
Masters Theses

Student Theses and Dissertations

1969

Analog simulation of mass transfer in droplets with turbulent internal circulation

Jeffrey Tsai-hwa Kuo

Follow this and additional works at: https://scholarsmine.mst.edu/masters_theses



Part of the [Chemical Engineering Commons](#)

Department:

Recommended Citation

Kuo, Jeffrey Tsai-hwa, "Analog simulation of mass transfer in droplets with turbulent internal circulation" (1969). *Masters Theses*. 5282.

https://scholarsmine.mst.edu/masters_theses/5282

This thesis is brought to you by Scholars' Mine, a service of the Missouri S&T Library and Learning Resources. This work is protected by U. S. Copyright Law. Unauthorized use including reproduction for redistribution requires the permission of the copyright holder. For more information, please contact scholarsmine@mst.edu.

ANALOG SIMULATION OF MASS TRANSFER IN DROPLETS
WITH TURBULENT INTERNAL CIRCULATION

BY

758

JEFFREY TSAI-HWA KUO, 1945

A

THESIS

submitted to the faculty of

THE UNIVERSITY OF MISSOURI - ROLLA

in partial fulfillment of the requirements for the

Degree of

MASTER OF SCIENCE IN CHEMICAL ENGINEERING

Rolla, Missouri

1969

Approved by

Robert M. Usher (advisor) W. Wagoner
Craig S. Langston

T2202
9/1
145P

154455

ABSTRACT

The object of this thesis is to simulate the Handlos and Baron Model for mass transfer into droplets by using an iterative analog computer in order to obtain eigenvalue and other parameters in a series solution. The eigenvalues λ_n calculated in this work are compared with the results obtained by Wellek-Skelland using a variational technique and by Patel using numerical approaches on the digital computer. From the analytical series solution, one can calculate the fraction of solute extracted in the droplets as a function of droplet contact time.

PACTOLUS, a digital-analog simulator, provides a check on the validity of analog simulation. The PACTOLUS simulation confirmed the results obtained from the analog simulation.

ACKNOWLEDGEMENT

The author wishes to express his indebtedness to Dr. Robert M. Wellek for suggesting this investigation and for serving as the research advisor. His help, guidance and encouragement are sincerely appreciated.

Gratefulness is acknowledged to Dr. R. C. Waggoner for his assistance and helpful suggestions.

TABLES OF CONTENTS

	PAGE
LIST OF FIGURES	vi
LIST OF TABLES	ix
CHAPTER	
I. INTRODUCTION	1
1.1. Prologue	1
1.2. Hydrodynamics and Droplet size	2
1.3. Mass transfer mechanism	2
1.3.1 Inside the droplets	3
1.3.1.1 Stagnant droplets	3
1.3.1.2 Circulating Drop	3
1.3.1.3 Individual mass transfer coefficient, k_{dr}	6
1.3.2 Outside of the droplet	8
1.4. Evaluation of overall mass transfer coefficient K_{dr}	9
II. MATHEMATICAL MODIFICATION FOR MASS TRANSFER INTO A DROPLET AT HIGH REYNOLDS NUMBERS	11
2.1. Handlos and Baron Model	11
2.2. Wellek and Skelland Modification of the Handlos and Baron Model	15
2.3. Mathematical Solution of the Model of Wellek-Skelland Modification	17
III. GENERAL ANALOG COMPUTATION TECHNIQUES IN SOLVING PARTIAL DIFFERENTIAL EQUATION	22
3.1 Separation of Variables	22

	PAGE
3.2. Finite Difference Method	23
IV. ANALOG SIMULATION OF THE MODEL	25
4.1. Two-point boundary value problem	25
4.2. Proposed method of solution	27
4.3. Magnitude and Time scaling of the problem	30
4.3.1. Magnitude Scaling	30
4.3.2. Time scaling	32
4.4. The digital logic	39
4.5. PACTOLUS simulation	41
V. RESULTS AND DISCUSSION	43
5.1. Computer results of eigenvalues and eignfunctions	43
5.2. Solution in terms of fraction of solute extracted	45
5.3. Comparison of results from analog computer with Patel's and Wellek-Skelland's results	62
5.4. Application of the results	63
VI. SUMMARY AND CONCLUSIONS	67
VII. NOMENCLATURE	71
VIII. BIBLIOGRAPHY	74
APPENDICES	77
1. APPENDIX (1)	78
2. APPENDIX (2)	81
3. APPENDIX (3)	85
4. APPENDIX (4)	87
5. APPENDIX (5)	91

PAGE

6.	APPENDIX (6)	97
7.	APPENDIX (7)	102
8.	APPENDIX (8)	113
9.	APPENDIX (9)	117
10.	APPENDIX (10,1)	126
11.	APPENDIX (10,2)	127
12.	APPENDIX (10,3)	128
13.	APPENDIX (11)	129
14.	APPENDIX (12)	132
15.	APPENDIX (13)	133
VITA		135

LIST OF FIGURES

FIGURE	PAGE
1. Hadamard Streamlines	4
2. Handlos and Baron Streamlines	12
3. Unscaled brief computer circuit	28
4. Block diagram for the trial and error procedure on analog computer	34
5. Iterative analog computer setup for Handlos and Baron Model	35
6. Digital logic setup for Handlos and Baron Model	36
7. Solution of Handlos and Baron Model on an iterative analog computer, λ_1	49
8. Solution of Handlos and Baron Model on an iterative analog computer, λ_2	50
9. Solution of Handlos and Baron Model on an iterative analog computer, λ_3	51
10. Solution of Handlos and Baron Model on an iterative analog computer, λ_4	52
11. Solution of Handlos and Baron Model on digital-analog simulator, λ_1	53
12. Solution of Handlos and Baron Model on digital-analog simulator, λ_2	54
13. Solution of Handlos and Baron Model on digital-analog simulator, λ_3	55
14. Solution of Handlos and Baron Model on digital-analog simulator, λ_4	56
15. Fraction extracted versus dimensionless time (Analog computer)	57

16.	Fraction extracted versus dimensionless time (PACTOLUS)	58
17.	Fraction extracted versus dimensionless time (Iterative analog computer)	59
A.1	Conventional analog computer program for Handlos and Baron Model	103
A.2	PACTOLUS program with relay switch for $y=1.0$	106
A.3	PACTOLUS program without time scale for the first type circuit arrangement	109
A.4	PACTOLUS program with time scale for the first type circuit arrangement	110
A.5	PACTOLUS program with time scale for the second type circuit arrangement	111
A.6	PACTOLUS program without time scale for the second type of circuit arrangement	112
A.7	Fraction extracted versus dimensionless time (Runge-Kutta method by Patel)	114
A.8	Fraction extracted versus dimensionless time (Hamming's method by Patel (28))	115
A.9	Fraction extracted versus dimensionless time (Finite-difference method by Patel (28))	116
A.10	Solution of Handlos and Baron Model on an iterative analog computer, λ_1	118
A.11	Solution of Handlos and Baron Model on an iterative analog computer, λ_2	119
A.12	Solution of Handlos and Baron Model on an iterative analog computer, λ_3	120

A.13	Solution of Handlos and Baron Model on an iterative analog computer, λ_4	121
A.14	Solution of Handlos and Baron Model on a conventional analog computer, λ_1	122
A.15	Solution of Handlos and Baron Model on a conventional analog computer, λ_2	123
A.16	Solution of Handlos and Baron Model on a conventional analog computer, λ_3	124
A.17	Solution of Handlos and Baron Model on a conventional analog computer, λ_4	125

LIST OF TABLES

	PAGE
1. Static Pot Settings and Amplifier Identification	37
2. Binary logic signal on the control line for different mode control	41
3. Digital logic for the Track-Hold system	41
4. Eigenvalues and Coefficients for Handlos and Baron Model (by trial and error on an iterative analog computer)	46
5. Eigenvalues and Coefficients for Handlos and Baron Model (by trial and error on a conventional analog computer)	47
6. Eigenvalues and Coefficients for Handlos and Baron Model (by trial and error on a digital-analog simulator)	48
A1 Eigenvalues and coefficients for stagnant drops due to Grober (15)	92
A2 Eigenvalues for Handlos and Baron Model calculated by Wellek and Skelland (11)	93
A3 Eigenvalues and coefficients for circulating drops calculated by Elzinga and Banchero(12)	94
A4 Eigenvalues and coefficients for Wellek-Skelland Modification (Runge-Kutta method by Patel(28))	95
A5 Eigenvalues and coefficients for Wellek-Skelland Modification (Hamming's method by Patel (28))	96
A6 Static pot settings and amplifier identification	104
A7 Block representations and numerical settings	107

"ANALOG SIMULATION OF MASS TRANSFER IN DROPLETS
WITH TURBULENT INTERNAL CIRCULATION"

I. INTRODUCTION

1.1 Prologue

Handlos and Baron (1) have proposed a mathematical model which describes mass transfer from a single liquid droplet or gas bubble (which possesses a special type of circulation and oscillation within the droplet) to a continuous phase of another liquid in which it is freely rising or falling. Examples of such processes are liquid-liquid extraction and gas-liquid absorption. The factors affecting the mass transfer rate are: (1) transfer area, (2) mass transfer coefficient, (3) driving force. A number of investigators (5,6,7,8,9,10, 11,19) have studied mass transfer from a single droplet to the continuous phase. It is essential to be able to predict the rate of mass transfer which is related to the mass transfer coefficient for the dispersed phase system. (1)

The purpose of this investigation is to present a theoretical relation for predicting the dispersed phase mass transfer coefficient of circulating and/or oscillating liquid droplets based on the modification of the Handlos and Baron.

In order to study the reason for the occurrence of oscillation and turbulent internal circulation of droplets which enhances the rate of extraction, a review of fluid dynamics and mass transfer aspects of droplet phenomena is

presented in the remainder of this chapter.

1.2 Hydrodynamics and Droplet size

In studying mass transfer from single liquid droplet, most of the previous work was based on the assumption of spherical droplets (6,7,8,9,10,11). At low droplet Reynolds numbers, $(d \cdot u_c / \mu_c)$, the droplet shape is approximately spherical. However, at high Reynolds numbers the droplet will be distorted from a spherical form. The change in shape of the droplet affects not only the interfacial area but also the continuous and dispersed phase mass transfer coefficient. The shape of a drop moving in a liquid continuous phase is determined by the force acting along the surface of the drop. Basically, the shape is dependent upon the balance between fluid dynamics pressure and the interfacial forces which tend to make the drop a sphere. As the Reynolds number is increased, droplet oscillation will occur. As the Reynolds number continues to increase, the drop will break. Elzinga and Banchemo (12) have suggested that internal circulation has little effect on distortion of the droplet dispersed in a gas, but is not necessarily true for a liquid continuous phase.

1.3 Mass transfer mechanism

Mass transfer between a drop and the fluid in the extraction column takes place in three stages. The first is during the period of drop formation; the second is during free fall or rise of the drop; and the third stage is the extraction at coalescent layer. In this work, only mechanisms postulated for the second stage are discussed.

1.3.1 Inside the droplet

1.3.1.1 Stagnant droplets: There is generally no internal circulation in small droplets. For heat and mass transfer rates inside the drop, recent studies by Elzinga and Banchero (12), Calderbank and Korchinski (13) have used the theory for a stagnant (non-oscillating) drop(sphere) or for a drop which possessed circulation patterns which were developed by Hadamard (14). (See Figure 1.) For a constant molecular diffusivity, uniform initial concentration and a spherical drop shape, Grober (15) derived an expression for the fraction extracted for a drop which encounters finite resistance in the continuous phase.

$$E_m = 1 - 6 \sum_{n=1}^{\infty} B_n \exp \left[-\lambda_n^2 \frac{Dt}{a^2} \right] \quad (1.1)$$

Newman (16) derived the following expression for mass transfer in a stagnant spherical drop from Fick's second law. It is applicable if there is no resistance in the continuous phase.

$$E_m = 1 - \frac{6}{a^2} \sum_{n=1}^{\infty} \frac{1}{n^2} \exp \left[-\frac{n^2 D \pi t}{a^2} \right] \quad (1.2)$$

1.3.1.2 Circulating Drop: As the drop size increases, the droplet begins to have internal circulation currents, which exist inside the droplet because of viscous flow between fluids. This increases the rate of extraction when compared with the rate of extraction in an internally stagnant drop. For drop Reynolds numbers less than unity, Kronig and Brink (17) derived the following equation to be used if continuous phase resistance is negligible:

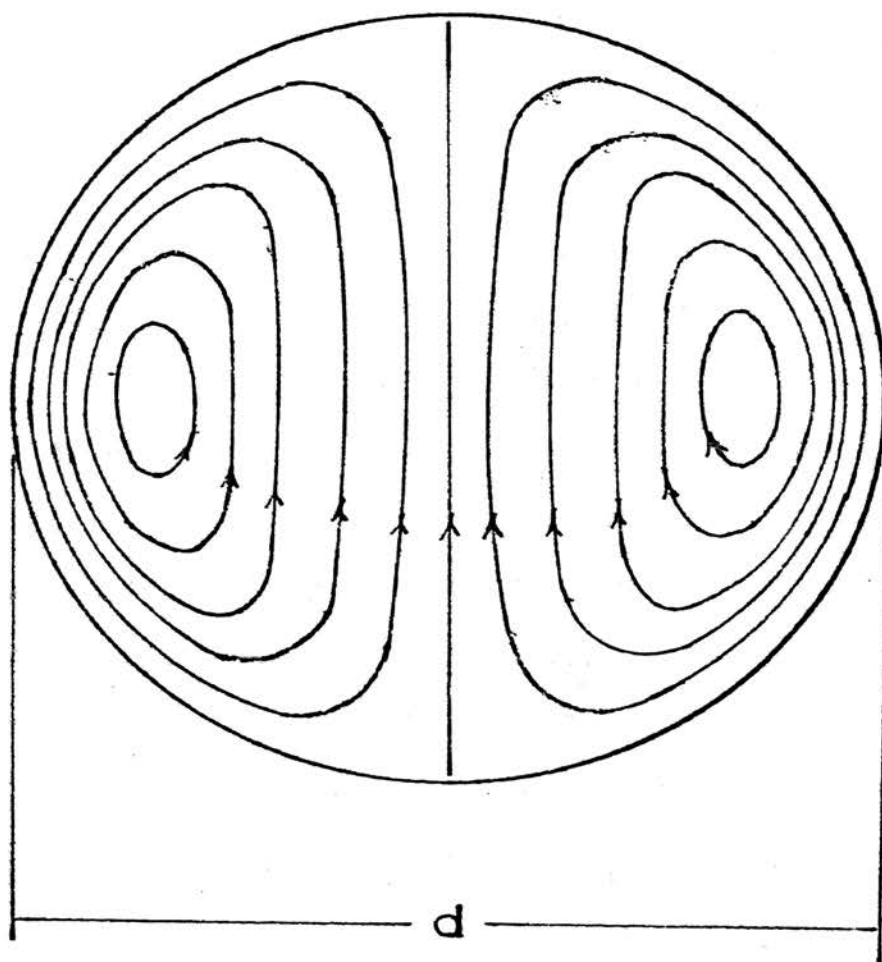


Figure 1: Hadamard Streamlines

$$E_m = 1 - \frac{3}{8} \sum_{n=1}^{\infty} B_n^2 \exp\left[-\lambda_n \frac{16Dt}{a^2}\right] \quad (1.3)$$

While investigating the heat transfer rate to drops in liquid-liquid systems, Elzinga and Banchemo (12) modified the Kronig and Brink Model to consider the effect of finite resistance in the continuous phase by revising the boundary condition at the surface. It should be emphasized that the Kronig and Brink Model and the Elzinga and Banchemo Model theoretically hold only for Reynolds numbers less than one and for Peclet numbers approaching unity.

Kronig and Brink (17) proposed a method for illustrating the increased rate of mass transfer which results from internal circulation. They consider that effectively the molecular diffusivity, D , has been increased by a factor of about 2.4 as compared with the case of a stationary droplet.

I. J. Q. Korchinski (13) studied heat transfer in single droplet systems. He observed rigid, oscillating and circulating behavior of droplets. At Reynolds numbers of about 200, drop oscillation commenced. He concluded that internal circulation in the liquid drop raised the effective diffusivity to a value approaching 2.25 times the molecular diffusivity. He also pointed out that no precise data is available to determine the limits between the regimes of pure circulation and drop oscillation. But, Korchinski listed a table for various liquid systems to show that at the time oscillation occurs, the empirical correction factor R increases greatly. He defines this correction factor, R , as

$$R = \frac{D(\text{effective diffusivity due to internal circulation})}{D(\text{molecular diffusivity})} \quad (1.4)$$

For non-circulating drops, it is apparent that R equals unity.

For drops with turbulent circulation R should be larger.

Johnson and Hamielec (5) state that intense circulation may cause R to be even greater than 2.5. When the drop oscillates, the large increase described by R causes the rate of extraction to increase dramatically.

Garner and Skelland (18) stated that overall mass transfer coefficients increased with drop size but decreased with increases of interfacial tension.

1.3.1.3 Individual mass transfer coefficient, k_{dr} :

For droplets which are internally stagnant and with no resistance in the continuous phase, Newman (16) derived:

$$k_{dr} = \frac{-d\rho}{6Mt} \ln \left[\frac{6}{\pi^2} \sum_{n=1}^{\infty} \frac{1}{n^2} \exp \left[\frac{-n^2 D_v \pi^2 t}{(d/2)^2} \right] \right] \quad (1.5)$$

Vermeulen's (33) empirical equation fits Newman's expression well when the fraction extracted, E_m , is less than 0.5 during free fall (or rise)

$$k_{dr} = \frac{-d\rho}{6Mt} \ln \left[1 - \frac{\pi D_v \frac{1}{2} t^{\frac{1}{2}}}{(d/2)} \right] \quad (1.6)$$

Johnson and Hamielec (5) introduced Korchinski's (13) expression as a dimensionless correction factor R into Grober's expression. This factor is a multiplier for the molecular diffusivity to account for transfer rate increases in drops which contain internal motion.

$$K_{dr} = \frac{-d\rho}{6Mt} \ln \left[\frac{6}{\pi^2} \sum_{n=1}^{\infty} B_n \exp \left[-\lambda_n^2 \frac{RD_v t}{(d/2)^2} \right] \right] \quad (1.7)$$

When transfer resistance is zero in the continuous phase and laminar circulation exists inside the drop, the Kronig and Brink expression becomes

$$k_{dr} = \frac{-d \rho}{6Mt} \ln \left[\frac{3}{8} \sum_{n=1}^{\infty} B_n^2 \exp \left[-\lambda_n \frac{16D_v t}{(d/2)^2} \right] \right] \quad (1.8)$$

Korchinski's (13) empirical equation fits Kronig and Brink expression well only for E_m values of less than 0.5

$$k_{dr} = \frac{-d \rho}{6Mt} \ln \left[1 - \frac{R^{\frac{1}{2}} \pi D_v^{\frac{1}{2}} t^{\frac{1}{2}}}{(d/2)} \right] \quad (1.9)$$

where $R \cong 2.5$

Elzinga and Banchero (12) modified Kronig and Brink's expression for the case of a finite resistance in the continuous phase.

Higbie's (34) equation has been applied to the case where internal circulation prevails in the drops

$$k_{dr} = \frac{2\rho}{M} \sqrt{\frac{D_v}{\pi t e}} \quad (1.10)$$

Handlos and Baron proposed a mechanism in which a form of turbulence (radial motion due to oscillation) is superimposed on circulation within the drop. Their expression for zero resistance in the continuous phase is given as follows:

$$k_{dr} = \frac{-d\rho}{6Mt} \ln \left[2 \sum_{n=1}^{\infty} B_n \exp \left[\frac{-\lambda_n 16D_v t N_{pe}}{2048d^2} \right] \right] \quad (1.11)$$

Wellek and Skelland modified the Handlos and Baron Model to consider the finite resistance in the continuous phase

$$k_{dr} = \frac{\lambda_1 V \rho}{768(1 + \mu_d / \mu_c)} \quad (1.12)$$

where the first eigenvalue λ_1 is a function of resistance in the continuous phase.

Skelland and Wellek provided the most comprehensive correlation for k_{dr} based on extensive experimental data for non-oscillating and oscillating droplets:

For non-oscillating droplets:

$$k_{dr} = 31.4 \frac{D_v \rho}{dM} \left(\frac{4D_v t}{d} \right)^{-0.34} \left(\frac{\mu_d}{\rho D_v} \right)^{-0.125} \left(\frac{dV^2 \rho_c}{\sigma} \right)^{0.37} \quad (1.13)$$

For oscillating droplets;

$$k_{dr} = 0.32 \frac{D_v \rho}{dM} \left(\frac{4D_v t}{d} \right)^{-0.14} \left(\frac{dV \rho_c}{\mu_c} \right)^{0.68} \left(\frac{\sigma 3 \rho_c^2}{g \mu_c^4 \Delta \rho} \right)^{0.225} \quad (1.14)$$

1.3.2 Outside of the droplet. Many theoretical and empirical relations are available for predicting the individual mass transfer coefficient in the continuous phase. The continuous phase mass transfer coefficient for a rigid (non-oscillating) droplet may be predicted by an expression based on boundary layer theory and empiricism derived by Frossling (20).

$$k_{cr} = \frac{D_v \rho}{dM} \left[2 + 0.55 (N_{Rec})^{\frac{1}{2}} (N_{Scc})^{\frac{1}{2}} \right] \quad (1.15)$$

valid for $2 < Re < 1000$

For droplets with internal circulation, Boussinesq (35) has shown that

$$k_{cr} = \frac{D \rho}{dM} \left[\frac{2}{\sqrt{\pi}} (N_{Rec})^{\frac{1}{2}} (N_{Scc})^{\frac{1}{2}} \right] \quad (1.16)$$

For continuous phase mass transfer from droplets which were internally circulating but not oscillating, Garner and

Treyban (36) found experimentally:

$$k_{cr} = \frac{D_v \rho}{dM} \left[0.6 (N_{Rec})^{\frac{1}{2}} (N_{Scc})^{\frac{1}{2}} \right] \quad (1.17)$$

For drops which were both circulating and oscillating, Garner and Treyban (36) developed the relation:

$$k_{cr} = \frac{D_v \rho}{dM} \left[50 + 0.085 (N_{Rec})^{1.0} (N_{Scc})^{0.7} \right] \quad (1.18)$$

Nearly all of the above expressions assume that the droplet is spherical. However, droplets usually show large deformation into an oblate spheroidal shape as indicated by Wellek, Agrawal and Skelland (19).

Skelland and Cornish (4) correlated data on the rate of mass transfer from rigid oblate spheroids in an air stream as follows:

$$k_{cr} = 0.74 \frac{D_v \rho}{d \rho M} \left(\frac{d_p V \rho}{\mu_c} \right) \left(\frac{\mu_c}{\rho D_v} \right)^{1/3} \quad (1.19)$$

where d_p is the total surface area of the spheroid divided by its perimeter normal to the flow (32). This equation is useful in calculating k_{dr} for non-oscillating drops which assume the shape of oblate spheroids.

1.4 Evaluation of overall mass transfer coefficient K_{dr}

With the assumption of interfacial equilibrium, an overall mass transfer coefficient can be expressed in terms of the individual dispersed phase coefficients k_{dr} and a continuous phase coefficient k_{cr} during the free fall (or rise) period.

$$\frac{1}{K_{dr}} = \frac{1}{k_{dr}} + \frac{m}{k_{cr}} \quad (1.20)$$

Individual mass transfer coefficients in the dispersed phase and the continuous phase can be calculated from the theoretical and empirical equations in section 3 of this chapter.

II. MATHEMATICAL MODIFICATION FOR MASS TRANSFER INTO A DROPLET AT HIGH REYNOLDS NUMBERS

2.1 Handlos and Baron Model

Handlos and Baron modified the Kronig and Brink (17) theory and devised a turbulent mixing model with an internal circulation pattern of concentric circles. They assumed that the liquid between two streamlines becomes radially mixed after one circulation period. The mechanism which they proposed predicted the very low resistance to mass transfer inside circulating and/or oscillating droplets. This model is based on the assumption that internal circulation is fully developed and that the velocities of falling (or rising) droplets can be predicted.

Handlos and Baron (1) further assumed that the circulation within the spherical droplet is a system of circular tori-Figure(2) and that "random radial vibrations" are superimposed upon the streamlines. Handlos and Baron did not specifically state the source of these vibrations but the presence of the oscillation due to the skin friction at the droplet surface may account for them. These vibrations provide mixing between streamlines. It should be emphasized that mass transfer is assumed to take place within the outer surface of each torus. Resistance to transfer within the volume of the droplet between the outer surface of the torus and the interfacial area of the sphere is neglected.

Handlos and Baron propose that the mass flux of solute

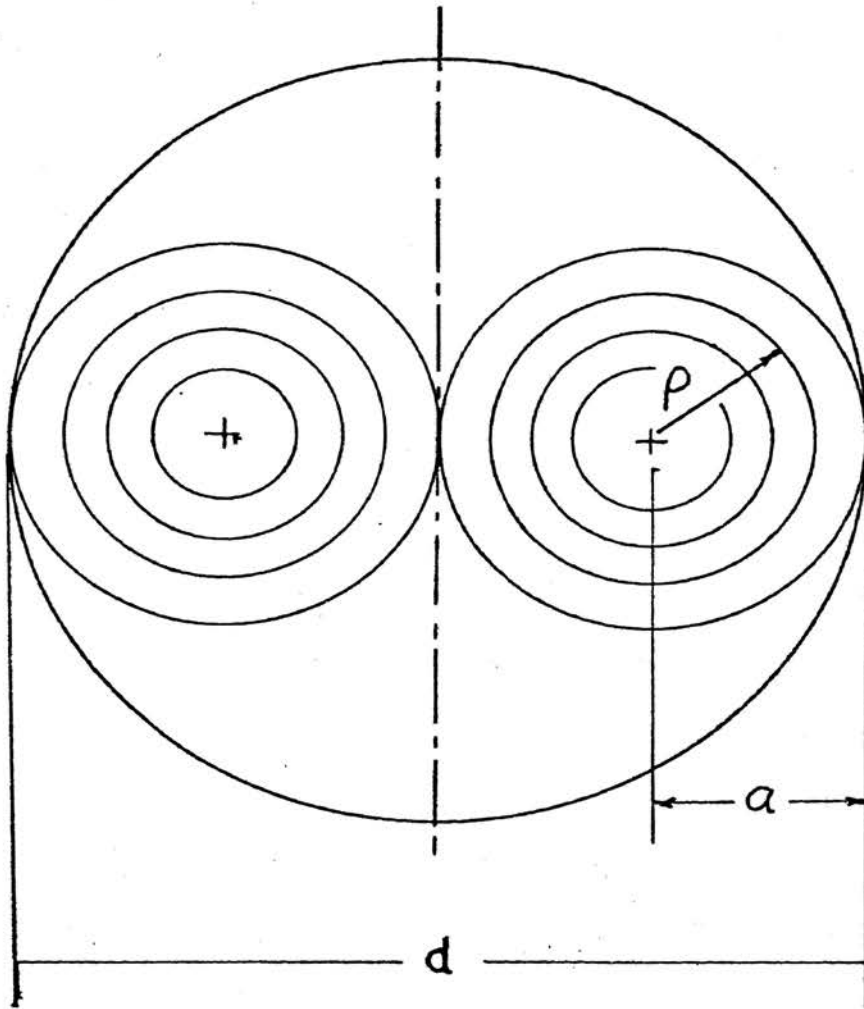


Fig. 2 : Handlos and Baron Streamlines

at any point follows the following relation

$$\bar{N} = -\bar{E}\nabla C \quad (2.1)$$

where \bar{N} is the flux of the solute and ∇C is the concentration vector gradient. When this relation is substituted into the equation of continuity, equation (2.2) is obtained for the case in which no chemical reaction takes place.

$$\frac{\partial C_a}{\partial t} = -\nabla \bar{N} = \nabla(\bar{E}\nabla C) \quad (2.2)$$

In order to derive the expression for the eddy mass diffusivity $E(r)$, Handlos and Baron suggest that the transfer process can be represented by the Einstein eddy diffusion equation (for two dimensions):

$$\bar{E} = \frac{\bar{Z}^2}{4\bar{t}} \quad (2.3)$$

where \bar{Z} is the mean square displacement of an element of fluid during the average circulation time \bar{t} . Handlos and Baron assumed that for this model \bar{t} can be approximated by the value of \bar{t} as derived by Kronig and Brink from the Hadamard (14) dispersed phase stream function.

$$\bar{t} = \frac{16}{3} \frac{d}{U} \left(1 + \frac{\mu_d}{\mu_c}\right) \quad (2.4)$$

A relation for \bar{Z} is developed as follows: a particle is considered initially to have a radius ρ . After a time sufficient for one circuit along the streamlines, the particle is displaced to a point ρ' as a result of random radial motions. In the limiting case of complete mixing in one circulation period, the probability that a particle is found between ρ'

and $\rho + d\rho$ is the ratio of the differential element of volume at ρ' to the total volume of the torus

$$P(\rho')d\rho' = \frac{32\rho'}{d^2} d\rho' \quad (2.5)$$

Since $\underline{r} = \frac{4\rho}{d}$

expression (2.5) becomes $P(\underline{r}')d\underline{r}' = 2\underline{r}'d\underline{r}'$

The displacement \bar{Z} of the element of fluid during the circulating period is given by

$$\bar{Z} = \rho' - \rho = \frac{d_e}{4} (\underline{r}' - \underline{r}) \quad (2.6)$$

According to Handlos and Baron, the mean square displacement is

$$\begin{aligned} \bar{Z}^2 &= \int_0^1 Z^2 P(\underline{r}') d\underline{r}' = \frac{d^2}{8} \int_0^1 \underline{r}' (\underline{r}' - \underline{r})^2 d\underline{r}' \\ &= \frac{d_e^2}{96} (6\underline{r}^2 - 8\underline{r} + 3) \end{aligned} \quad (2.7)$$

Now, substituting the relation of \bar{Z} and \bar{t} into the Einstein Equation

$$\bar{E}(\underline{r}) = \frac{\bar{Z}^2}{4\bar{t}} = \frac{d_e U}{2048} \frac{(6\underline{r}^2 - 8\underline{r} + 3)}{(1 + (\mu_d/\mu_c))} \quad (2.8)$$

If mass transfer takes place in the radial direction only, equation (2.2) for the chosen coordinate system is

$$\frac{\partial C_a}{\partial t} = \frac{16}{d_e^2} \frac{1}{\underline{r}} \frac{\partial}{\partial \underline{r}} \left(\bar{E}(\underline{r}) \cdot \underline{r} \frac{\partial C}{\partial \underline{r}} \right) \quad (2.9)$$

Substituting the relation for eddy diffusivities $\bar{E}(\underline{r})$ into equation (2.9)

$$\frac{\partial C}{\partial t} = \frac{1}{r} \frac{\partial}{\partial r} \left((6r^2 - 8r + 3)r \frac{\partial C}{\partial r} \right) \quad (2.10)$$

U

where $b = \frac{U}{128(1 + \mu_d/\mu_c)d_e}$

If $r = 1-y$, equation (2.10) is transformed to

$$\frac{\partial C}{\partial t} = \frac{b}{1-y} \frac{\partial}{\partial y} (1-5y+10y^2-6y^3) \frac{\partial C}{\partial y} \quad (2.11)$$

The boundary conditions are

$$C = 0, \quad y = 0, \quad t > 0 \quad (2.12)$$

$$C \text{ is finite}, \quad y = 1, \quad t = t \quad (2.13)$$

$$C = C_0, \quad 0 \leq y \leq 1, \quad t = 0 \quad (2.14)$$

The first boundary condition indicates that there is no resistance to transfer in the continuous phase, and also that the concentration of the continuous phase remains unchanged throughout the transfer period. The second boundary condition is equivalent to

$$\frac{\partial C}{\partial y} = 0, \quad y = 1, \quad t = t \quad (2.15)$$

The third boundary condition implies that the initial concentration of the drop is uniform.

2.2 Wellek and Skelland Modification of the Handlos and Baron Model

Wellek and Skelland assumed a finite resistance to mass transfer in the continuous phase. Hence, the boundary conditions are changed to:

$$C = C_0, \quad 0 \leq y \leq 1, \quad t = 0 \quad (2.16)$$

$$C \text{ is finite}, \quad y = 1, \quad t = t \quad (2.17)$$

$$\frac{\partial C}{\partial y} = hC, \quad y = 0, \quad t > 0 \quad (2.18)$$

$$\text{Where } h = \frac{512 k_c (1 + \mu_d/\mu_c)}{mU}$$

The third boundary condition at the surface of the droplet is obtained as follows:

$$-\bar{E}(\rho) \frac{\partial C}{\partial \rho} = \frac{k_c}{m} C, \quad \rho = \frac{d}{4}, \quad t > 0 \quad (2.19)$$

$$-\bar{E}(\underline{r}) \frac{4}{d} \frac{\partial C}{\partial r} = \frac{k_c}{m} C, \quad \underline{r} = 1, \quad t > 0$$

$$-\bar{E}(y) \frac{4}{d} \left(-\frac{\partial C}{\partial y} \right) = \frac{k_c}{m} C, \quad y = 0, \quad t > 0$$

$$\frac{\partial C}{\partial y} = \frac{d}{4} \frac{1}{\bar{E}(y)} \frac{k_c}{m} C = \frac{k_c}{m} \frac{d}{4} \frac{1}{\bar{E}(y)}$$

$$\begin{aligned} \bar{E}(y) &= -\frac{z^2}{4t} = \frac{d^2/96}{4(16/3)(d/U)(1+\mu_d/\mu_c)}, \quad \left(\bar{z}^2(1) = \frac{d^2}{96}(1) = \frac{d^2}{96} \right) \\ &= \frac{Ud}{(16)(32)(1+\mu_d/\mu_c)} \\ &= \frac{Ud}{2048(1+\mu_d/\mu_c)} \end{aligned} \quad (2.20)$$

Substitute $\bar{E}(y)$ at $y=0$ into equation (2.18)

$$\frac{\partial C}{\partial y} = \frac{k_c}{m} \frac{d}{4} \left(\frac{4 \cdot 512 (1 + \mu_d/\mu_c)}{Ud} \right) C, \quad y = 0, \quad t > 0$$

$$\frac{\partial C}{\partial y} = hC \quad y = 0, \quad t > 0 \quad (2.21)$$

Since h is assumed to remain constant during operation, the continuous phase mass transfer coefficient k_c , distribution

ratio, n , viscosity of both phases and droplet free fall (or rise) velocity must be held uniform during the transfer period. These assumptions are good enough to describe most situations.

2.3 Mathematical Solution of the Model of Wellek-Skelland Modification

The linear partial differential equation which describes the model is

$$\frac{\partial C}{\partial t} = \frac{b}{1-y} \frac{\partial}{\partial y} (1-5y+10y^2-6y^3) \frac{\partial C}{\partial y} \quad (2.11)$$

The relevant boundary conditions are

$$(1) \quad \frac{\partial C}{\partial y} = hc, \quad y = 0, \quad t > 0 \quad (2.18)$$

$$(2) \quad c \text{ is finite}, \quad y = 1, \quad t = t \quad (2.17)$$

$$(3) \quad c \text{ is } c_0, \quad 0 \leq y \leq 1, \quad t = 0 \quad (2.16)$$

To solve a linear partial differential equation when the separation of variables technique is used, the solution is assumed to have the form

$$C = T(t) Y(y) \quad (2.22)$$

where t and y are the two independent variables in the equation. Now, the equation can be separated into two ordinary differential equations as:

$$\frac{dT}{dt} + b\lambda T = 0 \quad (2.23)$$

$$\frac{d}{dy} \left(P(y) \cdot \frac{dy}{dy} \right) + \lambda \cdot Q(y)Y = 0 \quad (2.24)$$

$$\text{Where } P(y) = 1 - 5y + 10y^2 - 6y^3 \quad (2.25)$$

$$Q(y) = 1 - y \quad (2.26)$$

The solution of Equation (2.23) is

$$T(t) = B_n \exp(-b\lambda_n t) \quad (2.27)$$

The boundary conditions for Equation (2.24) are

$$\frac{dY}{dy} = hY, \quad y = 0 \quad (2.28)$$

$$\text{and } Y \text{ is finite, } y = 1 \quad (2.29)$$

Equations (2.24), (2.25) and (2.26) represent a Sturm-Liouville system. Non-trivial solutions to that system exist in most cases only for a discrete set of values of $\lambda_1, \lambda_2, \lambda_3, \dots$ called eigenvalues. The series of orthogonal eigenfunctions Y_1, Y_2, Y_3, \dots are not known but are considered normalized with the factor included in the coefficient B_n . Combining the solution of the two differential equations, one obtains the complete solution

$$C(y, t) = C_0 \sum_{n=1}^{\infty} B_n Y_n \exp(-b\lambda_n t) \quad (2.30)$$

This complete solution (2.30) represents the solute concentration at any value of y and t . For the derivation of the general solution refer to Appendix (2).

The mass of solute $M(t)$ in the drop at any time can be expressed as

$$M(t) = \int_0^{V_t} C dV \quad (2.31)$$

The volume of torus is

$$V_p = 2\pi^2 \left(\frac{d_e}{4}\right) (\rho^*)^2$$

$$dV_p = 4\pi^2 \left(\frac{d_e}{4}\right) \rho d\rho, \quad \underline{r} = 1-y, \quad \underline{r} = \frac{\rho}{d/4}$$

$$dV_y = -\frac{\pi^2 d^3}{16} (1-y) dy$$

$$M(t) = \frac{C_o \pi^2 d^3}{16} \sum_{n=1}^{\infty} B_n \exp(-b\lambda_n t) \int_0^1 (1-y) Y_n dy \quad (2.32)$$

At t equals 0, the general solution can be written as:

$$C(y, 0) = C_o = C_o \sum_{n=1}^{\infty} B_n Y_n \quad (2.33)$$

Hence

$$\sum_{n=1}^{\infty} B_n Y_n = 1 \quad (2.34)$$

In order to obtain B_n , the condition of orthogonality is applied to Equation (2.34). Now, equation (2.34) can be modified to the equation

$$\int_0^1 (1-y) Y_n dy = B_n \int_0^1 (1-y) Y_n^2 dy \quad (2.35)$$

By application of the theory of orthonormal functions, equation reduces to

$$B_n = \int_0^1 (1-y) Y_n dy \quad (2.36)$$

Substituting this relation into Equation (2.32), leads to the expression for the mass in the drop at any time

$$M(t) = \frac{C_o \pi^2 d^3}{16} \sum_{n=1}^{\infty} B_n^2 \exp(-b\lambda_n t) \quad (2.37)$$

The initial mass of solute in the droplet is

$$M(0) = C_o V = C_o \cdot 2\pi^2 \left(\frac{d_e}{4}\right)^3$$

$$= C_o (2\pi^2) \frac{d_e^3}{64}$$

Therefore :

$$\frac{M(t)}{M(0)} = \frac{(C_0 \pi^2 d^3 / 16) \sum_{n=1}^{\infty} B_n^2 \exp(-b \lambda_n t)}{C_0 \pi^2 (d^3 / 32)}$$

$$\frac{M(t)}{M(0)} = 2 \sum_{n=1}^{\infty} B_n^2 \exp(-b \lambda_n t) \quad (2.38)$$

Johnson and Hamielec (5) prefer to express Equation (2.38) in terms of the fraction of solute extracted

$$E_m = 1 - 2 \sum_{n=1}^{\infty} B_n^2 \exp(-b \lambda_n t) = 1 - \frac{M(t)}{M(0)} \quad (2.39)$$

In this equation, B_n and λ_n have to be determined before E_m can be obtained.

Consider the equation

$$\frac{d}{dy} \left(P(y) \cdot \frac{dY}{dy} \right) + \lambda Q(y) Y = 0 \quad (2.40)$$

$$Q(y) Y_n = -\frac{1}{\lambda_n} \frac{d}{dy} \left(P(y) \frac{dY}{dy} \right) \quad (2.41)$$

$$Q(y) = (1 - y) \quad (2.26)$$

$$B_n = \int_0^1 Q(y) Y dy \quad (2.36)$$

Performing the integration:

$$B_n = \int_0^1 -\frac{1}{\lambda_n} \frac{d}{dy} \left(P(y) \frac{dY}{dy} \right) dy$$

$$B_n = -\frac{1}{\lambda_n} \left[P(y) \frac{dY}{dy} \right]_0^1$$

$$= \frac{-1}{\lambda_n} \left[P(1) \frac{dY_n(1)}{dy} - P(0) \frac{dY_n}{dy} \right]$$

$$P(1) = 0$$

$$P(0) = 1$$

Hence :

$$B_n = \frac{1}{\lambda_n} \frac{dY_n}{dy}(0) \quad (2.42)$$

This relation is used to calculate B_n after both the eigenvalues λ_n , and $dY_n(0)/dy$ have been obtained from iterative analog operations.

III. GENERAL ANALOG COMPUTATION TECHNIQUES IN SOLVING PARTIAL DIFFERENTIAL EQUATION

Analog computer techniques have been used successfully to solve systems described mathematically by partial differential equations. They may be used to obtain an approximation of an analytical solution when such solutions are either impossible or tedious. They may also serve as means of determining the range of validity of an approximate solution(21).

Two approaches have been applied to solve partial differential equations on the analog computer.

3.1 Separation of Variables

The integrators on an analog computer are limited to a single independent variable. A partial differential equation must be converted to a set of ordinary differential equations before the computer can simulate a mathematical model. In this approach, each equation is easily programmed on the computer, but solutions are not readily obtained if the boundary values for the problem specify for each ordinary differential equation both initial and final conditions. On the computer only the initial condition can be applied and it is thus necessary to determine by iteration parameter values on the initial condition that will satisfy the final condition.

In eigenvalue problems, there is often an infinite number of suitable parameter values (eigenvalues) and solutions (eigenfunctions).

Fortunately, it is usually necessary to include only the first few modes in any series. A complete solution of the partial differential equation may be obtained from the product of separate functions of the independent variables. The analog computer may be used to obtain both the eigenvalues and eigenfunctions. The computer is programmed and wired to solve one of the ordinary differential equations. The known initial conditions are applied. The parameter (eigenvalue) enters the solution as a trial initial value which is varied by adjusting a potentiometer until the final conditions are satisfied. The final value shown on the potentiometer is the eigenvalue and the corresponding solution of the dependent function gives the eigenfunction. Therefore, the original problem of solving the partial differential equation reduces to a series of solutions of an eigenvalue problem.

In recent years, the "iterative analog computer" has been designed. Several digital logic components have been added to the analog computer. They may be used to control its modes and to adjust parameters automatically. These operations are especially useful in eigenvalue problems.

3.2 Finite Difference Method

The finite difference method is applicable to both linear and non-linear systems. The partial differential equation is replaced by a set of ordinary differential equations with one independent variable as the continuous independent variable and the other independent variable

considered at discrete values. The partial derivatives are replaced by an appropriate difference expressions such as the backward, central, or forward differences. This technique requires that the "discreted" dependent variable of interest be only within bounded intervals of the additional independent variable(s). To maintain accuracy, division into a reasonable number of segments (or intervals) must be used so that the change of the dependent variable from point to point will not be too severe. The requirement is generally fulfilled in most physical problems. If the boundary interval is divided into segments, the resulting set of $n+1$ simultaneous differential equations can be solved on the analog computer or digital computer concurrently.

IV. ANALOG SIMULATION OF THE MODEL

4.1 Two-point boundary value problem

The mathematical expression to describe the Handlos and Baron model with the Wellek-Skelland modification(11) is

$$\frac{\partial C}{\partial t} = \frac{b}{1-y} \frac{\partial}{\partial y} (1-5y+10y^2-6y^3) \frac{\partial C}{\partial y} \quad (2.11)$$

The boundary conditions are

$$(1) \quad \frac{\partial C}{\partial y} = hC \quad , \quad y = 0 \quad , \quad t > 0 \quad (2.18)$$

$$(2) \quad C \text{ is finite,} \quad y = 1 \quad , \quad t = t \quad (2.17)$$

$$(3) \quad C = C_0 \quad , \quad 0 \leq y \leq 1, \quad t = 0 \quad (2.16)$$

Equation (2.11) is a linear partial differential equation. After using the method of separation of variable (refer to Appendix 2), two ordinary differential equations are obtained. The two-point boundary value problem to be simulated with the relevant boundary conditions is given as follows:

$$\frac{d}{dy} \left(P(y) \frac{dY}{dy} \right) + \lambda Q(y)Y = 0 \quad (2.24)$$

with boundary conditions

$$(1) \quad \frac{dY}{dy} = hY, \quad y = 0 \quad (2.28)$$

$$(2) \quad \frac{dY}{dy} = 0 \quad , \quad y = 1 \quad (2.29)$$

$$\text{where } P(y) = 1-5y+10y^2-6y^3 \quad (2.25)$$

$$\text{and } Q(y) = 1-y \quad (2.26)$$

The variable $Y(y)$ is the dependent variable in equation (2.24).

Equation (2.24) may be rearranged to obtain the following expression:

$$\frac{d^2Y}{dy^2} - \frac{(18y^2 - 20y + 5)}{(1 - 5y + 10y^2 - 6y^3)} \frac{dY}{dy} + \frac{\lambda_n Y}{(6y^2 - 4y + 1)} = 0 \quad (4.1)$$

The analog computer results in later chapters* show that the normalized boundary condition used by Patel

$$Y(1) = 1, \quad y = 1 \quad (4.2)$$

is also applicable in this work.

The second term in equation (4.1) becomes indeterminate when y approaches unity. However, a limiting value for d^2Y/dy^2 may be obtained by the application of L'Hospital's Rule (23) which results in the following equation:

$$\frac{d^2Y}{dy^2} = \frac{-\lambda_n Y}{2(6y^2 - 4y + 1)} \quad (4.3)$$

and hence at $y = 1$

$$\frac{d^2Y}{dy^2} = -\frac{\lambda_n}{6} \quad (4.4)$$

Equation (4.1) is the basis of the simulation. In order for it to be compatible with the limitation of an analog computer, it must be magnitude scaled and time scaled.

As shown by Figure 5, the independent variable y in equation (4.1) and equation (4.3) is measured in time by the time-generated integrator 4 on analog computer. The function generators to generate functions $G_1(y)$, $G_2(y)$, $G_3(y)$ indicated on Figure 3 are obtained from non-linear elements. Scaled

* refer to Chapter V

values of the dependent variables, dY/dy and Y are generated in voltage by integrators 1 and 2.

4.2 Proposed method of solution

After the problem has been stated above in Equation (4.1), the next step is the formulation of a logical procedure to be programmed on the iterative analog computer.* This procedure is outlined in an abbreviated computer diagram, Figure 3. The values for the modified continuous phase resistance, h , used in this work are the same values as used by Wellek-Skelland (9). The object of this iterative analog computer program is to determine the value of $Y(0)$ for which the final condition, $dY(1)/dy = 0$, is satisfied.

The eigenvalue λ_n is selected arbitrarily and is revised during each run. A search procedure must be devised so that two variables, λ_n and $dY(0)/dy$ may be obtained as a set of conditions. If both parameters, $Y(0)$ and λ_n must be adjusted manually, the operation may become time-consuming. Therefore, the digital logic portion of the iterative analog computer is programmed to find automatically the initial value of $dY(0)/dy$ which satisfies the problems boundary conditions.

The computer must be programmed with a criterion ϵ to control the problems on each iteration so that when $dY/dy(1) < \epsilon$ (where ϵ is small enough to determine the accuracy to which the boundary condition is satisfied), $dY(y)/dy$ is close to $dY_n(y)/dy$ for the desired mode. The criterion to be used is based on the zero-crossing property of the normal mode. For necessarily larger eigenvalues, λ_n , the zeroes (* refer to APPENDIX 13)

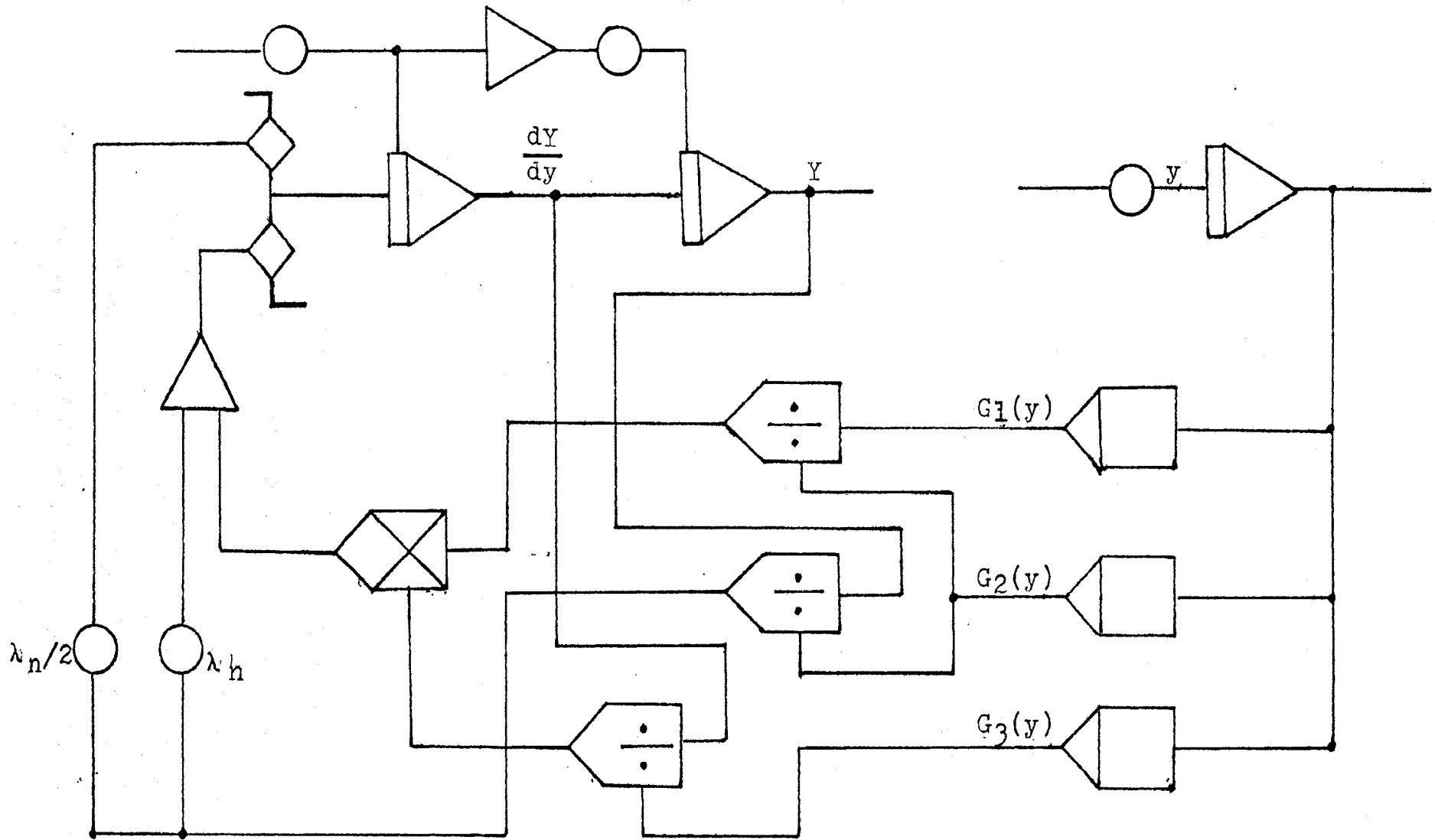


Figure 3: Unscaled brief computer circuit where

$$G_1(y) = (18y^2 - 20y + 1)$$

$$G_2(y) = (6y^2 - 4y + 1)$$

$$G_3(y) = 1 - y$$

of the normal mode, $dY_n(y)/dy$, (22) lie closer together.

Let the eigenvalues be ordered numerically so that $0 < \lambda_1 < \lambda_2 < \lambda_3 \dots \lambda_n$. This ordering is possible since the eigenvalues are all real and positive. If $Y_n(y)$ and $Y_{n+1}(y)$ are solutions of the equation with $\lambda = \lambda_n$ and $\lambda = \lambda_{n+1}$ respectively, it is found that $Y_{n+1}(y)$ has at least one zero-crossing more than $Y_n(y)$ within the interval. After estimating the small region close to the boundary at $y=1$ in which equation (4.3) can be applied, a scheme to obtain the eigenvalues λ_n and $Y(0)$ can be set up. The following procedure for programming the problem will be used:

- (1) An eigenvalue λ_n^i is assumed (i is the number of iteration).
- (2) Set $dY(0)/dy$ at its initial approximate values $dY(0)/dy|_i$
- (3) Put the computer in IC position and track the value of $dY(0)/dy$ stored in the Track-Hold system.
- (4) Put computer in Operate position (checking program in Appendix 13).
- (5) Integrate from $y=0$ to $y=1$ to find the final condition $dY(1)/dy$.
- (6) Test $dY(1)/dy$, if $dY(1)/dy = 0$ (smaller than ϵ), the search is completed. If not, go to next step.
- (7) Adjust the initial value of dY/dy , i.e.

$$dY(0)/dy|_{i+1} = dY(0)/dy|_i + k \cdot dY(1)/dy|_i$$
 (where k is a correction factor) and return to step (2). If convergence is not obtained in step (6), a correction (+ or -) must be applied to the eigenvalue and the

iterative scheme reentered at step (2).

If the value $dY(1)/dy$ being tested at step (6) becomes negative, the eigenvalue assumed in step (1) is too large. As the mode increases, the successive eigenvalues become closer together and it became increasingly difficult to pre-select the correct value for λ_n^i . Quite often an estimated value would lead to a solution for an entirely different mode index. The repetitive operation has to be continued until the final boundary condition is satisfied i.e.

$$dY(1)/dy|_1 < \epsilon.$$

It should be pointed out that if initial guesses are used for $dY(0)/dy$ and $Y(0)$ an iteration is performed on λ_n , there is only one curve that satisfies the boundary conditions for $dY(0)/dy$ and $Y(0)$.

Fadden (24) had suggested one way to choose λ_n as follows

$$\lambda_n^{i+1} = \lambda_n^i + k \frac{dY_n}{dy}(0) \quad (4.6)$$

However, the problem he worked with only involved one unknown parameter λ_n .

Since an iterative procedure has been formulated for the problem, the next step is to obtain a computer circuit for implementing this procedure.

4.3 Magnitude and Time scaling of the problem

4.3.1 Magnitude Scaling: On the computer, magnitude scaling is necessary to obtain a meaningful solution since dependent variables are limited to ± 100 volts. Magnitude scale factors are used to relate the voltages from the

computer elements to the dependent variables and its derivatives

Cadem and Smith (24) suggest that the output from high gain amplifiers in an analog computer should be maintained near the reference voltage for the computer but should never exceed it. This procedure leads to the best utilization of the computer capacity. To select scale factors for the dependent variable and its functions, the maximum value of these variables must be estimated. The scale factors for the derivatives given in (25) are

$$k_y = \frac{100}{\dot{Y}_{\max}}, \quad k_{\ddot{y}} = \frac{100}{\ddot{Y}_{\max}}, \quad k_y = \frac{100}{Y_{\max}}$$

The maximum values of \dot{Y}_{\max} , \ddot{Y}_{\max} , Y_{\max} are estimated from the digital-analog simulator for different values of h and λ_n . (Appendix 6). In practice, the scale factors in this work are selected to be somewhat less than $100/Y_{\max}$, $100/\dot{Y}_{\max}$, $100/\ddot{Y}_{\max}$. These values make the best use of the voltage range available and ensure that the amplifier will never be overloaded in normal operation (refer to Appendix 6).

The original differential equation

$$\frac{d^2Y}{dy^2} = \frac{(18y^2-20y+5)}{(1-5y+10y^2-6y^3)} \frac{dY}{dy} - \frac{\lambda_n Y}{(6y^2-4y+1)} \quad (4.1)$$

After magnitude scaling Equation (4.1) becomes :

$$\frac{1}{10} \frac{d^2\{10Y\}}{dy^2} = \frac{1}{10} \frac{(18y^2-20y+5)}{(1-5y+10y^2-6y^3)} \frac{d\{10Y\}}{dy} - \frac{1}{10} \frac{\lambda_n\{10Y\}}{(6y^2-4y+1)} \quad (4.7)$$

Let $\{Y\}$ equal $10Y$.

The variable $\{Y\}$ is the scaled variable (sometimes called the normalized variable); thus,

$$\frac{d^2[Y]}{dy^2} = \frac{(18y^2 - 20y + 5)}{(1 - 5y + 10y^2 - 6y^3)} \frac{d[Y]}{dy} - \frac{\lambda_n[Y]}{(6y^2 - 4y + 1)} \quad (4.8)$$

The solution in the normalized form is the basis for the analog programming procedure. For instance, if the normalized variable $Y(y)$ as shown on Figure 7 is 1.5 volt, the unscaled variable would have a value of 0.15. One unit magnitude for the unscaled variable is equivalent to 10 volts on the computer.

4.3.2 Time scaling: In many problems to assure a feasible operating time, the program must be time-scaled. If the physical problem takes too long to complete, the analog solution must be speeded up. The analog computer integrates with respect to the actual time in seconds. Let τ designate the time measured in computer-seconds to distinguish it from independent variable y . If the problem is not scaled, one second of computer time will be equivalent to one unit of the independent variable. The time scaled factor β (25) is defined as follows:

$$\beta = \frac{\tau}{y} = \frac{\text{computer time, sec}}{\text{independent problem variable}}$$

Since the independent variable, y , varies from zero to one, unscaled time would be too short to record accurately in computer voltages. The recorder pen would tend to lag behind the computer signal. Therefore, the problem must be scaled to run at one-tenth the unscaled rate.

$$\tau = \beta y \quad (4.9)$$

If Beta is greater than unity, the problem is slowed down (25)

$$y = \frac{1}{\beta} \tau = 0.1\tau \quad (4.10)$$

In this case, after 5 sec. of computer time y has a value of 0.5.

A general expression for the n th derivative may be used to relate the derivative terms of the unscaled variable y to the computer time.

$$\frac{d^n f}{d\tau^n} = \frac{1}{\beta^n} \frac{d^n f}{dy^n} \quad (4.11)$$

$$\text{Hence, } \frac{d^2 Y_n}{dy^2} = \beta^2 \frac{d^2 Y_n}{d\tau^2} ; \quad \frac{d^2 Y_n}{dy^2} = 100 \frac{d^2 Y_n}{d\tau^2} \quad (4.12)$$

$$\frac{dY_n}{dy} = \beta \frac{dY_n}{d\tau} , \quad \frac{dY_n}{dY} = 10 \frac{dY}{d\tau} \quad (4.13)$$

When these relations are substituted into the magnitude scaled equation, the following expressions are obtained:

$$\beta^2 \frac{d^2 Y}{d\tau^2} = \frac{18(0.01)\tau^2 - 20(0.1\tau) + 5}{(1 - 0.1\tau)[6(0.01)\tau^2 - (0.4)\tau + 1]} (\beta) \frac{dY}{d\tau} - \frac{\lambda_n Y}{(0.06\tau^2 - 0.4\tau + 1)} \quad (4.14)$$

$$\frac{d^2 Y}{d\tau^2} = \frac{1}{10} \frac{(0.18\tau^2 - 2.0\tau + 5)}{(1 - 0.1\tau)(1 - 0.4\tau + 0.06\tau^2)} \frac{dY}{d\tau} - \frac{(0.01\lambda_n Y)}{(0.06\tau^2 - 0.4\tau + 1)} \quad (4.15)$$

which may be simplified

$$\frac{d^2 Y}{d\tau^2} = 0.1 \frac{(0.18\tau^2 - 2.0\tau + 5)}{(1 - 0.5\tau + 0.1\tau^2 - 0.006\tau^3)} - (0.01) \frac{\lambda_n Y}{(0.06\tau^2 - 0.4\tau + 1)} \frac{dY}{d\tau} \quad (4.16)$$

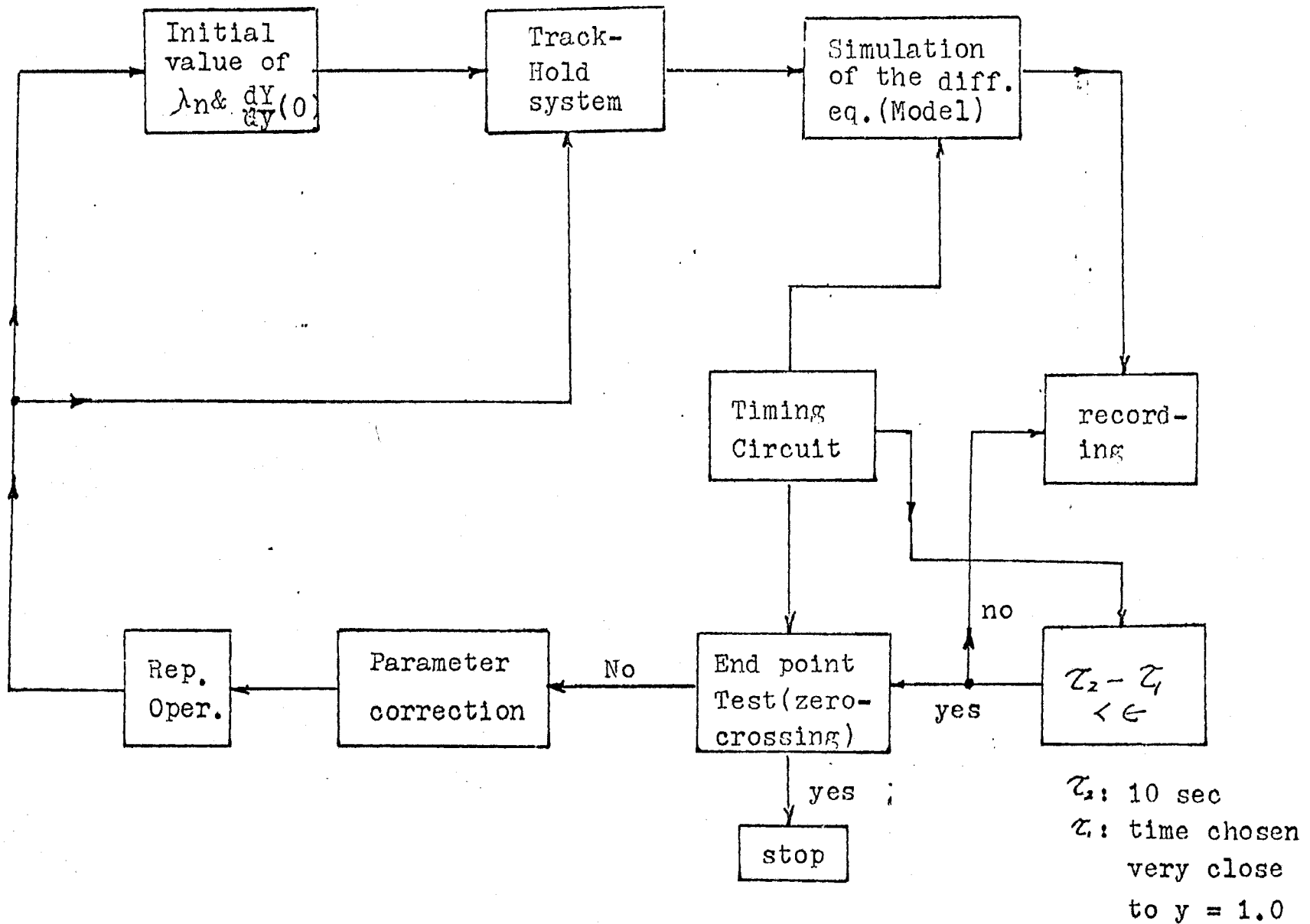


Figure 4: Block diagram for the trial and error procedure on analog computer

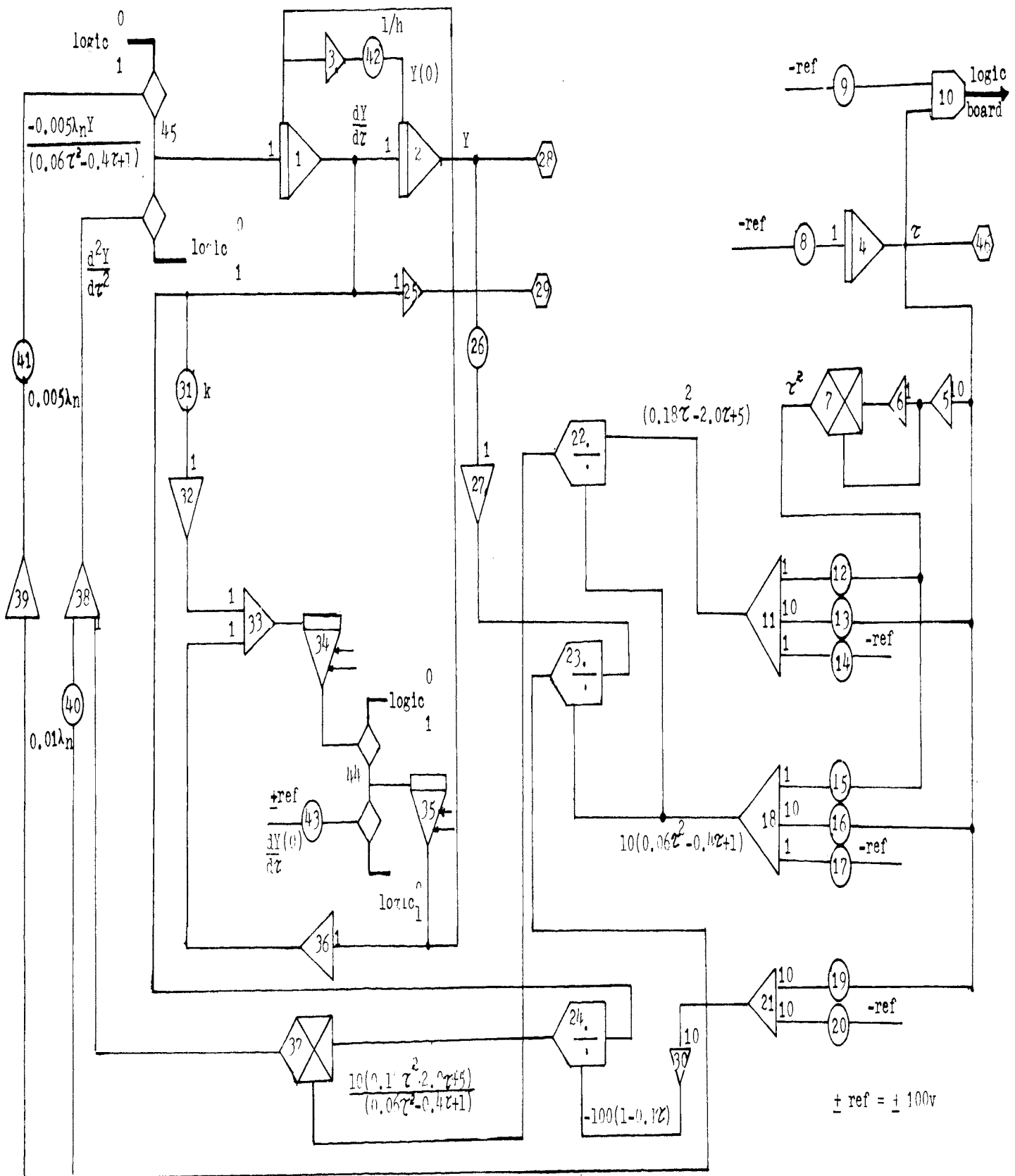


Figure 5: Iterative analog computer setup for Handlos and Baron Model

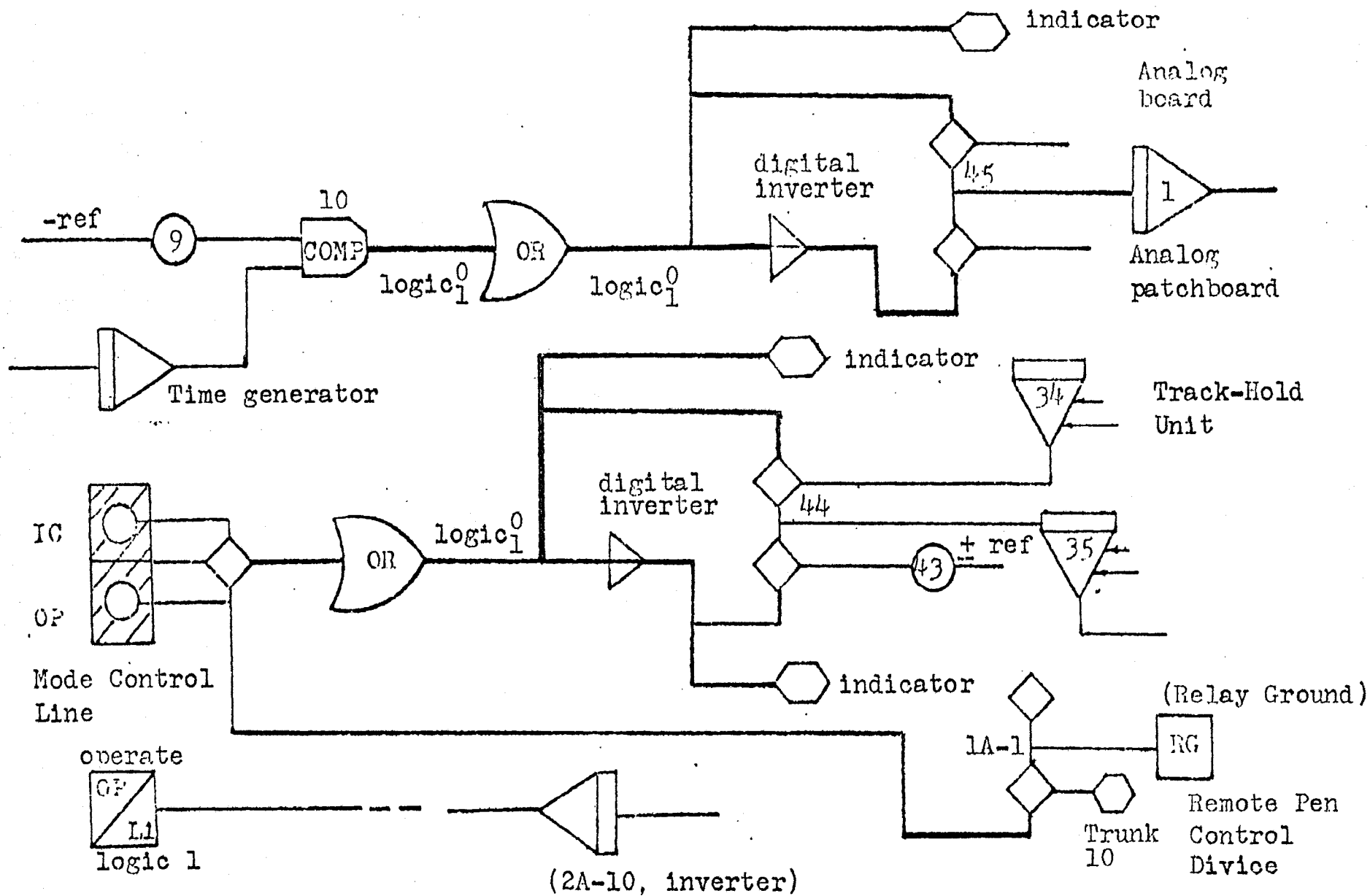


Figure 6: Digital logic setup for Handlos and Baron Model

TABLE 1: STATIC POT SETTINGS AND AMPLIFIER IDENTIFICATION

(I)			
<u>Amp. No.</u>	<u>Amp. Purpose</u>	<u>Amp. Output</u>	<u>Corresponding Patchboard Component</u>
01	Int.	$dY/d\tau$	A-2
02	Int.	Y	A-3
03	High gain or Inverter	Y(0)	A-4
04	Int.	τ	A-1
05	High gain	10τ	B-1
06	Inverter	-10τ	B-2
07	Multiplier (square)	τ^2	A-5
11	+	$(0.18\tau^2 - 2.0\tau + 5)$	B-3
18	+	$10(0.06\tau^2 - 0.4\tau + 1)$	B-4
21	+ ((high gain)	$10(1 - 0.1\tau)$	C-2
22	Divider	$\frac{10(0.18\tau^2 - 2.0\tau + 5)}{(0.06\tau^2 - 0.4\tau + 1)}$	A-7, 8
23	Divider	$\frac{Y}{(0.06\tau^2 - 0.4\tau + 1)}$	B-5, 6
24	Divider	$\frac{1}{(1 - 0.1\tau)} \cdot \frac{dY}{d\tau}$	B-7, 8
25	Inverter	$dY/d\tau$	2A-9
27	Inverter	$-0.1 \cdot Y$	2B-10
30	High gain	$100(1 - 0.1\tau)$	C-3
32	Inverter	$k \cdot dY/d\tau$	2C-10
33	+	$\frac{dY(0)}{d\tau} \Big _i + k \cdot \frac{dY(1)}{d\tau} \Big _i$	D-2
34	Amp. (Track-hold)	"	2C-9
35	Amp.	"	2D-9
36	Inverter	"	2D-10

37	Multiplifier	$\frac{-0.1(0.18\tau^2 - 2.0\tau + 5)}{(1 - 0.1\tau)(0.06\tau^2 - 0.4\tau + 1)}$	D-4
38	+	$d^2Y/d\tau^2$	D-1
39	High gain	$\frac{d^2Y}{d\tau^2} = \frac{-0.01\lambda_n Y}{2(0.06\tau^2 - 0.4\tau + 1)}$	D-3

<u>Pot No.</u>	<u>Numerical Settings</u>	<u>Corresponding Patchboard component</u>
08	0.01	AP-2
09	~ 0.01	AP-3
12	0.18	AP-5
13	0.20	AP-4
14	0.05	AP-6
15	0.60	AP-8
16	0.40	AP-7
17	0.10	AP-8
19	0.10	BP-2
20	0.01	BP-3
26	0.10	BP-1
31	$k < 1.0$	BP-7
40	$0.01\lambda_n$	BP-4
41	$0.005\lambda_n$	BP-5
42	1/h	AP-1
43	Init. Value of Y(0)	BP-8

<u>Component No.</u>	<u>Component Output</u>	<u>Component Identification</u>
10	Logic $\begin{matrix} 0 \\ 1 \end{matrix}$	Comparator
28	$dY/d\tau$	Trunk
29	Y	Trunk
44, 45	Logic $\begin{matrix} 0 \\ 1 \end{matrix}$	Electronic Switch

As shown in equation (4.3) a revised expression must be used when y is close to unity. Equation (4.3) may be time and magnitude scaled to obtain this relationship

$$\frac{d^2y}{d\tau^2} = (0.01) \frac{-0.5\lambda_n y}{(0.06\tau^2 - 0.4\tau + 1)} \quad (4.17)$$

When the independent variable y is close to 1.0 the input to comparator 10 changes sign and makes the control switch connect the opposite direction to Equation (4.17).

It should be emphasized that the boundary conditions of the differential equation have to be magnitude and time scaled before they are programmed on the computer.

4.4 The digital logic

After the equation has been magnitude and time scaled, it can be readily programmed on the analog patchboard, Figure 5. Each input of a high-gain amplifier or integrator has been clearly marked. The settings for pot 8 of the time-generator is 0.01. The values of pots 12, 13 and 14 to generate the time function $(0.18\tau^2 - 2.0\tau + 5)$ are 0.18, 0.20, and 0.05, respectively. Pots 15, 16 and 17 used to generate $(0.06\tau^2 - 0.4\tau + 1)$ are 0.06, 0.40 and 0.10, respectively. Pots 19 and 20 to generate $(1 - 0.1\tau)$ are 0.10 and 0.01, respectively. Pots 40 and 41 represent $0.01 \lambda_n$ and $0.005 \lambda_n$, respectively. The value for $1/h$ is set on pot 42. The settings of pot 9 are selected very close to 0.01 as a basis for switching near the end of the integration period where y approaches unity.

The iterative procedures formulated for the problem are performed by components of the digital logic. The symbols

for the elements of the computer program are described in Appendix 1. The logic signal generated by the comparator is used to control the operating modes for the analog computer as well as selected electronic switches in its program. A track-hold system is developed for use in the iterative procedures. When the computer is placed in Reset mode, a binary logic 1 signal is applied to the IC control line. Concurrently it sets amplifier 35 in the track-hold system into track mode and puts electronic switch 2A2 in the DOWN position. At this moment, amplifier 35 tracks the initial approximation of $dY(0)/dy$ which is supplied to the system thru switch 2A2. As the computer is turned to the OP(or "REPOP")*, a binary logic 0 signal is applied to the IC control line and amplifier 34 tracks the error $k \left[\frac{dY_n}{dy} - dY(0)/dy \right]$. Also, the binary logic 1 signal from the OR-Gate on the logic patchboard makes the electronic switch 2A2 close whenever the computer is in the REPOP mode.

Near the end of the programmed operate period, the sign change of the input to the comparator switches the binary logic signal 1 from the OR-Gate into its complementary logic signal 0. Therefore, the switch 2A1 changes from the DOWN position to the UP position and switches the solution to the equation derived from L'Hospital's Rule. When the computer returns to IC(REPOP) after one integration period, amplifier

*REPOP is a term used to refer to repetitive operation on the analog computer.

34 holds the last value tracked by amplifier 35 $\left[k \frac{dY(1)}{dy} \Big|_n - \frac{dY(0)}{dy} \Big|_n \right]$. The repetitive operation is continued until a value of $\frac{dY(0)}{dy}$ is obtained for which $\frac{dY(1)}{dy} = 0$. A block diagram of the computer program is shown in Figure 4. The analog and digital logic details are contained in Figures 5 and 6. The timing circuit made up of elements 4, 8, 9 and 10 is used to control the reset (IC) and operate period.

Table 2: Binary logic signal on the control line for different mode control

Control line	MODE		
	Reset	Hold	OP
IC	1	0	0
OP	0	0	1

Table 3: Digital logic for the Track-Hold system

RS	REPOP		
	Element	OP	RS
RS	A-1(dY/dy)	OP	RS
RS	A-2(Y)	OP	RS
H	2C9(34)	T	H
T	2D9(35)	H	T
DN	Switch 2A-2	UP	UP

4.5 PACTOLUS simulation

The development of MIDAS (modified integration DAS) from DAS (digital analog simulator) is based on a fourth-order Runge-Kutta Merson integration method with an automatic

stepsize adjustment to make it reliable and accurate. PACTOLUS, developed by Brennen (26) of IBM Research Laboratory, is similar to the MIDAS system and uses a block-oriented interpretive digital-analog simulator with a second-order Runge-Kutta integration method.

Mass transfer in droplets can also be simulated on a digital computer by using the program, PACTOLUS. In addition to the use of such elements as summers, integrators, multipliers, etc., a simulated relay switch also is used to switch the problem to the equation derived by the use of L'Hospital's Rule to eliminate the undetermined term when y approaches unity.

A plot of the results from the digital computer calculation can be compared with a plot of the results from the analog computer in Figures 11, 12, 13 and 14. The main difference between the programming on the analog computer and PACTOLUS is that the signs of the output from the summers and integrators in PACTOLUS are not changed. The PACTOLUS simulation is presented by a PACTOLUS flow diagram in Appendix 7. The simulation on PACTOLUS follows the arrangement of the circuit of the analog computer program. Programs with and without time scaling are set up to check the difference. All the symbols for the flow diagram are shown in Reference 20.

V. RESULTS AND DISCUSSION

5.1 Computer results of eigenvalues and eigenfunctions

Iterative analog computer results of eigenvalues λ_n and eigenfunctions $Y_n(0)$ are shown in Appendix 10. Values of B_n are calculated from the following equation:

$$B_n = \frac{1}{\lambda_n} \frac{dY_n(0)}{dy} \quad n = 1 \dots 4 \quad (5.1)$$

For instance, when $h = 10.0$, $\lambda_2 = 18.90$, and $dY(0)/dy = -3.04$. Hence, B_n is obtained from Equation (5.1) and has the value -0.1608 .

The calculated eigenvalues and series constants B_n for various values of the modified continuous phase mass transfer coefficient, h , obtained from the different schemes on the analog computer and digital-analog simulator are summarized in tables 4, 5 and 6. Only the first four eigenvalues and series constants are calculated, in part because, for $n > 5$, the additional terms have an almost negligible effect on the concentration profile (except at very short contact times).

The solutions using the different schemes mentioned above must be compared.

The digital-analog simulator print-out shows that the results with or without time and magnitude scaling are very close.

The results plotted from the X-Y recorder on the analog computer are shown on Figures 7 to 10. The results from the digital-analog simulator are shown on Figures 11 to 15. These figures are based on a constant n . As n increases, the value

of λ_n increase rapidly.

The results are also expressed in terms of the fraction of the solute extracted from the droplet, E_m , as a function of dimensionless time, bt . See Figures 15, 16, and 17.

Upon comparison of the first four eigenvalues λ_1 , λ_2 , λ_3 and λ_4 for different values of h used by Wellek-Skelland (9), (except when $h = 40$), it is apparent that the three eigenvalues λ_2 , λ_3 and λ_4 increase slowly for the low continuous phase resistance, h , especially for $h < 0.1$; but the first eigenvalue increases rapidly with h . When h is larger than 0.1, all four eigenvalues increase rapidly as a function of h . After reaching 10, the first three eigenvalues λ_1 , λ_2 and λ_3 remain approximately constant or increase very slowly. For very high continuous phase resistances, all the eigenvalues seem to remain nearly constant. This is consistent with the physical situation because as the modified continuous phase resistance h increases, the resistance to mass transfer in the continuous phase becomes less. As h approaches infinite, ($k_c \rightarrow \infty$), all the resistance to mass transfer will be in the droplet.

The results of this work using the iterative analog computer have been compared with Patel's results (30) using the Runge-Kutta and Hamming's numerical approach to solve this problem; the four eigenvalues calculated by the two methods on iterative analog computer and digital computer, respectively, agree with each other within about 5%. But the results obtained for the higher eigenvalues λ_3 , λ_4 on a conventional

analog computer differ by 10% with Patel's results. Rogers and Connolly (29) state that this difference arises, in fact, because at low eigenvalues which correspond to the low-frequency normal mode, the results can be found quite accurately since it depends simply on potentiometer settings. But the higher frequency normal-modes require high gain in the computer circuit, which causes less satisfactory operation.

Digital-analog simulator results coincide with results of Patel's numerical solution within about 3%.

The possible inaccurate part of this work is that for very small values of h , the noise begins to affect the low voltage of the initial approximation of $dY(0)/dy$. Corcos, Howe, Rauch and Sellars (23) indicate that the values of the recorded eigenfunctions never have the same degree of accuracy as the eigenvalues. Because of the possible inaccurate values of the eigenfunctions $Y(0)$, the coefficient B_n calculated may also be slightly inaccurate.

The coefficient B_1 is positive for all values of h . All values of B_2 are negative. B_3 is negative for $h > 10$ and positive for h less than 10. The values of B_4 are always negative.

5.2 Solution in terms of fraction of solute extracted

The complete solution for the fraction extracted can be computed from the following relation:

$$E_m = 1 - 2 \sum_{n=1}^{\infty} B_n^2 \exp(-b\lambda_n t) \quad (5.2)$$

The values B_n and λ_n obtained by three different approaches

Table 4: Eigenvalues and Coefficients for Handlos and Baron Model
 (by trial and error on an iterative analog computer)

h	λ_1	λ_2	λ_3	λ_4	B ₁	B ₂	B ₃	B ₄
0.0010	0.0018	6.630	31.20	354.0	0.4130	-0.799(10) ⁻⁴	0.154(10) ⁻⁴	-0.762(10) ⁻⁶
0.0020	0.0039	6.600	31.20	353.0	0.5436	-0.162(10) ⁻³	0.250(10) ⁻⁴	-0.161(10) ⁻⁵
0.0100	0.0185	6.790	31.20	353.0	0.4214	-0.788(10) ⁻³	0.146(10) ⁻³	-0.850(10) ⁻⁵
0.0500	0.0950	6.810	31.20	355.0	0.4895	-0.418(10) ⁻²	0.695(10) ⁻³	-0.415(10) ⁻⁴
0.1000	0.2000	6.900	31.20	352.0	0.4375	-0.884(10) ⁻²	0.140(10) ⁻²	-0.852(10) ⁻⁴
0.5000	0.7900	8.010	32.90	354.0	0.3987	-0.399(10) ⁻¹	0.699(10) ⁻²	-0.452(10) ⁻³
1.0000	1.2800	9.300	36.20	355.0	0.3477	-0.731(10) ⁻¹	0.134(10) ⁻¹	-0.794(10) ⁻³
2.5000	1.9900	12.40	35.60	365.0	0.2804	-0.1153	0.351(10) ⁻¹	-0.194(10) ⁻²
5.0000	2.3600	15.60	41.40	369.0	0.2542	-0.1288	0.492(10) ⁻¹	-0.376(10) ⁻²
7.0000	2.5100	17.10	45.30	373.0	0.2789	-0.1316	0.476(10) ⁻¹	-0.517(10) ⁻²
10.000	2.5900	18.90	87.00	376.0	0.2317	-0.1608	-0.212(10) ⁻¹	-0.697(10) ⁻²
25.000	2.7300	18.90	90.90	393.0	0.1905	-0.1217	-0.429(10) ⁻¹	-0.119(10) ⁻¹
30.000	2.7500	18.90	92.00	396.0	0.1964	-0.1333	-0.394(10) ⁻¹	-0.128(10) ⁻¹
40.000	2.7700	19.00	96.90	402.0	0.2076	-0.1247	-0.388(10) ⁻¹	-0.139(10) ⁻¹
50.000	2.7800	19.10	95.10	404.0	0.2032	-0.1238	-0.394(10) ⁻¹	-0.144(10) ⁻¹
70.000	2.7850*	19.15*	96.60	411.0	0.2011	-0.1227	-0.375(10) ⁻¹	-0.143(10) ⁻¹
100.00	2.8000	19.30	96.80	415.8	0.2004	-0.1166	-0.386(10) ⁻¹	-0.145(10) ⁻¹
250.00	2.8200	20.20	97.10	416.8	0.1993	-0.1337	-0.395(10) ⁻¹	-0.145(10) ⁻¹
500.00	2.8200	20.80	97.20	417.0	0.1986	-0.1154	-0.388(10) ⁻¹	-0.146(10) ⁻¹
700.00	2.8200	20.90	97.80	418.5	0.2021	-0.1077	-0.387(10) ⁻¹	-0.145(10) ⁻¹
1000.0	2.8200	22.30	98.00	418.5	0.2021	-0.1108	-0.384(10) ⁻¹	-0.144(10) ⁻¹
	2.8200	22.40	98.10	419.0	0.2021	-0.982(10) ⁻¹	-0.387(10) ⁻¹	-0.145(10) ⁻¹

* Approximate values due to the 3-digits of the null dial on the computer.

Table: 5: Eigenvalues and Coefficients for Handlos and Baron Model
 (by trial and error on a conventional analog computer)

h	λ_1	λ_2	λ_3	λ_4	B_1	B_2	B_3	B_4
0.0010	0.0018	6.30	35.40	394.0	0.522	-0.870(10) ⁻⁴	0.114(10) ⁻⁴	-0.731(10) ⁻⁶
0.0020	0.0036	6.35	34.90	394.0	0.519	-0.173(10) ⁻³	0.227(10) ⁻⁴	-0.146(10) ⁻⁵
0.0100	0.0200	6.40	35.30	394.0	0.472	-0.867(10) ⁻³	0.111(10) ⁻³	-0.733(10) ⁻⁵
0.0500	0.0963	6.40	35.10	394.0	0.493	-0.462(10) ⁻²	0.527(10) ⁻³	-0.367(10) ⁻⁴
0.1000	0.1870	6.45	35.20	394.0	0.476	-0.898(10) ⁻²	0.107(10) ⁻²	-0.711(10) ⁻⁴
0.5000	0.7950	7.45	35.00	394.5	0.347	-0.416(10) ⁻¹	0.536(10) ⁻²	-0.321(10) ⁻³
1.0000	1.2900	8.50	35.70	395.0	0.287	-0.800(10) ⁻¹	0.108(10) ⁻¹	-0.696(10) ⁻³
2.5000	1.9850	12.0	37.60	397.0	0.239	-0.1500	0.239(10) ⁻¹	-0.166(10) ⁻²
5.0000	2.3600	15.5	41.60	403.0	0.201	-0.1677	0.420(10) ⁻¹	-0.333(10) ⁻²
7.0000	2.4800	17.0	43.70	404.0	0.215	-0.1610	0.494(10) ⁻¹	-0.460(10) ⁻²
10.000	2.5600	17.4	87.50	409.0	0.180	-0.1736	-0.263(10) ⁻¹	-0.648(10) ⁻²
25.000	2.7100	19.3	93.30	420.5	0.184	-0.1580	-0.356(10) ⁻¹	-0.982(10) ⁻²
30.000	2.7300	19.5	94.90	425.0	0.186	-0.1477	-0.360(10) ⁻¹	-0.107(10) ⁻¹
40.000	2.7500	19.8	96.70	428.0	0.189	-0.1495	-0.372(10) ⁻¹	-0.114(10) ⁻¹
50.000	2.7600	19.8	97.50	432.0	0.190	-0.1461	-0.369(10) ⁻¹	-0.112(10) ⁻¹
70.000	2.7750	20.1	97.60	439.0	0.189	-0.1393	-0.365(10) ⁻¹	-0.121(10) ⁻¹
100.00	2.8100	20.2	101.0	451.0	0.187	-0.1348	-0.322(10) ⁻¹	-0.132(10) ⁻¹
250.00	2.8250	20.6	101.5	451.0	0.188	-0.1341	-0.327(10) ⁻¹	-0.139(10) ⁻¹
500.00	2.8250	20.7	101.5	451.0	0.198	-0.1342	-0.337(10) ⁻¹	-0.139(10) ⁻¹
700.00	2.8450	20.7	101.5	452.0	0.204	-0.1343	-0.327(10) ⁻¹	-0.136(10) ⁻¹
1000.0	2.8500	20.8	102.0	452.0	0.205	-0.1341	-0.329(10) ⁻¹	-0.136(10) ⁻¹
	2.8600	20.8	102.0	452.0	0.206	-0.1356	-0.332(10) ⁻¹	-0.138(10) ⁻¹

Table 6: Eigenvalues and Coefficients for Handlcs and Baron Model
 (by trial and error on a digital-analog simulator)

h	λ_1	λ_2	λ_3	λ_4	B_1	B_2	B_3	B_4
0.0010	0.0020	6.80	31.30	363.0	0.500	-0.822(10) ⁻⁴	0.153(10) ⁻⁴	-0.826(10) ⁻⁶
0.0020	0.0040	6.80	31.30	363.0	0.500	-0.179(10) ⁻³	0.306(10) ⁻⁴	-0.165(10) ⁻⁵
0.0100	0.0180	6.86	31.30	363.6	0.505	-0.893(10) ⁻³	0.153(10) ⁻³	-0.819(10) ⁻⁵
0.0500	0.0940	6.92	31.40	364.2	0.506	-0.446(10) ⁻²	0.764(10) ⁻³	-0.409(10) ⁻⁴
0.1000	0.1860	7.02	31.40	364.4	0.491	-0.891(10) ⁻²	0.153(10) ⁻²	-0.816(10) ⁻⁴
0.5000	0.7800	7.90	32.20	365.6	0.423	-0.421(10) ⁻¹	0.757(10) ⁻²	-0.407(10) ⁻³
1.0000	1.2690	9.04	33.12	365.3	0.372	-0.753(10) ⁻¹	0.147(10) ⁻¹	-0.816(10) ⁻²
2.5000	1.9600	12.06	35.80	367.0	0.307	-0.12380	0.545(10) ⁻¹	-0.202(10) ⁻²
5.0000	2.3000	14.96	39.20	372.6	0.278	-0.13840	0.524(10) ⁻¹	-0.392(10) ⁻²
7.0000	2.4600	16.30	41.60	376.4	0.264	-0.13520	0.593(10) ⁻¹	-0.531(10) ⁻²
10.000	2.5600	17.40	83.90	380.0	0.256	-0.13330	-0.142(10) ⁻¹	-0.714(10) ⁻²
25.000	2.7000	19.22	90.20	394.6	0.244	-0.12110	-0.415(10) ⁻¹	-0.120(10) ⁻¹
30.000	2.7200	19.35	91.40	399.0	0.243	-0.11990	-0.414(10) ⁻¹	-0.128(10) ⁻¹
50.000	2.7600	19.80	93.40	406.0	0.239	-0.11700	-0.413(10) ⁻¹	-0.138(10) ⁻¹
70.000	2.7700	20.20	94.60	410.0	0.238	-0.11410	-0.408(10) ⁻¹	-0.141(10) ⁻¹
100.00	2.7800	20.36	96.30	418.4	0.238	-0.11200	-0.399(10) ⁻¹	-0.141(10) ⁻¹
250.00	2.7900	20.38	96.40	418.5	0.238	-0.11190	-0.402(10) ⁻¹	-0.143(10) ⁻¹
500.00	2.8000	20.40	96.64	418.6	0.236	-0.11120	-0.401(10) ⁻¹	-0.143(10) ⁻¹
700.00	2.8060	20.42	97.70	420.0	0.235	-0.11120	-0.401(10) ⁻¹	-0.142(10) ⁻¹
1000.0	2.8070	20.42	96.70	420.0	0.235	-0.11120	-0.400(10) ⁻¹	-0.142(10) ⁻¹
	2.8100	20.50	96.92	420.4	0.235	-0.11120	-0.399(10) ⁻¹	-0.142(10) ⁻¹

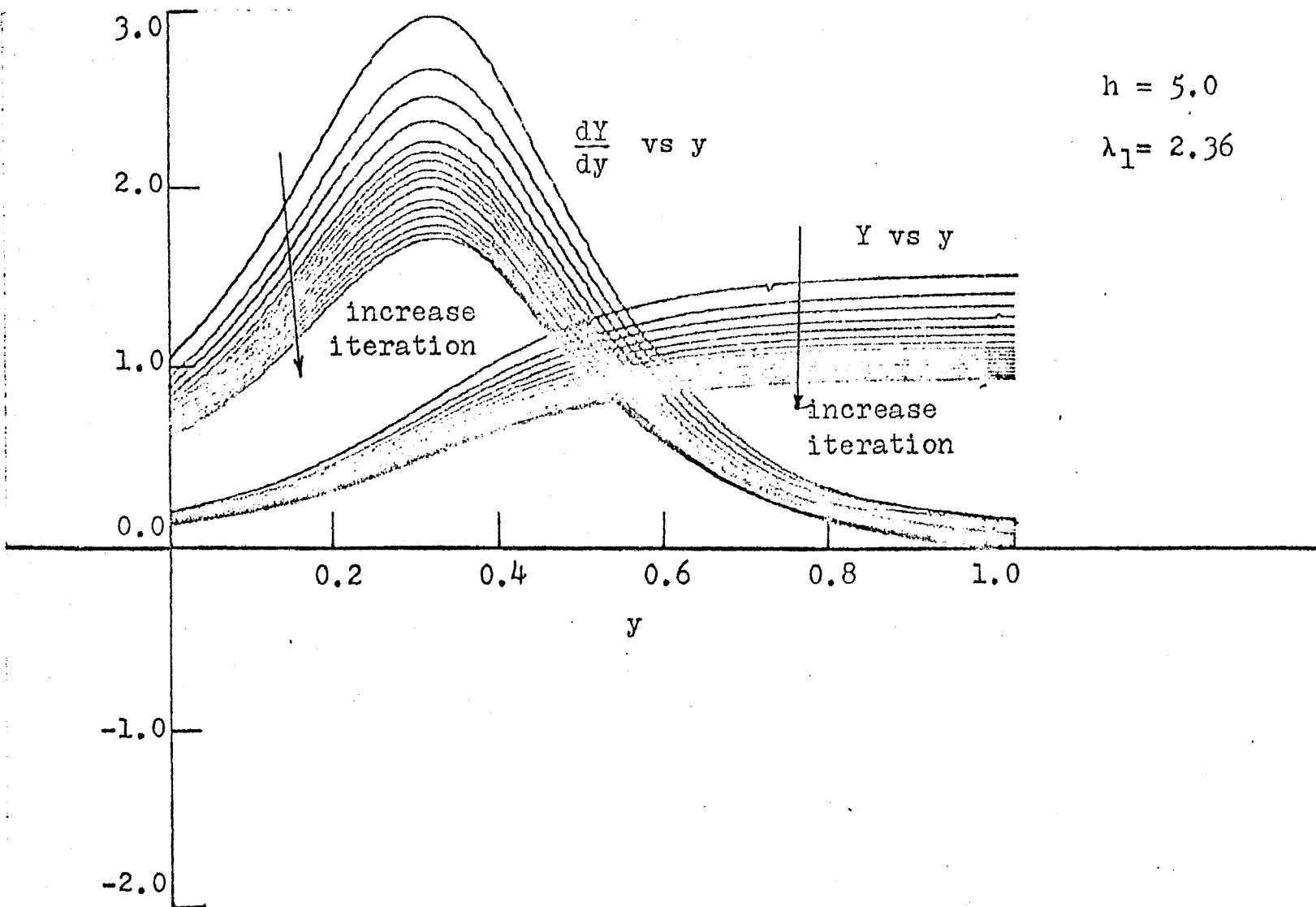


Figure 7: Solution of Handlos and Baron Model on an iterative analog computer

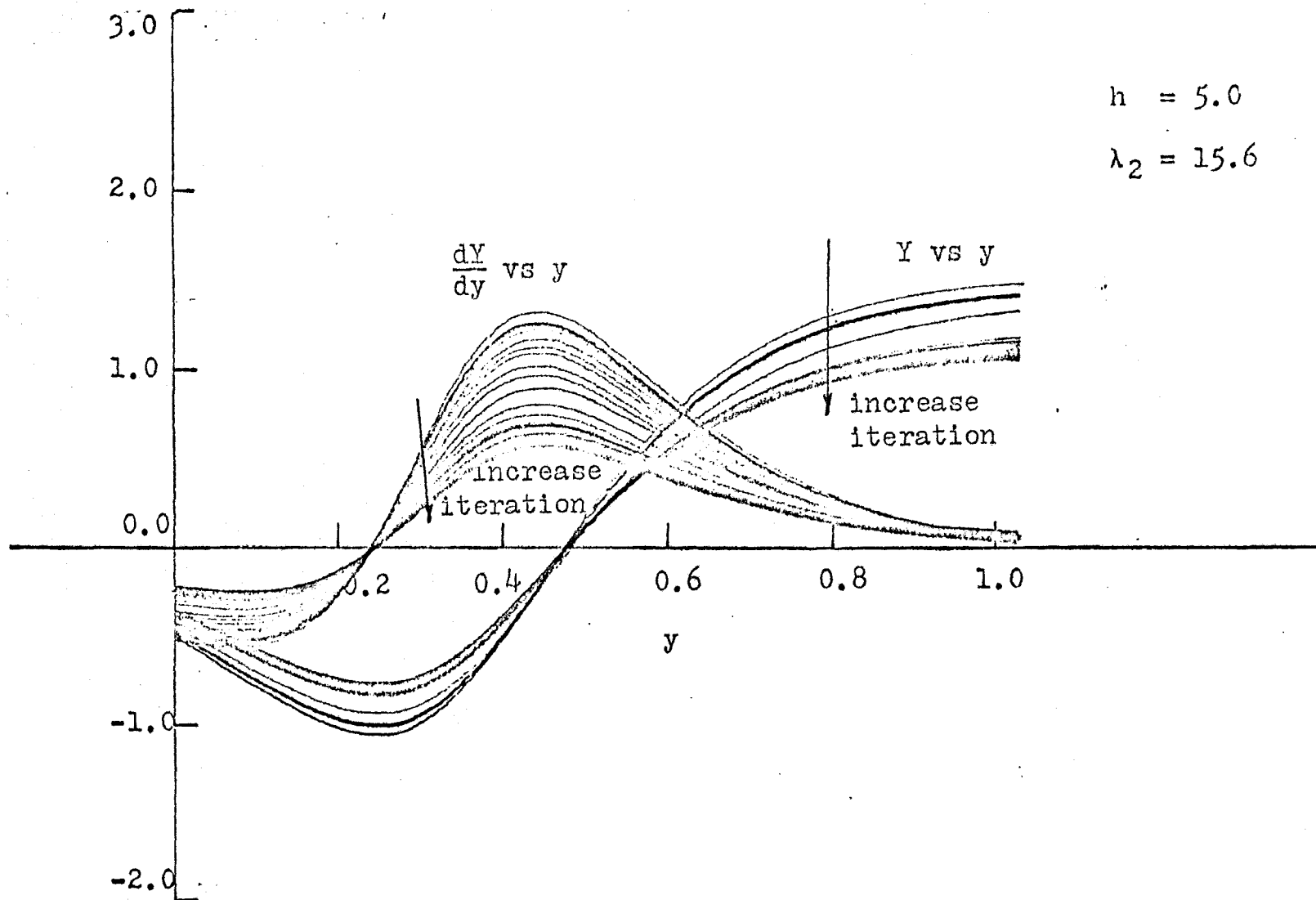


Figure 8: Solution of Handlos and Baron Model on an iterative analog computer

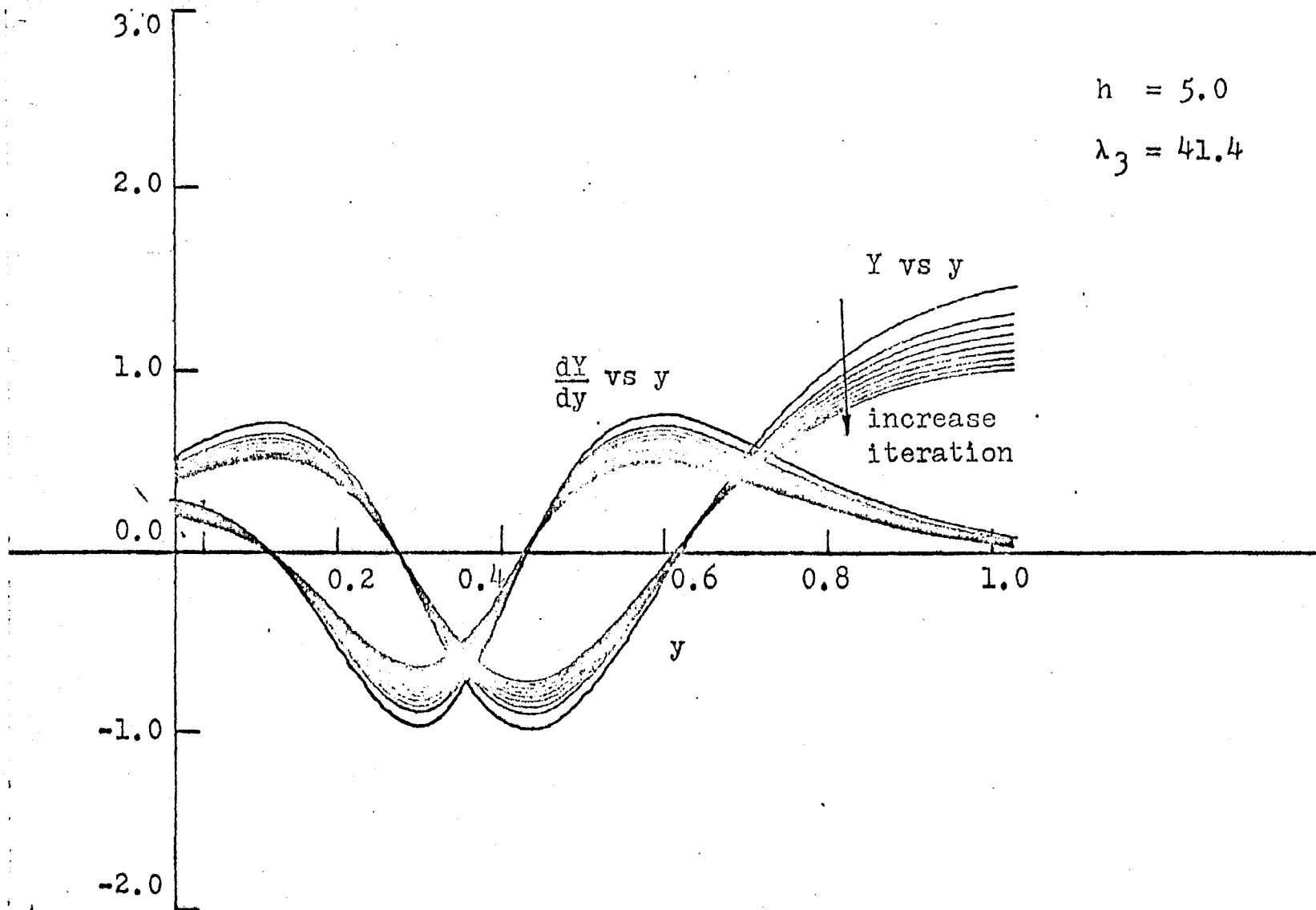


Figure 9: Solution of Handlos and Baron Model
on an iterative analog computer

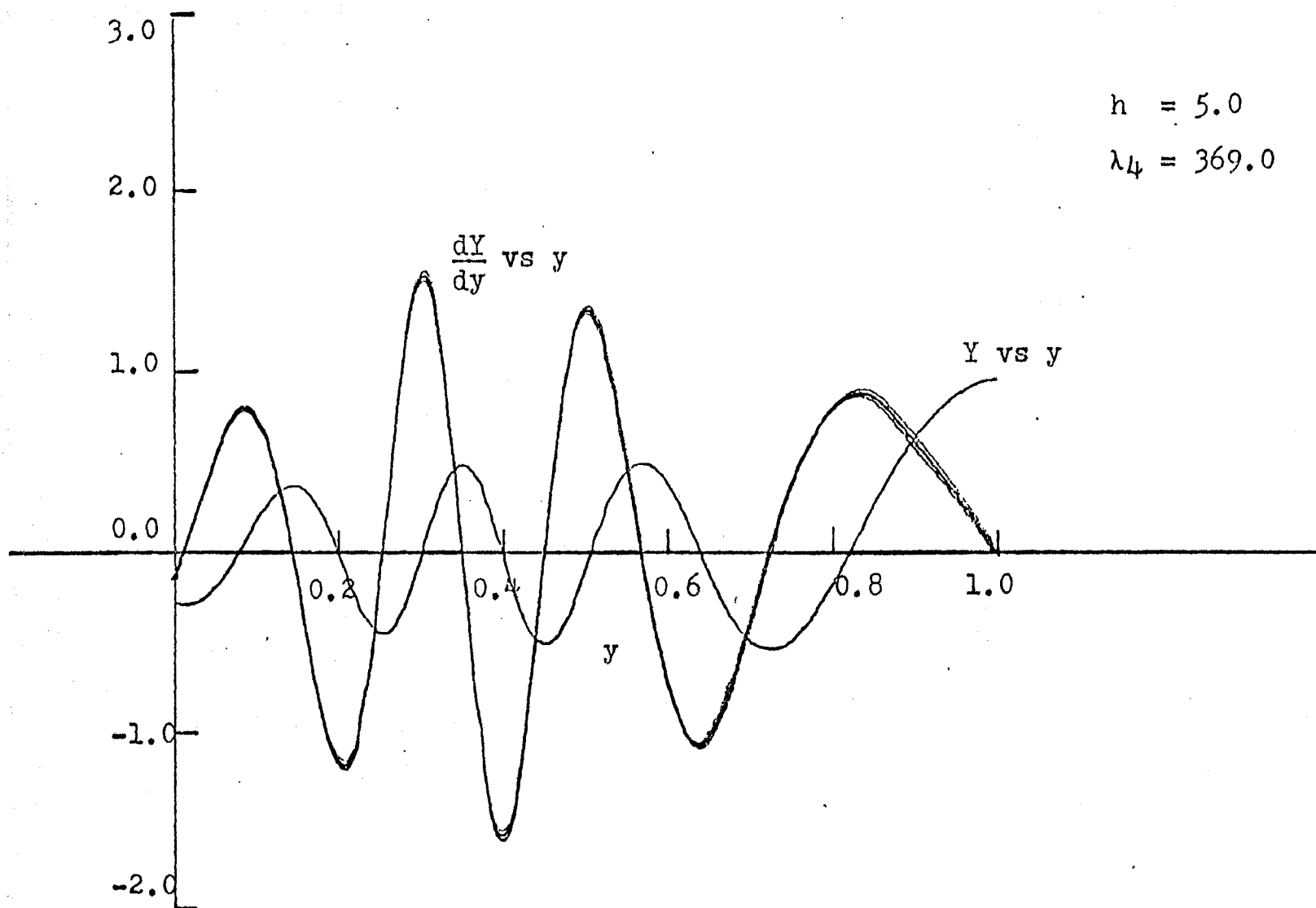


Figure 10: Solution of Handlos and Baron Model
on an iterative analog computer

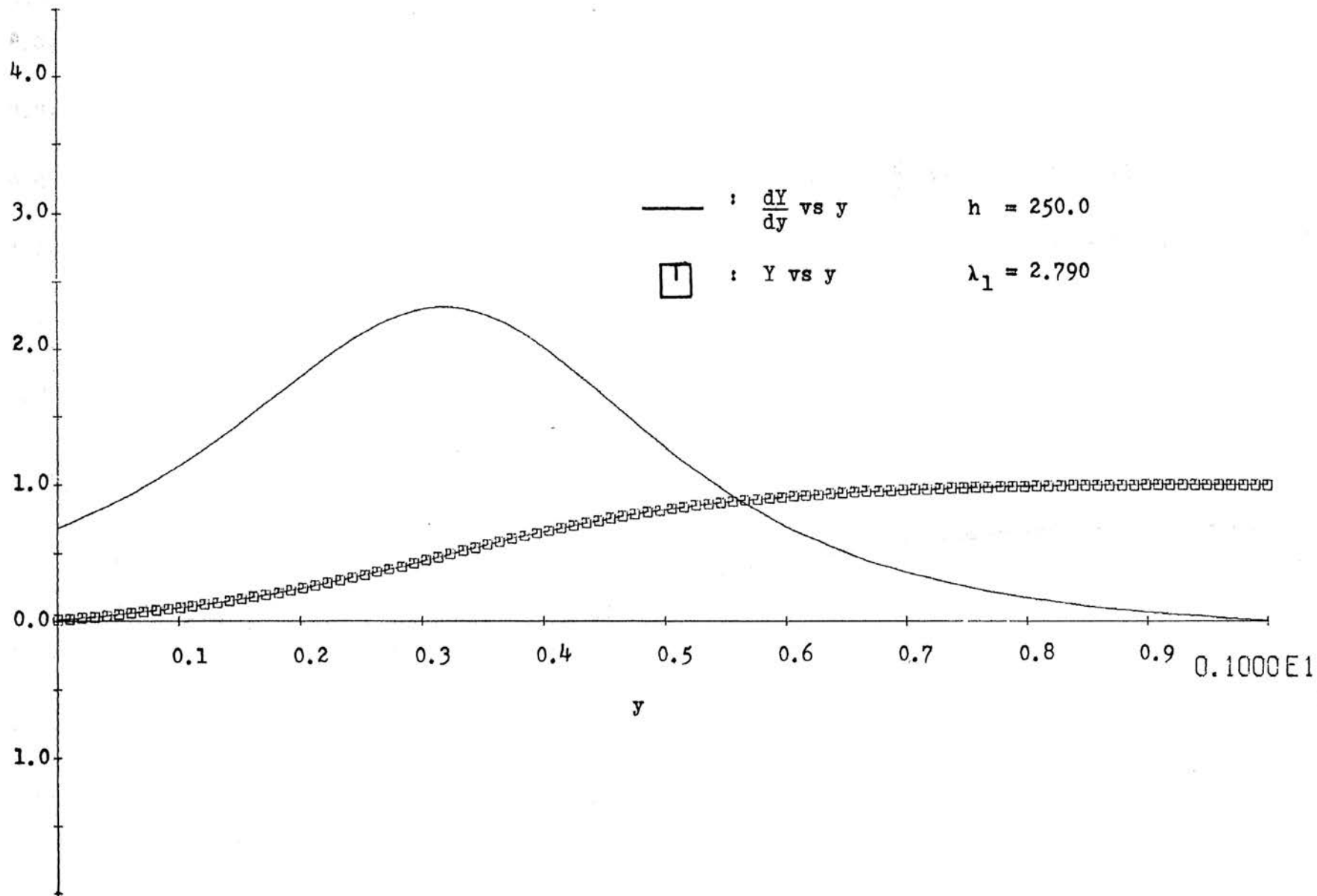


Figure 11: Solution of Handlos and Baron Model on digital-analog simulator

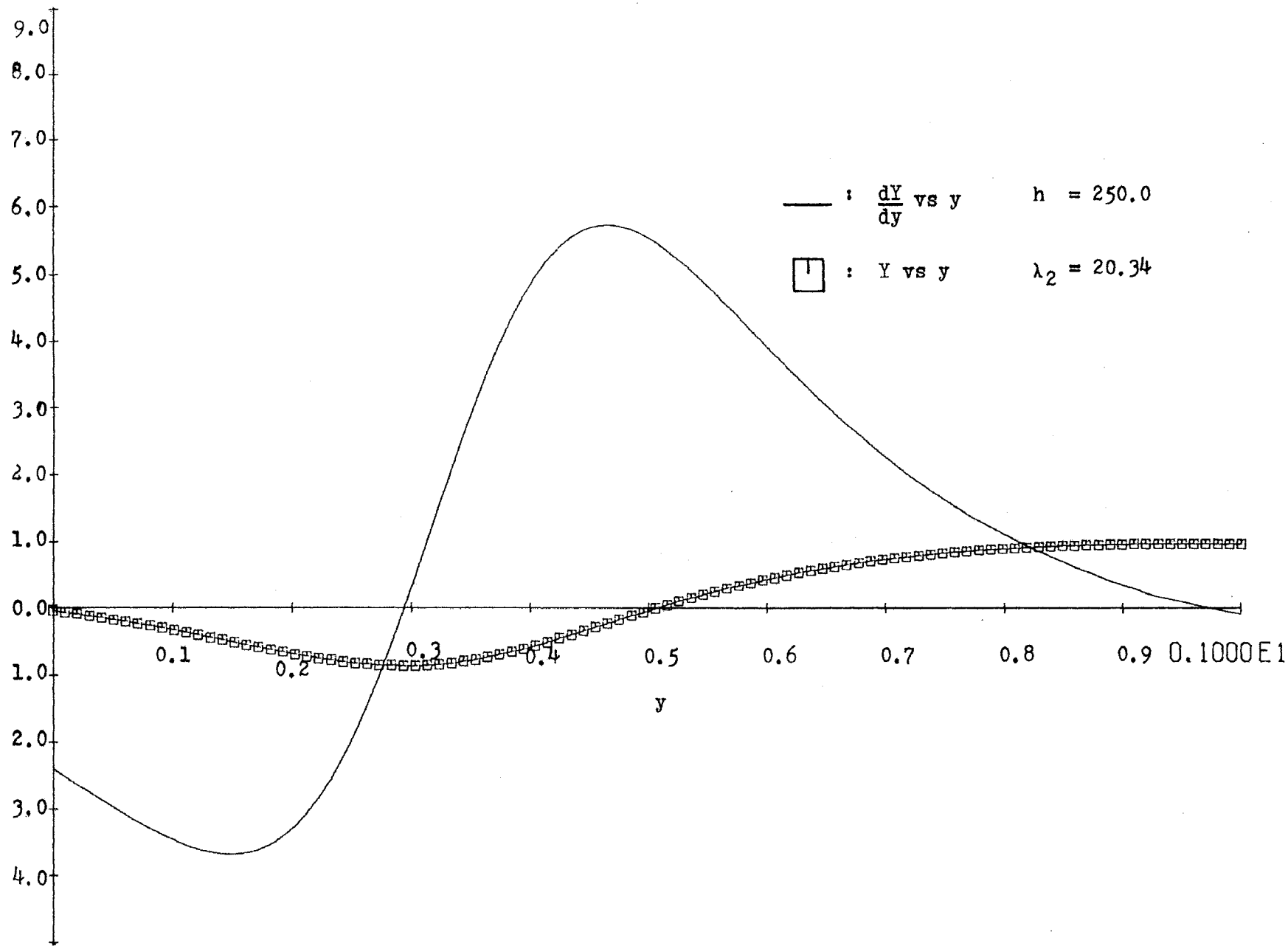


Figure 12: Solution of Handlos and Baron Model on digital-analog simulator

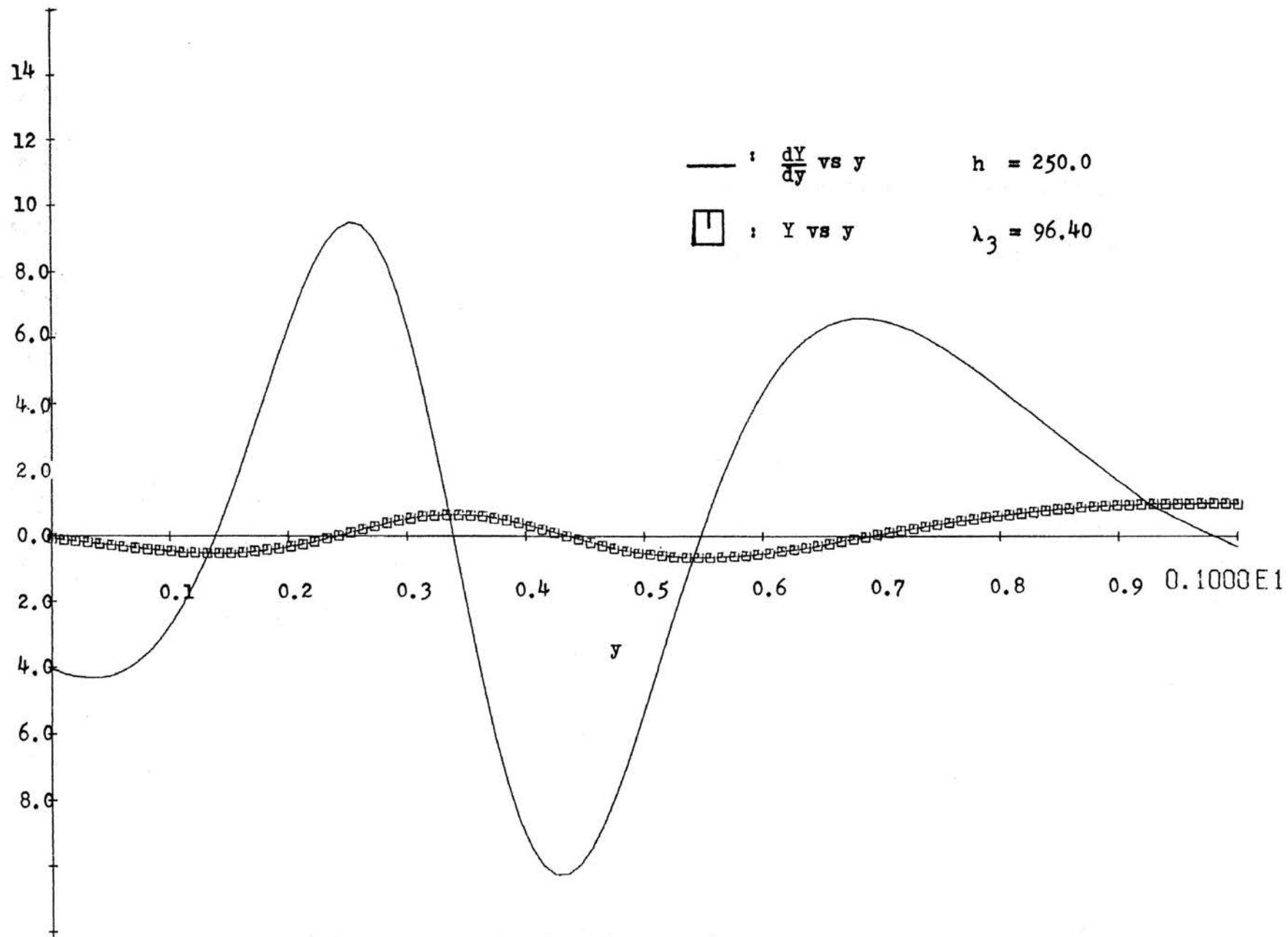


Figure 13: Solution of Handlos and Baron Model on digital-analog simulator

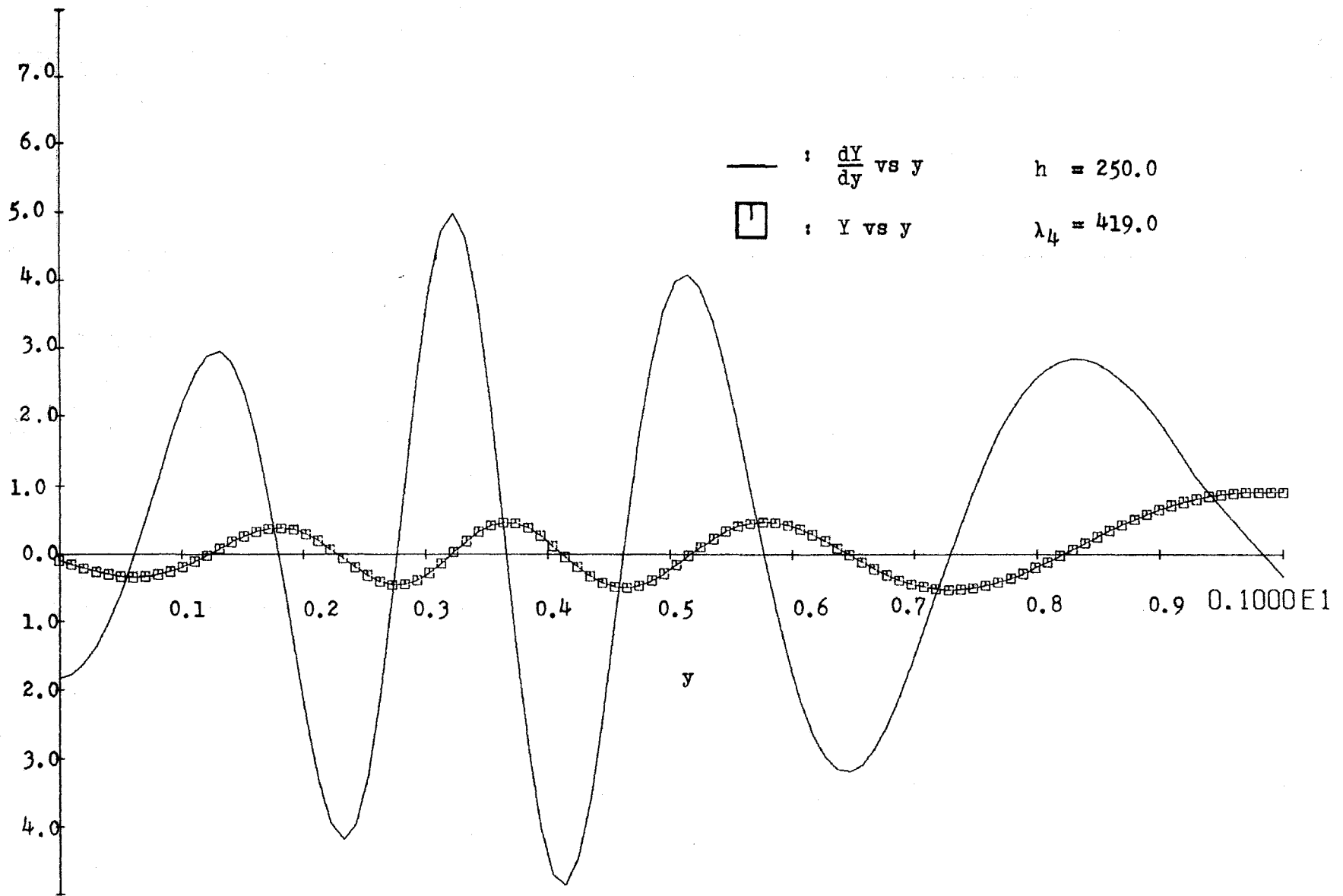


Figure 14: Solution of Handlos and Baron Model on digital-analog simulator

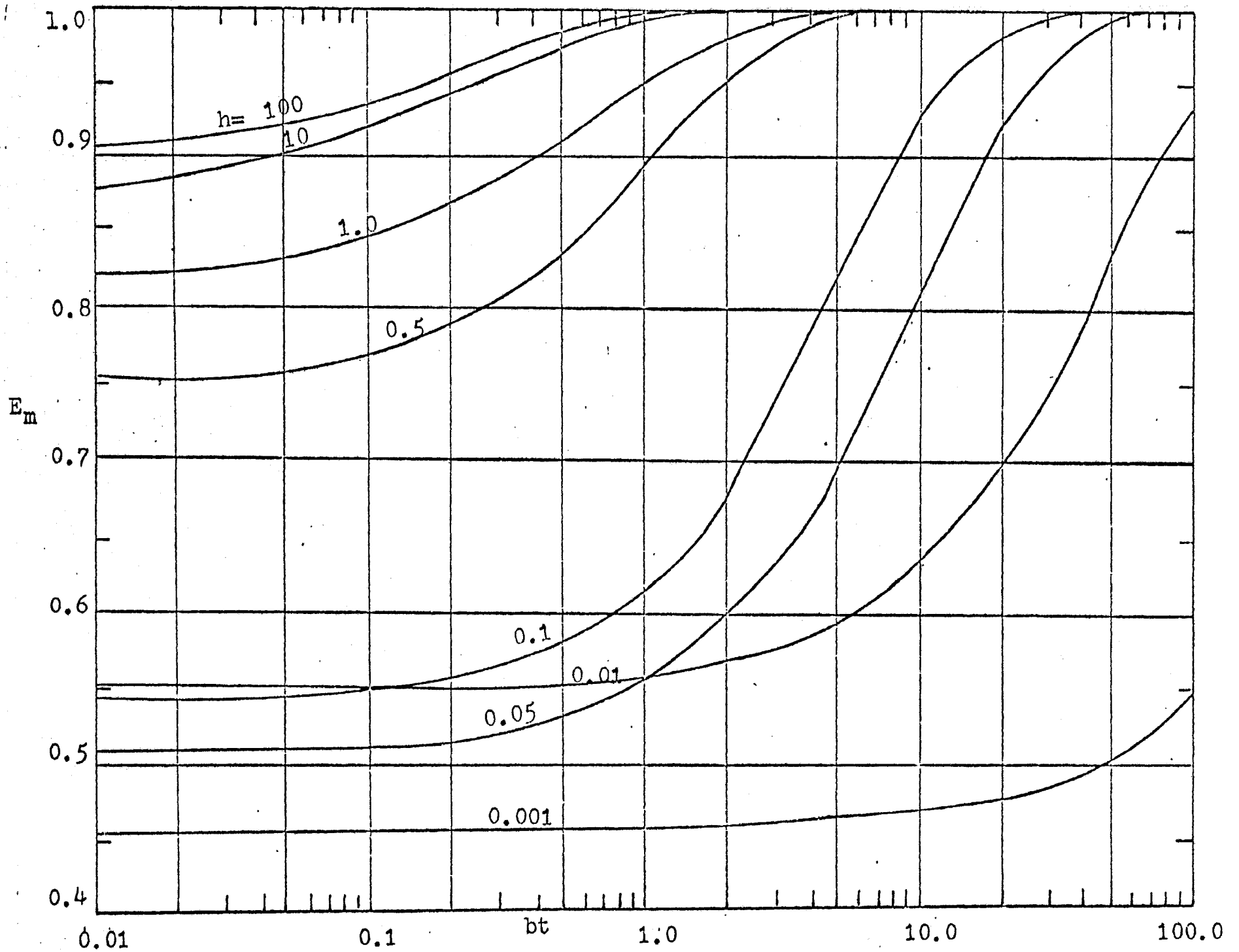


Figure 15: Fraction extracted versus dimensionless time(Analog computer)

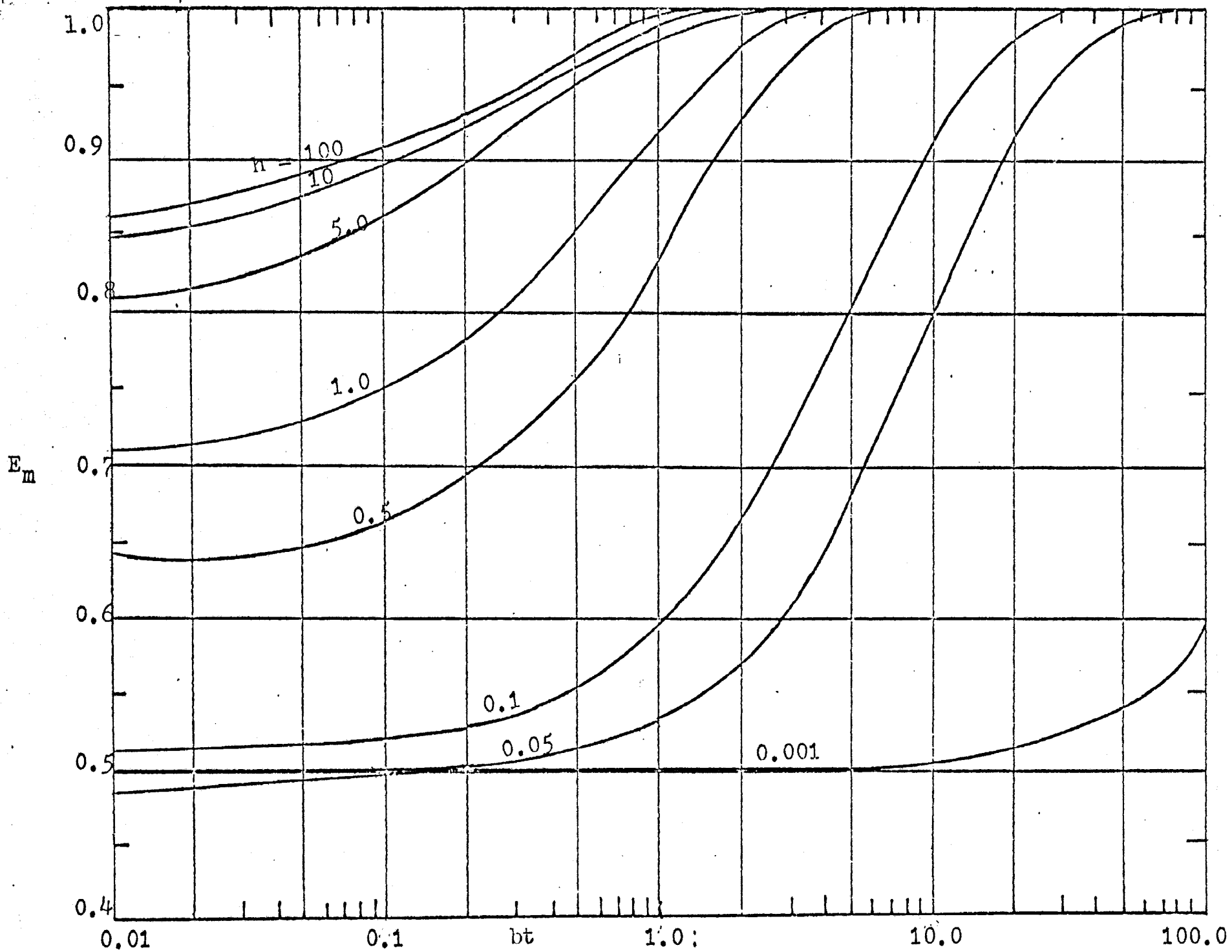


Figure 16: Fraction extracted versus dimensionless time(PACTOLUS)

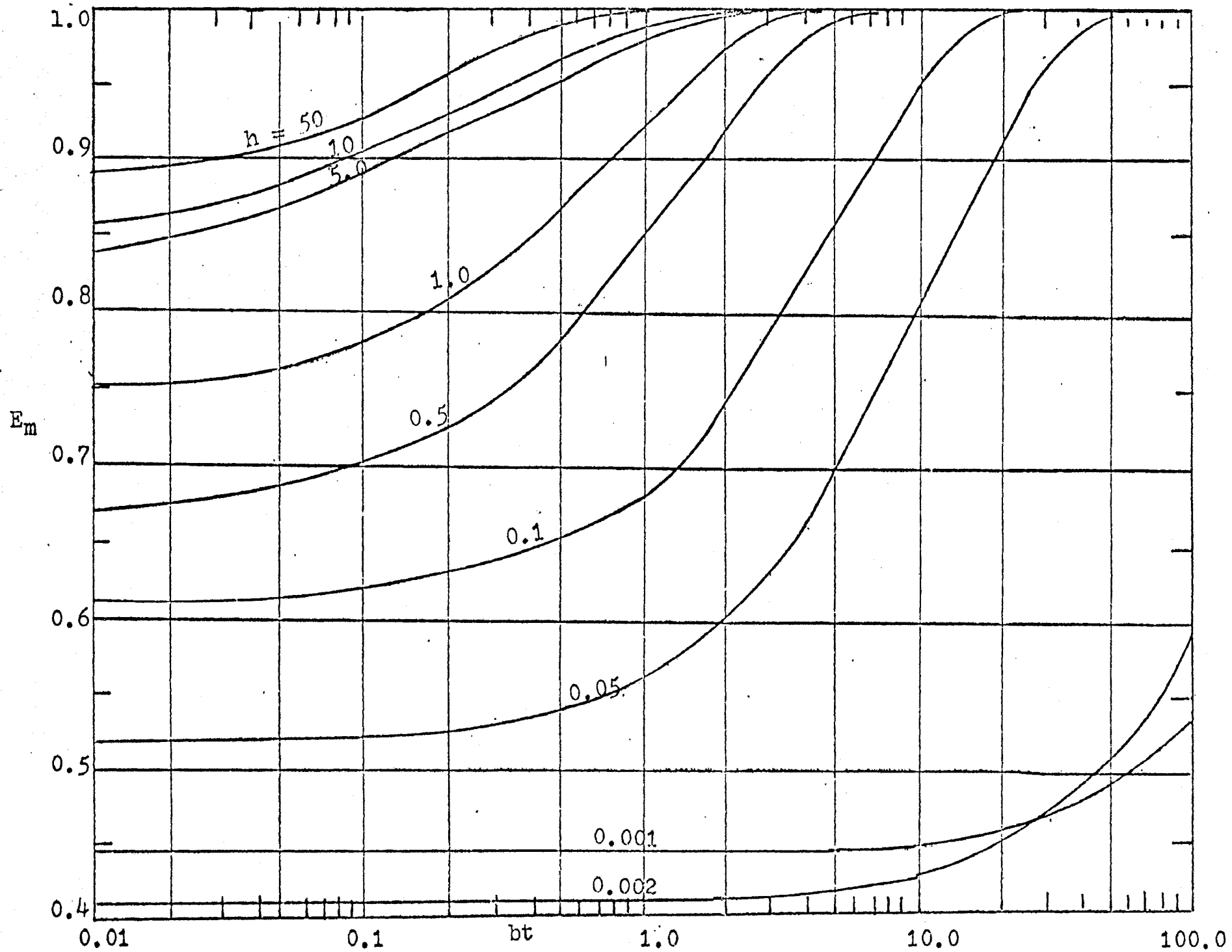


Figure 17: Fraction extracted versus dimensionless time (Iterative analog computer)

mentioned before have been substituted into the above equation to obtain the fraction extracted predicted by these approaches. It can be observed from Figures 14, 15 and 16 that for a particular value of bt the fraction extracted increases as the modified continuous phase resistance h increases. This is quite true because as h becomes larger ($h > 0.5$) the fraction extracted approach unity at a lower value of bt . This is consistent with expectations because as h gets larger, k_c gets larger and therefore, the resistance in the continuous phase decreases. For low value of bt , the fraction extracted remains approximately constant at non-zero values. As bt becomes larger, the fraction extracted increases and approaches unity asymptotically, which is expected physically.

Refer to appendix * , the calculation of the deviation between $E_m(n=4)$ and $E_m(n=3)$ indicates that the solution for $n=4$ is approximated satisfactorily. For low value of h , B_n and λ_n are small enough that only first term is dominant, especially for high values of bt . For high values of h , at low value of bt , small deviations of the order of about 0.05% exists between $E_m(n=4)$ and $E_m(n=3)$.

A similar family of curves were obtained in Patel's work using numerical methods with the digital computer. Comparing the results presented in Appendix 8, it is observed that the results of the iterative analog computer and digital-analog simulator agree best with solution obtained by either the Runge-Kutta or Hamming's method. The solution obtained using * supplementary appendix

the conventional analog computer deviates slightly from the iterative analog computer results.

When bt is zero, E_m should be zero; thus the following relation should exist at time equal to zero:

$$1 = 2 \sum_{n=1}^{\infty} B_n^2 \quad (5.3)$$

But in this work, the results apparently do not satisfy the above relation. For larger dimensionless time, (bt), the values of E_m do approach unity as bt approaches infinity, which is the expected physical behavior.

It is very important to realize that in the trial and error procedures in this work, $dY(0)/dy$, one of the two parameters, only affects the curves of dY/dy versus y in magnitude (amplitude) and another parameter being searched decides the position of the zero-crossing position in order to meet the final condition. Two kinds of recording equipments, cathode-ray oscilloscope and a servo-meter driven X-Y recorder have been used in this work. The oscilloscope has the advantage that problems with an end point to meet can be solved more quickly, especially in this work, an approximate value of the two parameters λ_n and $dY(0)/dy$ are obtained on the oscilloscope. However, using the oscilloscope it is also somewhat difficult to obtain the same degree of accuracy as the slower recording device (21).

Frequency response was not critical in the problem situations generated by the iterative analog computer. The question of precision arises for the dividers which are the

least exact components used in the simulation. Whenever it was impossible to prevent the use of low values of voltages or very small pot settings, electrical noise, both internal and external, could affect the solution. Low voltage outputs from the dividers show them to be operating at the least precise section of their range.

5.3 Comparison of results from analog computer with Patel's and Wellek-Skelland's results

Compare the eigenvalues obtained by Wellek-Skelland (9), Patel (28) and this work, the first eigenvalue for the three works are generally in agreement within $\pm 5\%$. But the deviation becomes larger in the third and fourth eigenvalues λ_3 , λ_4 . Since only the first eigenvalue is important at large contact time, the results of E_m obtained by the three works agree with each other very well at large contact time.

At short contact times, Patel obtained a numerical solution by a finite difference method which can be applied very satisfactorily.

Although the results obtained by Wellek-Skelland are consistent with the physical situation which at bt equals to zero, E_m equals to zero, the solution is strictly valid for large contact times.

The values of E_m calculated by the various method are presented below for the specific case of $h=0.5$, and $bt=1.0$.

$$E_m = 0.836 \quad (\text{digital-analog simulator})$$

$$E_m = 0.891 \quad (\text{conventional analog computer})$$

$$E_m = 0.856 \quad (\text{iterative analog computer})$$

$$E_m = 0.834 \quad (\text{Runge-Kutta method by Patel})$$

$$E_m = 0.832 \quad (\text{Hamming's method by Patel})$$

$$E_m = 0.663 \quad (\text{Finite difference method by Patel})$$

$$E_m = 0.750 \quad (\text{Wellek-Skelland})$$

It can be seen that the three results obtained in this work are in agreement with each other within about 5%. The value of E_m obtained by finite difference method of Patel and by Wellek-Skelland are lower than the values of E_m in this work. For larger values of h , all the curves of E_m versus bt tend to coincide.

When bt is close to zero, the deviation becomes very large from the actual physical situation which is bt equal zero, E_m equals zero.

One particular behavior of the family of curves obtained in this work which is similar to the behavior of the family of curves (E_m versus bt) obtained by Elizinga and Banchemo (12). The similarity is the intersection of various curves.

5.4 Application of the results

Two different single droplets systems are chosen to describe the application of the analytical series solution of the model. The first system has the most of the resistance to mass transfer in the droplet phase. In the second system, resistance is about equally distributed between both phases.

The experimental data for the following comparisons are provided by Handlos and Baron (1).

System (I)

solute: acetic acid

dispersed phase: benzene

continuous phase: water

droplet velocity: 11.3 cm/sec

droplet diameter: 0.503 cm

Reynolds number = 597

Using the Garner and Tayeban correlation to calculate the continuous phase mass transfer coefficient

$$k_c = 0.01565 \text{ cm/sec}$$

$$h = 50.29$$

dimensionless time $bt = 0.952$

The following values for the over-all mass transfer coefficient are obtained for the different methods:

$$K_d = 0.0409 \text{ cm/sec (Runge-Kutta method by Patel)}$$

$$K_d = 0.0241 \text{ cm/sec (Wellek-Skelland)}$$

$$K_d = 0.0318 \text{ cm/sec (Finite difference method by Patel)}$$

$$K_d = 0.0470 \text{ cm/sec (conventional analog computer)}$$

$$K_d = 0.0409 \text{ cm/sec (digital-analog simulator)}$$

$$K_d = 0.0457 \text{ cm/sec (iterative analog computer)}$$

$$K_d = 0.0258 \text{ cm/sec (Handlos and Baron, } h \rightarrow \infty)$$

$$K_d = 0.0211 \text{ cm/sec (experimental)}$$

The results show that the Wellek-Skelland and Handlos and Baron calculations and the experimental value agree fairly well with each other. (It should be emphasized that the Handlos and Baron calculation is based on the continuous phase resistance being negligible). The values of K_d obtained by Patel using the Runge-Kutta and Hamming's method agree with this work satisfactorily.

System (II)

solute: Acetone

Dispersed phase: benzene

Continuous phase: water

Droplet diameter: 0.481 cm

rising (falling) velocity: 10.6 cm/sec

Reynolds number = 535

Using the Garner and Tayeban correlation the continuous phase mass transfer coefficient is

$$k_c = 0.0134 \text{ cm/sec}$$

$$h = 1.133$$

dimensionless time = $bt = 0.995$

The following values of the over-all mass transfer coefficient are obtained for the different methods:

$$K_d = 0.00845 \text{ cm/sec (Runge-Kutta method by Patel)}$$

$$K_d = 0.00880 \text{ cm/sec (Wellek-Skelland)}$$

$$K_d = 0.00655 \text{ cm/sec (Finite difference method by Patel)}$$

$$K_d = 0.00846 \text{ cm/sec (digital-analog simulator)}$$

$$K_d = 0.00915 \text{ cm/sec (conventional analog computer)}$$

$$K_d = 0.00870 \text{ cm/sec (iterative analog computer)}$$

$$K_d = 0.01090 \text{ cm/sec (Handlos and Baron } h \rightarrow \infty)$$

$$K_d = 0.01260 \text{ cm/sec (experimental)}$$

From the above results, it can be seen that the value calculated by Handlos and Baron ($h \rightarrow \infty$) and the experimental value of K_d are higher than the other computer solutions. For this case, the values of K_d obtained in this work and by the numerical methods (Runge-Kutta, Hamming's) by Patel agree

with each other satisfactorily.

For short contact time (such as $bt=0.1$), the results obtained by the Runge-Kutta method and analog computer method differ considerably from the results by the method of finite difference. However, the results using finite difference method agree better with the physical situation for low contact time. But the results of this work as well as the results obtained by Patel using the Runge-Kutta and/or Hamming's method can be applied for large contact times (especially for $bt > 0.5$).

VI: SUMMARY AND CONCLUSIONS

The aim of this study was to successfully simulate on an analog computer the modification of the Handlos and Baron Model for mass transfer to droplets with turbulent internal circulation and a finite continuous phase resistance. Apparently, no solution to a similar type of mathematical problem (i.e. an eigenvalue problem with split boundary condition) exists in the literature (37) which has been simulated on an iterative analog computer. The two-variable iteration which is used constitutes a special feature of this work.

The project was divided into three schemes:

- (1) using a conventional analog computer to determine both the parameters λ_n and $dY(0)/dy$ and ultimately B_n . The trial and error procedure is performed manually on the computer.
- (2) using the iterative analog computer to perform the iterative procedures more accurately and rapidly.
- (3) using a digital-analog simulator to calculate the eigenvalues λ_n and $dY(0)/dy$.

The results obtained by these three schemes are then compared with results in the literature using different approaches.

The results show that for long contact time, the different schemes used in this work satisfactorily agree with the previous work done by Patel (28). For short contact time the finite difference method of Patel is recommended.

Upon comparison of the results obtained in this thesis with several previous approaches in the literature, the following conclusions can be made:

(1) The low eigenvalues (λ_1 and λ_2) obtained in all the schemes in this work agree with each other within 3%. For the higher eigenvalues (λ_3 and λ_4) the results from the conventional analog computer show a 5% to 10% deviation from the digital-analog simulator.

(2) The values of the coefficients B_n calculated by the three schemes in this work differ by no more than 10% from the results of each method. The results obtained using the analog computer with digital logic are closer to the values obtained by the digital-analog simulator.

(3) The eigenvalues λ_n obtained by Patel using numerical methods (Runge-Kutta and Hamming's) and by Wellek-Skelland using the Rayleigh-Ritz variational technique and this work are in agreement within 5%. The higher eigenvalues differ considerably. But the results of this work are closer to the Runge-Kutta results obtained using the digital computer than the finite difference method using the digital computer.

(4) For long dimensionless times ($bt > 50$), all the curves of E_m versus bt tend to coincide with each other; that is, they approach the results for h equal to infinity for the Handlos and Baron Model ($k_c \rightarrow \infty$).

(5) The families of curves E_m versus bt (with varying h values) obtained in this work are similar in nature to those results obtained from the Runge-Kutta and Hamming's method by

Patel, the Grober (stagnant drop) result, and the Elzinga and Banchemo (laminar circulation) results. That is, as bt approaches zero, (or for short dimensionless time, bt), E_m (fraction extracted) does not approach zero. This is not consistent with the physical situation.

(6) The overall mass transfer coefficients, K_{dr} , obtained by using the Runge-Kutta or Hamming's method and the results in this work agree with each other within 10%.

(7) For the experimental system chosen for the calculation of K_{dr} (with most of the resistance to mass transfer in the droplet), K_{dr} calculated by using Wellek and Skelland method differs considerably from the values of K_{dr} calculated by using the Runge-Kutta method, Hamming's method and the analog computation. But the Wellek and Skelland method predicts K_{dr} values which are closer to the experimental values. The system with resistance to mass transfer in both phases shows that all predicted values of K_{dr} (using all the methods) are in agreement with each other, although they are less than the experimental value by about 30%.

(8) For very short contact times ($bt < 0.1$), the value of K_{dr} calculated by the finite difference method of Patel and by the results of this work differ by as much as 40%. But the results from the Runge-Kutta and Hamming's method by Patel agree with this work very satisfactorily.

(9) Further study in this work is recommended to use the numerical approach to simulate the mathematical model on the hybrid computer and to transform the partial differential

equation into a difference equation using a technique to avoid truncation errors. The hybrid computer has the advantage of a larger storage capacity for digital values than than that of the iterative analog computer. This advantage is on the order of 1000 to 1 so that entire functions may be stored numerically.

VII. NOMENCLATURE

- A_n = Coefficients in series solution
 a = radius of droplet (cm)
 B_n = Coefficients in series solution, dimensionless
 b = $\frac{u}{128(1 + \mu_d/\mu_c)d_e}$
 C & c = Concentration of solute in dispersed phase. $\frac{\text{g-mole}}{\text{liter}}$
 C_o = initial concentration (g-mole/liter)
 D = Molecular diffusivity (cm^2/sec)
 d_e = droplets diameter (cm)
 E = Eddy diffusivity
 E_m = Fraction Extracted, $\frac{C_o - C}{C_o}$
 e_o = output voltage
 e_i = input voltage
 g = Acceleration due to gravitation (cm/sec^2)
 h = Modified continuous phase resistance, $\frac{512kc(1 + \mu_d/\mu_c)}{\mu}$
 h_o = heat transfer coefficients ($\text{cal cm}^{-2} \text{sec}^{-1} \text{ } ^\circ\text{K}^{-1}$)
 K_{dr} = Overall coefficients of mass transfer in terms of disperse phase concentration during droplet free rising (or falling) period. (cm/sec)
 K = Thermalconductivity ($\text{cal sec}^{-1} \text{cm}^{-1} \text{ } ^\circ\text{K}^{-1}$)
 k = correction factor
 k_y = magnitude scaled factor
 k_c, k_d = individual mass transfer coefficient (continuous and dispersed phase), respectively (cm/sec)

- $M(t)$ = mass of solute in droplet phase (drop phase) at time t
 $M(0)$ = mass of solute in droplet phase at $t=0$
 m = distribution coefficient, dispersed phase concentration/continuous phase concentration at equilibrium
 n = an integer number (number of modes)
- (N_{Re}) = Reynolds number $\frac{d_e u \rho_c}{\mu_c}$
- $(N_{Sc})_c$ = Continuous phase Schmit number, $\frac{\mu}{\rho_c D}$
 N_{Nu} = Nusselt number, $\frac{h_o d_e}{k}$
- N_{Pe} = Peclet number, $\frac{d_e u}{D}$
- N_{Sh} = Sharewood number, $\frac{k_c d_e}{D}$
- \underline{r} = $\frac{4\rho}{d_e}$, torus radius
- t = time during free fall (or rise) period (sec.)
 bt = dimensionaless time
 \bar{t} = average circulation time droplet (sec)
- U, u = droplet free fall (or rise) velocity (cm/sec)
 \bar{Z} = average displacement of fluid
 n = eigenvalues
- μ_d, μ_c = viscosity of dispersed phase and continuous phase respectively (centipoise)
- ρ_d, ρ_c = density of dispersed phase and continuous phase respectively (g/cm^3)
- ρ = torus radius
- τ = Scaled time (computer time) (sec)
- β = Scaled factor for time scale

ξ = radial direction of Hadamard type circulation
Y = Magnitude scaled variable
Y = Problem variable

VIII: BIBLIOGRAPHY

- (1) Handlos, A. E. and T. Baron, A.I.Ch.E.J. 3, 127 (1957).
- (2) Mickley, H. S., T. K. Sherwood and C. E. Reed, "Applied Mathematics in Chemical Engineering," McGraw-Hill Book Co., New York (1957), 2nd Edition.
- (3) Operation Manual for AD-40 analog computer, Applied Dynamics, Ann Arbor, Michigan.
- (4) Skelland, A. H. P. and A. R. H. Cornish, Can. J. Ch. E., 43, 302, Dec. (1965).
- (5) Johnson, A. I. and A. E. Hamielec, A.I.Ch.E.J., 6, 145 (1960).
- (6) Griffith, R. M., Chem. Engr. Sci., 12, 198 (1960).
- (7) Olney, R. B. and R. S. Miller, Modern Chemical Eng., 1, 89, Acrivos, A., P. Reinhold, eds., New York (1963).
- (8) Linton, M. and K. L. Sutherland, Chem. Eng. Sci., 12, 214 (1960).
- (9) Skelland, A. H. P. and R. M. Wellek, A.I.Ch.E.J., 9, 73, (1963).
- (10) Treybal, R. G. "Liquid Extraction", 2, 186, McGraw-Hill, New York (1963).
- (11) Wellek, R. M. and A. H. P. Skelland, A.I.Ch.E.J., 11, 577 (1965).
- (12) Elizingsa, E. R. and J. T. Eanchedero, Chem. Engr. Symp. Ser., No. 29, 55, Chicago.
- (13) Calderbank, P. H. and I. J. O. Korchinski, Chem. Engr. Sci., 6, 65 (1965).

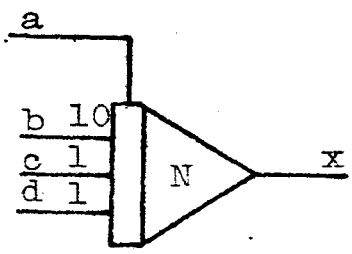
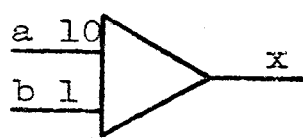
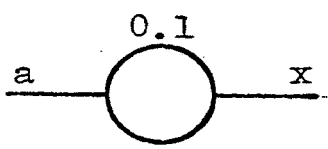
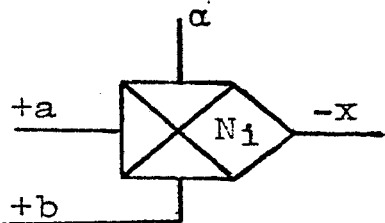
- (14) Hadamard, J., Comp. Rend., 152, 1735 (1911).
- (15) Grober, H. Z., Ver. Dent. Ing., 69, 705 (1925).
- (16) Newman, A. B., Trans. Am. Inst. Chem. Engr., 27, 203 (1931).
- (17) Kronig R. and J. E. Brink, Applied Sci. Res., A-2, 142.
- (18) Garner, F. H. and A. H. R. Skelland, Ind. Engr. Chem. 46, 1255 (1945).
- (19) Wellek, R. M., A. K. Agrawal and A. H. P. Skelland, A.I.Ch.E.J., 11, 854 (1966).
- (20) Frossling, N. Gerland Beitr. Geophysik, 52, 170 (1938).
- (21) G. W. Corcus, R. M. Howe, L. L. Ranch, and J. R. Sellars, Project Cyclone, Synp (II), Part 2, (1952).
- (22) Fadden, E. J., 55th National Meeting, A.I.Ch.E.
- (23) Olmsted, J. M. H., "Advanced Calculus", 95, Appleton-Century-Crofts, Inc., New York (1959).
- (24) Cadem, T. W. and T. G. Smith, Series in Hydrocarbon Processing begins from Feb., 47, No. 2 (1968).
- (25) Coughhanour, D. R. and L. B. Koppel, "Process Systems Analysis and Control", 420 (1965).
- (26) Chao, H. T., M. S. Thesis, Univ. of Missouri-Rolla (1968).
- (27) Alcorn, H. R. "Instruction for programming, PACTOLUS", Computer Science Center, Univ. of Missouri-Rolla (1966).
- (28) Patel, J. M., M. S. Thesis, Univ. of Missouri-Rolla (1966).
- (29) Rogers, A. E. and T. W. Connolly, "Analog Computation in Engineering Design", McGraw-Hill Book Co., Inc. (1960).

- (30) Tamiya Nomura and R. M. Dieters, 11, No. 2, Simulation, Aug. (1968).
- (31) R. B. Bird, W. E. Stewart and E. N. Lightfoot "Transport Phenomena", John Wiley & Sons, Inc., New York, 356.
- (32) Pasternak, I. S. and Gauvin, W. H., Can. J. Chem. Eng. 38, 35 (1960).
- (33) Vermeulen, Theodore, Ind. Eng. Chem. 45, 1664 (1953).
- (34) Higbie, R., Trans. Am. Inst. Chem. Engr. 31, 365 (1935).
- (35) Boussinesq, J., J. de Math. Pures et appliques, ser 6, 1, 285 (1905).
- (36) Garner, F. H., Tayeban M., Anales de la Real Sociedad Espanola de Fisica y Quimica, serie B-Quimica Tomo LVI (B) 479 (1960).
- (37) Simulation Survey and Literature Review edited by Lawrence W. Ross, "Simulation"

APPENDICES

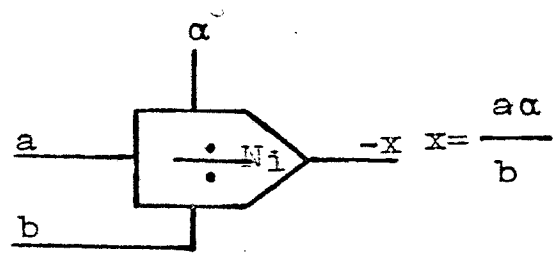
APPENDIX (1)

Analog and hybrid symbols for the elements used in the computer circuit. (The symbols are published in December, 1967, Simulation issue by Simulation Council, Inc.).

<u>SYMBOLS</u>	<u>FUNCTION</u>	<u>DEFINATION</u>
<p>(1) Integrator</p> 	$x = -a - \int_0^t (10b + c + d) dt$	<p>a is the initial condition for the integration</p>
<p>(2) Summer</p> 	$x = -(10a + b)$	<p>"N" indicates the number of the amplifier, it has 10 and 1 gain in AD-40</p>
<p>(3) Potentiometer</p> 	$x = 0.1a$	<p>Two-terminal pot k value is less than 1 and always positive</p>
<p>(4) Multiplier</p> 	$x = \frac{ab}{\alpha}$	<p>= some reference positive or negative voltage output possible</p>

(5) Divider

The denominator has to be always positive

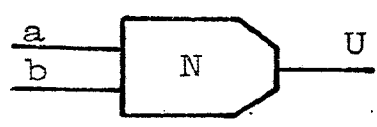


(6) Comparator
With binary output

$U=1 (a+b)>0$

$U=1 (a+b)<0$

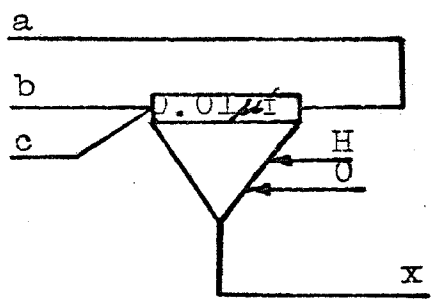
The symbol for a relay comparator can be made by combining either of these symbols with that of a relay



(7) Track-hold

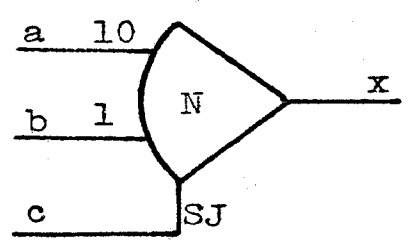
Track when IC
Hold when in hold

When used in this way the size of the integrating capacitor is important. The quantity being track and held is $-(a+b+c)$



(8) High Gain amplifier

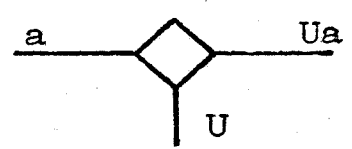
The curve back indicates that the feedback resistor has been removed.



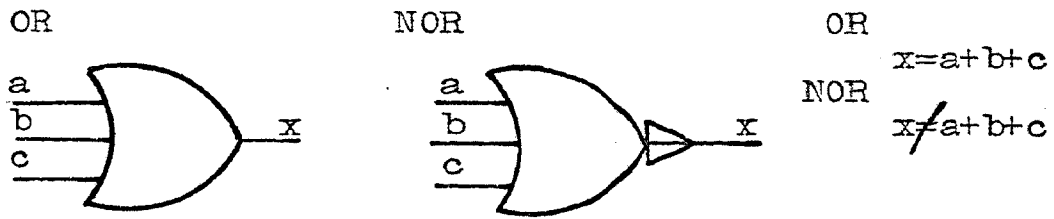
(9) Analog/digital switch $U_a=0 (U=0)$

ON when binary signal U is digital "one"

$U_a=a(U=1)$



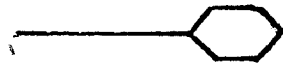
(10) Logic gate



(11) Indicator

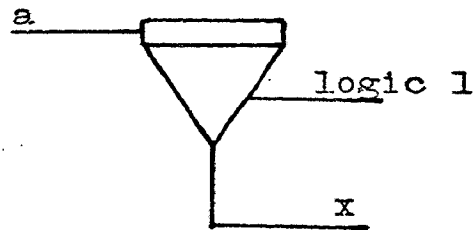


(12) Trunk



(13) Track-hold integrator as inverter

$x=-a$



(14) Signal flow

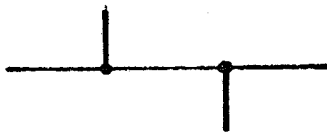
Analog

Hybrid



Connection

No connection



APPENDIX (2)

The partial differential equation to describe the Model with the relevant boundary conditions:

$$\frac{\partial C}{\partial t} = \frac{b}{1-y} \frac{\partial}{\partial y} (1-5y+10y^2-6y^3) \frac{\partial C}{\partial y} \quad (\text{A.1})$$

Boundary condition

(1) Weltek-Skelland modification

$$\frac{\partial C}{\partial y} = h(C-C_1) \quad y = 0 \quad t > 0 \quad (\text{A.2})$$

$$(2) \quad \frac{\partial C}{\partial y} = 0 \quad y = 1 \quad t = t \quad (\text{A.3})$$

$$(3) \quad C = C_0 \quad 0 < y < 1 \quad t = 0 \quad (\text{A.4})$$

Applying the technique of separation of variables:

$$C = T(t) Y(y) \quad (\text{A.5})$$

$$\frac{\partial C}{\partial t} = T'(t)Y(y)$$

$$\frac{\partial C}{\partial y} = T(t)Y'(y)$$

$$\frac{\partial^2 C}{\partial t^2} = T(t)Y''(y)$$

Substitute into equation (A.1)

$$T'(t)Y(y) = \frac{6}{(1-y)} (1-5y+10y^2-6y^3)T(t)Y''(y) + \frac{6}{(1-y)} T(t)Y'(y)(-5+20y-18y^2)$$

$$\frac{T'(t)}{bT(t)} = \frac{1}{(1-y)} (1-5y+10y^2-6y^3) \frac{Y''(y)}{Y(y)} + (-5+20y-18y^2) \frac{Y'(y)}{Y(y)} = -\lambda \quad (\text{A.6})$$

Rearranging the equation, a set of ordinary differential equations are obtained:

$$\frac{dT}{dt} + b\lambda T = 0 \quad (\text{A.7})$$

$$(1-5y+10y^2-6y^3)Y''(y) + (-5+20y-18y^2)Y'(y) + \lambda(1-y)Y(y) = 0 \quad (\text{A.8})$$

$$\frac{d^2Y}{dy^2} = - \frac{(-5+20y-18y^2)}{(1-5y+10y^2-6y^3)} \frac{dY}{dy} - \frac{\lambda(1-y)Y}{(1-5y+10y^2-6y^3)} \quad (\text{A.9})$$

$$\text{or } \frac{d^2Y}{dy^2} = \frac{18y^2-20y+5}{1-5y+10y^2-6y^3} \frac{dY}{dy} - \frac{\lambda_n Y}{(6y^2-4y+1)}$$

Boundary conditions

$$(1) \quad \frac{dY}{dy} = hY \quad y = 0 \quad (\text{A.10})$$

$$(2) \quad \frac{dY}{dy} = 0 \quad y = 1 \quad (\text{A.11})$$

In order to obtain the analytical solution, let

$$P(y) = 1-5y+10y^2-6y^3$$

$$Q(y) = 1-y$$

For $\lambda =$ positive value

$$T(t) = B \exp(-b\lambda t) \quad (\text{A.12})$$

For $\lambda =$ negative

$$T(t) = A \exp(b\lambda t) \quad (\text{A.13})$$

$$\text{For } \lambda = 0 \quad T(t) = D \quad (\text{A.14})$$

Where A, B and D are constants

$$\text{For } \lambda = \text{positive} \quad Y(y) = Y(y) \quad (\text{A.15})$$

$$\lambda = \text{negative} \quad Y(y) = Y^*(y) \quad (\text{A.16})$$

$$\lambda = 0 \quad P(y) \frac{dY}{dy} = C$$

$$\int dY = \int \frac{C}{(1-5y+10y^2-6y^3)} dy$$

$$Y(y) = \int \frac{C}{(1-5y+10y^2-6y^3)} dy \quad (\text{A.17})$$

Applying the principle of superposition, the complete solution is

$$C(y,t) = \sum_{n=1}^{\infty} b_n Y_n \exp(-b\lambda_n t) + \sum_{n=1}^{\infty} a_n Y_n \exp(b\lambda_n t) + \int_0^1 \frac{C}{(1-5y+10y^2-6y^3)} dy \quad (\text{A.18})$$

As t approaches infinity

$$C(y,\infty) = \text{infinite}$$

Hence, the second term is omitted.

$$C(y,t) = C_1 = \int \frac{C}{(1-5y+10y^2-6y^3)} dy \quad (\text{A.19})$$

$$= C_2 Y(y) + C_3$$

$$C_3 = C_1, \quad C_2 = 0$$

Now, the complete solution should have the form

$$C(y,t) = \sum_{n=1}^{\infty} b_n Y_n \exp(-b\lambda_n t) + C_1 \quad (\text{A.20})$$

In this work, C_1 (continuous phase solute concentration) is very dilute.

$$C_1 = 0 \quad (\text{A.21})$$

Therefore,

$$C(y,t) = \sum_{n=1}^{\infty} b_n Y_n \exp(-b\lambda_n t) \quad (\text{A.22})$$

Equations (A.9), (A.10) and (A.11) belong to the Sturm-Liouville system, and hence the solution has an infinite number of eigenvalues as indicated in Equation (A.18).

From the initial condition

$$C(0,y) = C_0 = \sum_{n=1}^{\infty} b_n Y_n \quad (\text{A.23})$$

From the orthogonal properties of Sturm-Liouville systems:

$$\begin{aligned} \int_0^1 C_0 (1-y) Y_n dy &= \sum_{n=1}^{\infty} b_n \int_0^1 (1-y) Y_n dy \\ b_n \int_0^1 (1-y) Y_n^2 dy &= C_0 \int_0^1 (1-y) Y_n dy \\ b_n &= C_0 \int_0^1 (1-y) Y_n dy \end{aligned} \quad (\text{A.24})$$

$$\text{Let } B_n = \int_0^1 (1-y) Y_n dy$$

Therefore

$$C(y,t) = C_0 \sum_{n=1}^{\infty} B_n Y_n \exp(-b \lambda_n t)$$

At the boundary ($y=1$) one term in the equation is undeterminable

$$\frac{d^2 Y}{dy^2} = 3 \left(\frac{0}{0} \right) - \frac{Y_n(1)}{3} \quad (\text{A.25})$$

Therefore, the L-Hospital's Rule has to be applied before the end condition is reached.

$$\begin{aligned} \frac{d^2 Y}{dy^2} &= \frac{(18y^2 - 20y + 5)}{(-5 + 20y - 18y^2)} \frac{d^2 Y}{dy^2} - \frac{\lambda_n Y}{(6y^2 - 4y + 1)} \\ &= - \frac{d^2 Y}{dy^2} - \frac{\lambda_n Y}{(6y^2 - 4y + 1)} \end{aligned} \quad (\text{A.26})$$

$$2 \frac{d^2 Y}{dy^2} = \frac{\lambda_n Y}{(6y^2 - 4y + 1)} \quad (\text{A.27})$$

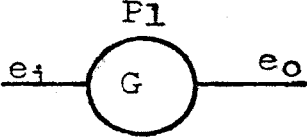
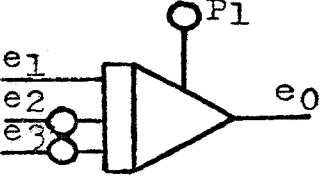
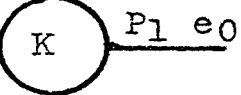
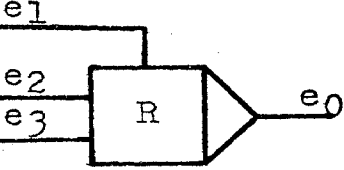
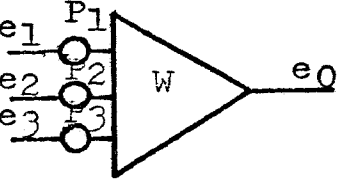
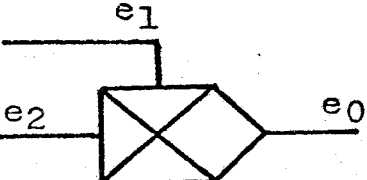
at $y=1$,

$$\frac{d^2 Y(1)}{dy^2} = - \frac{\lambda_n}{6} \quad (\text{A.28})$$

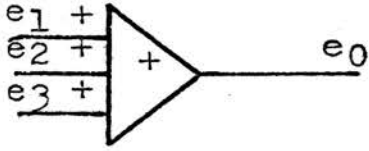
This is the same result as obtained by Patel (28) using a series expansion approach.

APPENDIX (3)

PACTOLUS element symbols are given in the notes of the Computer Science Center of University of Missouri-Rolla.

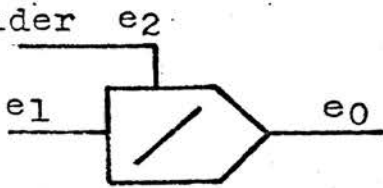
<u>Name</u>		<u>Type</u>	<u>Description</u>
Gain		G	$e_o = P_1 e_i$
Integrator		I	$e_o = P_1 + (e_1 + e_2 P_2 + e_3 P_3) dt$
Constant		K	$e_o = P_1$
Relay		R	$e_o = \begin{matrix} e_2 & \text{for } e_1 > 0 \\ e_3 & \text{for } e_1 < 0 \end{matrix}$
Weighted summer		W	$e_o = P_1 e_1 + P_2 e_2 + P_3 e_3$
Multiplier		X	$e_o = e_1 e_2$

Summer



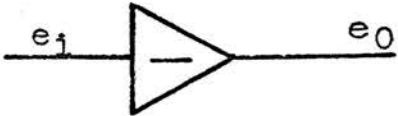
$$+ \quad e_0 = e_1 + e_2 + e_3$$

Divider



$$/ \quad e_0 = e_1 / e_2$$

Sign Inverter



$$- \quad e_0 = -e_1$$

APPENDIX (4)

Sample calculation of overall mass transfer coefficient K_{dr}

System (I)

Solute: Acetic acid

dispersed phase: benzene

continuous phase: water

droplet velocity: 11.3 cm/sec

droplet diameter: 0.503 cm

Reynolds number = 597

The Garner and Tayeban correlation is used to evaluate the continuous phase mass transfer coefficient k_c

$$k_c = \frac{D_{ab}}{d_e} \left[50 + 0.0095(Re)^{1.0} (Sc)^{0.7} \right]$$

Sc = continuous phase Schmidt number = $\frac{\mu_c}{\rho_c D_{ab}}$

$$k_c = 0.01565 \text{ cm/sec (computer result)}$$

It is defined:

$$h = \frac{512k_c(1 + \mu_d/\mu_c)}{\mu}$$

$$= 50.29$$

$$b = \frac{u}{128(1 + \mu_d/\mu_c)d_e} = 0.1075$$

Dimensionless time = $bt = 0.95$

For the droplet rising (falling) 100 cm, the contact time

$$t = 100/11.3 = 8.50 \text{ sec}$$

Relation used to evaluate the dispersed mass transfer coefficient is given as follows:

$$k_d = -(d_e/6t) \ln(1-E_m) \quad (\text{A.29})$$

From the dimensionless time bt and h , E_m can be obtained by interpolation from Figures 15, 16 and 17.

$$E_m = 0.994 \text{ (conventional analog computer)}$$

$$E_m = 0.990 \text{ (digital-analog simulator)}$$

$$E_m = 0.993 \text{ (iterative analog computer)}$$

Substituting E_m and t into equation (A.29) to obtain k_d :

$$k_d = 0.0468 \text{ cm/sec (analog computer with digital logic)}$$

$$k_d = 0.0481 \text{ cm/sec (conventional analog computer)}$$

$$k_d = 0.0436 \text{ cm/sec (digital-analog simulator)}$$

Interpolation in the figures of E_m versus bt of Patel's work

$$E_m = 0.990 \text{ (Hamming's method by Patel)}$$

$$E_m = 0.970 \text{ (finite difference method by Patel)}$$

$$k_d = 0.0436 \text{ cm/sec (Hamming's method)}$$

$$k_d = 0.0333 \text{ cm/sec (finite difference method)}$$

k_d of Wellek and Skelland modification

$$k_d = \frac{u}{768(1+\mu_d/\mu_c)} = 0.0257 \text{ cm/sec}$$

Combining the individual dispersed and continuous phase coefficients during free (or, fall) rise to give the overall mass transfer coefficient K_{dr} on the assumption of interfacial equilibrium:

$$\frac{1}{K_{dr}} = \frac{1}{k_{dr}} + \frac{m}{k_{cr}}$$

Since the distribution factor m has the value 0.023, the following results of K_{dr} can be obtained:

$$K_d = 0.0409 \text{ cm/sec (Runge-Kutta by Patel)}$$

$$K_d = 0.0241 \text{ cm/sec (Wellek-Skelland modification)}$$

$$K_d = 0.0318 \text{ cm/sec (finite difference method by Patel)}$$

$$K_d = 0.0457 \text{ cm/sec (iterative analog computer)}$$

$$K_d = 0.0470 \text{ cm/sec (conventional analog computer)}$$

$$K_d = 0.0409 \text{ cm/sec (digital-analog simulator)}$$

$$K_d = 0.0258 \text{ cm/sec (Handlos and Baron, } h \rightarrow \infty)$$

$$K_d = 0.0211 \text{ cm/sec (experimental)}$$

System (II)

solute: Acetone

dispersed phase: benzene

continuous phase: water

drop velocity: 10.6 cm/sec

drop diameter: 0.481 cm

Reynolds number = 535

The calculation of k_c , h , b , and t follows the same approach as indicated previously in system (I), except the distribution factor, m , is 0.939.

$$K_d = 0.00845 \text{ cm/sec (Runge-Kutta method by Patel)}$$

$$K_d = 0.00880 \text{ cm/sec (Wellek-Skelland modification)}$$

$$K_d = 0.00655 \text{ cm/sec (Finite difference method by Patel)}$$

$$K_d = 0.00846 \text{ cm/sec (digital-analog simulator)}$$

$$K_d = 0.00915 \text{ cm/sec (conventional analog computer)}$$

$$K_d = 0.00870 \text{ cm/sec (iterative analog computer)}$$

$$K_d = 0.01091 \text{ cm/sec (Handlos and Baron, } h \rightarrow \infty)$$

$$K_d = 0.02161 \text{ cm/sec (experimental)}$$

For the contact time bt equals 0.1, interpolate the values

E_m from the Figures 15, 16, 17, A.8 and A.10 of E_m versus bt , then, the following values of K_{dr} are obtained:

$$K_d = 0.0127 \text{ cm/sec (Runge-Kutta method by Patel)}$$

$$K_d = 0.00725 \text{ cm/sec (finite difference method by Patel)}$$

$$K_d = 0.01275 \text{ cm/sec (digital-analog simulator)}$$

$$K_d = 0.0129 \text{ cm/sec (iterative analog computer)}$$

$$K_d = 0.0131 \text{ cm/sec (conventional analog computer)}$$

APPENDIX (5)

Eigenvalues for Patel (28), Wellek-Skelland (11),
Elzinga and Banchemo (12) and Grober (15).

Table:A1 Eigenvalues and coefficients for stagnant drops due to Grober(15)

$\frac{h_{od}}{k}$	ψ_1	ψ_2	ψ_3	ψ_4	A1	A2	A3	A4
4	2.209	4.913	7.979	11.086	0.159	0.00634		
6	2.289	5.087	8.069	11.173	0.153	0.01090		
8	2.456	5.233	8.205	11.256				
10	2.570	5.354	8.303	11.335	0.142	0.0179	0.00408	
12	2.654	5.454	8.391	11.409				
14	2.717	5.538	8.470	11.477	0.134	0.0220	0.00600	
16	2.765	5.608	8.541	11.541				
18	2.804	5.667	8.603	11.599	0.129	0.242	0.0119	0.00291
20	2.836	5.717	8.659	11.653				
22	2.863	5.761	8.708	11.703	0.125	0.0255	0.00858	0.00359
32	2.948				0.119			
42	2.993							
62	3.041				0.111			
82	3.065							
102	3.080				0.107			
∞	3.142				0.101			

Table A2:

Eigenvalues for Handlos and Baron Model calculated by Wellek and Skelland(1)

h	λ_1	λ_2	λ_3	λ_4
0.001	0.0020	7.46	39.0	300.0
0.010	0.022	7.49	39.1	300.0
0.100	0.270	7.85	39.3	300.0
0.500	1.337	10.7	41.6	302.0
1.000	1.980	14.27	45.4	304.0
2.500	2.445	19.54	55.9	311.0
5.000	2.674	23.42	77.2	322.0
7.000	2.708	23.76	80.0	327.0
10.00	2.731	23.72	78.6	332.0
25.00	2.821	25.26	97.4	355.0
50.00	2.847	25.54	99.5	366.0
70.00	2.850	25.24	91.2	365.0
100.0	2.852	24.88	83.5	364.0
250.0	2.861	24.85	80.9	367.0
500.0	2.864	24.76	78.8	367.0
700.0	2.864	24.64	77.0	366.0
1000.	2.865	24.56	75.8	366.0
∞	2.866	24.58	75.6	367.0

Table A3: Eigenvalues and coefficients for circulating drops
calculated by Elzinga and Banhero(14)

$\frac{H_{od}}{k}$	1	2	3	B ₁	B ₂	B ₃
3.20	0.262	4.24		1.49	0.107	
5.33	0.368					
8.00	0.534					
10.7	0.680	4.92		1.49	0.300	
16.0	0.860	5.26		1.48	0.382	
21.3	0.982	5.63		1.47	0.428	
26.7	1.082	5.90	15.7	1.49	0.495	0.205
53.3	1.324	7.04	17.5	1.43	0.603	0.298
107.0	1.484	7.88	19.5	1.39	0.603	0.384
213.0	1.560	8.50	20.80	1.31	0.588	0.396
320.0	1.600	8.62	21.3	1.31	0.583	0.386
∞	1.565	9.08	22.2	1.29	0.506	0.386

Table A4: Eigenvalues and coefficients for
Wellek-Skelland Modification
(Runge-Kutta method by Patel(28))

h	λ_1	λ_2	λ_3	λ_4	B_1	B_2	B_3	B_4
0.001	0.002	6.87	31.6	365	0.5073	-0.873(10) ⁻⁴	0.152(10) ⁻⁴	-0.814(10) ⁻⁶
0.002	0.004	6.88	31.6	365	0.5071	-0.178(10) ⁻³	0.303(10) ⁻⁴	-0.163(10) ⁻⁵
0.010	0.020	6.89	31.6	365	0.5053	-0.889(10) ⁻³	0.152(10) ⁻³	-0.816(10) ⁻⁵
0.05	0.096	6.98	31.7	365	0.4964	-0.443(10) ⁻²	0.757(10) ⁻³	-0.408(10) ⁻⁴
0.10	0.188	7.10	31.8	365	0.4859	-0.881(10) ⁻²	0.151(10) ⁻²	-0.815(10) ⁻⁴
0.50	0.785	8.03	32.5	366	0.4207	-0.414(10) ⁻¹	0.750(10) ⁻²	-0.407(10) ⁻³
1.00	1.276	9.20	33.3	367	0.3708	-0.740(10) ⁻¹	0.147(10) ⁻¹	-0.813(10) ⁻³
2.50	1.966	12.14	36.0	369	0.3063	-0.123	0.332(10) ⁻¹	-0.201(10) ⁻²
5.0	2.343	15.05	39.6	374	0.2736	-0.137	0.519(10) ⁻¹	-0.391(10) ⁻²
7.0	2.468	16.33	41.8	377	0.2631	-0.135	0.591(10) ⁻¹	-0.531(10) ⁻²
10.0	2.568	17.46	83.9	381	0.2549	-0.132	-0.142(10) ⁻¹	-0.712(10) ⁻²
25.0	2.714	19.24	90.8	396	0.2431	-0.121	-0.412(10) ⁻¹	-0.120(10) ⁻¹
30.0	2.731	19.44	91.7	400	0.2417	-0.119	-0.414(10) ⁻¹	-0.128(10) ⁻¹
50.0	2.765	19.86	93.8	407	0.2391	-0.116	-0.410(10) ⁻¹	-0.138(10) ⁻¹
70.0	2.779	20.04	94.7	411	0.2379	-0.115	-0.408(10) ⁻¹	-0.141(10) ⁻¹
100.0	2.790	20.18	95.4	414	0.2370	-0.113	-0.403(10) ⁻¹	-0.143(10) ⁻¹
250	2.806	20.37	96.4	418	0.2358	-0.112	-0.402(10) ⁻¹	-0.143(10) ⁻¹
500	2.811	20.43	96.7	419	0.2354	-0.111	-0.401(10) ⁻¹	-0.143(10) ⁻¹
700	2.812	20.45	96.8	420	0.2353	-0.111	-0.400(10) ⁻¹	-0.142(10) ⁻¹
1000	2.814	20.46	96.9	420	0.2352	-0.111	-0.400(10) ⁻¹	-0.142(10) ⁻¹
∞	2.816	20.49	97.1	421	0.2350	-0.111	-0.399(10) ⁻¹	-0.142(10) ⁻¹

Table A5: Eigenvalues and coefficients for
Wellek-Skelland Modification
(Hamming's method by Patel(28))

h	λ_1	λ_2	λ_3	λ_4	B ₁	B ₂	B ₃	B ₄
0.001	0.002	6.96	31.9	369	0.5150	-0.882(10) ⁻⁴	0.151(10) ⁻⁴	-0.827(10) ⁻⁶
0.002	0.004	6.96	31.9	369	0.5148	-0.177(10) ⁻³	0.303(10) ⁻⁴	-0.166(10) ⁻⁵
0.010	0.019	6.98	31.9	369	0.5129	-0.886(10) ⁻³	0.152(10) ⁻³	-0.829(10) ⁻⁵
0.10	0.185	7.18	32.1	369	0.4938	-0.878(10) ⁻²	0.151(10) ⁻²	-0.829(10) ⁻⁴
0.50	0.776	8.11	32.8	370	0.4289	-0.413(10) ⁻¹	0.750(10) ⁻²	-0.414(10) ⁻³
1.00	1.265	9.26	33.6	371	0.3789	-0.739(10) ⁻¹	0.147(10) ⁻¹	-0.825(10) ⁻³
2.50	1.961	12.19	36.2	373	0.3133	-0.124	0.333(10) ⁻¹	-0.205(10) ⁻²
5.0	2.345	15.12	39.9	377	0.2798	-0.139	0.523(10) ⁻¹	-0.399(10) ⁻²
7.0	2.473	16.42	42.1	381	0.2690	-0.138	0.597(10) ⁻¹	-0.541(10) ⁻²
10.0	2.575	17.56	84.5	385	0.2606	-0.134	-0.359(10) ⁻¹	-0.727(10) ⁻²
25.0	2.726	19.38	91.5	400	0.2483	-0.123	-0.420(10) ⁻¹	-0.123(10) ⁻¹
30.0	2.743	19.59	92.5	403	0.2469	-0.121	-0.422(10) ⁻¹	-0.130(10) ⁻¹
50.0	2.778	20.02	94.6	411	0.2442	-0.118	-0.421(10) ⁻¹	-0.143(10) ⁻¹
70.0	2.793	20.20	95.6	415	0.2430	-0.116	-0.418(10) ⁻¹	-0.146(10) ⁻¹
100.0	2.804	20.34	96.3	418	0.2421	-0.115	-0.416(10) ⁻¹	-0.148(10)

Appendix 6

Pactolus program for the for the first type arrangement
with time scaling

SOLVING EIGEN VALUES CHE490
PACTOLUS DIGITAL ANALOG SIMULATOR PROGRAM

CONFG

CONFIGURATION SPECIFICATION

BLOCK	TYPE	INPUT-1	INPUT-2	INPUT-3
1	I	0	22	0
2	I	1	0	0
3	X	76	76	0
4	X	76	3	0
5	G	3	0	0
6	G	76	0	0
7	K	0	0	0
8	G	76	0	0
9	G	3	0	0
10	K	0	0	0
11	G	4	0	0
12	G	76	0	0
13	G	3	0	0
14	K	0	0	0
15	+	5	6	7
16	+	8	9	10
17	+	11	12	13
26	+	17	14	0
18	/	2	15	0
19	/	16	26	0
20	X	1	19	0
21	G	18	0	0
22	+	21	30	0
29	/	1	26	0
END ICPAR	30	G	20	0

INITIAL CONDITIONS AND PARAMETERS

BLOCK	IC/PAR1	PAR2	PAR3
1	-0.23047	1.000000	0.0
2	-0.23047	0.0	0.0
5	-0.060000	0.0	0.0
6	-0.400000	0.0	0.0
7	1.000000	0.0	0.0
8	-2.000000	0.0	0.0
9	0.180000	0.0	0.0
10	5.000000	0.0	0.0
11	-0.006000	0.0	0.0
12	-0.500000	0.0	0.0
13	0.100000	0.0	0.0
14	1.000000	0.0	0.0
21	-0.17460	0.0	0.0
END TIMES	30	0.100000	0.0

INTEGRATION INTERVAL 0.01000000
TOTAL TIME 10.00000000
SAMPLE TIME INCREMENT 0.10000000

END
OUTPT

OUTPUT	1	2	3	4	5	6	7	8
END	15	22	1	2	19	20	18	16

Pactolus program for the first type arrangement
without time scale of the differential equation

SOLVING EIGEN VALUES CHE49C
PACTOLUS DIGITAL ANALOG SIMULATOR PROGRAM

1
CONFG

		CONFIGURATION SPECIFICATION			
BLOCK	TYPE	INPUT 1	INPUT 2	INPUT 3	
1	I	0	22	0	
2	I	1	0	00	
3	X	76	76	00	
4	Y	76	0	00	
5	G	3	0	00	
6	G	76	0	00	
7	K	0	0	00	
8	G	76	0	00	
9	G	3	0	00	
10	K	0	0	00	
11	G	4	0	00	
12	G	76	0	00	
13	G	3	0	00	
14	K	0	0	00	
15	+	5	6	7	
16	+	8	0	10	
17	+	11	12	13	
18	+	17	14	00	
19	/	2	15	00	
20	/	14	25	00	
21	Y	1	17	00	
22	G	18	0	00	
23	+	21	20	00	
24	/	1	25	00	
25	G	76	0	00	
26	G	76	0	00	
27	G	76	0	00	

END
ICPAR

INITIAL CONDITIONS AND PARAMETERS

BLOCK	IC/PAR1	PAR2	PAR3
1	0.65458	1.00000	0.0
2	0.06546	0.0	0.0
5	6.00000	0.0	0.0
6	-4.00000	0.0	0.0
7	1.00000	0.0	0.0
8	-20.00000	0.0	0.0
9	18.00000	0.0	0.0
10	5.00000	0.0	0.0
11	-6.00000	0.0	0.0
12	-8.00000	0.0	0.0
13	10.00000	0.0	0.0
14	1.00000	0.0	0.0
21	-2.56800	0.0	0.0
27	10.00000	0.0	0.0

END
TIMES

INTEGRATION INTERVAL 0.00100000
TOTAL TIME 1.00000000
SAMPLE TIME INCREMENT 0.01000000

END
OUTPUT

OUTPUT	1	2	3	4	5	6	7	8
END	27	22	1	2	10	20	18	22

Pactolus program with the relay to switch the equation
to the equation using L Hospital's rule

SOLVING EIGEN VALUES CHE490
PACTOLUS DIGITAL ANALOG SIMULATOR PROGRAM

CONFG

CONFIGURATION SPECIFICATION

BLOCK	TYPE	INPUT 1	INPUT 2	INPUT 3
1	I	0	25	0
2	I	1	0	0
3	X	76	76	0
4	G	75	0	0
5	G	3	0	0
6	K	0	0	0
7	+	4	5	6
8	G	75	0	0
9	G	3	0	0
10	K	0	0	0
11	+	8	9	10
12	/	7	11	0
13	/	2	11	0
14	G	76	0	0
15	K	0	0	0
16	+	14	15	0
17	/	1	16	0
18	X	12	17	0
19	G	13	0	0
20	G	13	0	0
22	G	13	0	0
23	K	0	0	0
24	+	23	76	0
25	R	24	22	21
END ICPAR	21	+	19	20

INITIAL CONDITIONS AND PARAMETERS

BLOCK	IC/PAR1	PAR2	PAR3
1	0.06493	1.00000	0.0
2	0.09276	0.0	0.0
4	-2.00000	0.0	0.0
5	0.18000	0.0	0.0
6	5.00000	0.0	0.0
8	-0.40000	0.0	0.0
9	0.06000	0.0	0.0
10	1.00000	0.0	0.0
14	-0.10000	0.0	0.0
15	1.00000	0.0	0.0
23	-0.30000	0.0	0.0
19	-0.02468	0.0	0.0
22	-0.01238	0.0	0.0
END TIMES	20	0.10000	0.0

INTEGRATION INTERVAL 0.01000000
TOTAL TIME 10.00000000
SAMPLE TIME INCREMENT 0.10000000

END
OUTPT

OUTPUT 1 2 3 4 5 6 7 8
END 1 2 12 13 21 18 7 11

154455

Pactolus program for the second type arrangement
without time scale of the differential equation

SOLVING EIGEN VALUES CHE490
PACTOLUS DIGITAL ANALOG SIMULATOR PROGRAM

CONFG

CONFIGURATION SPECIFICATION	
BLOCK	TYPE INPUT 1 INPUT 2 INPUT 3
1	I 0 19 0
2	I 1 0 0
3	X 76 76 0
4	G 76 0 0
5	G 3 0 0
6	K 0 0 0
7	+ 4 5 6
8	G 76 0 0
9	G 3 0 0
10	K 0 0 0
11	+ 9 9 10
12	/ 7 11 0
13	/ 2 11 0
14	K 0 0 0
15	+ 14 20 0
16	/ 1 15 0
17	X 12 16 0
18	G 13 0 0
20	G 76 0 0
19	+ 17 18 0

END
ICPAR

INITIAL CONDITIONS AND PARAMETERS

BLOCK	IC/PAR1	PAR2	PAR3
1	0.65458	1.00000	0.0
2	0.06546	0.0	0.0
4	-20.00000	0.0	0.0
5	18.00000	0.0	0.0
6	5.00000	0.0	0.0
8	-4.00000	0.0	0.0
9	6.00000	0.0	0.0
10	1.00000	0.0	0.0
14	1.00000	0.0	0.0
20	-1.00000	0.0	0.0
18	-2.56800	0.0	0.0

END
TIMES

INTEGRATION INTERVAL 0.00100000
TOTAL TIME 1.00000000
SAMPLE TIME INCREMENT 0.01000000

END
OUTPUT

OUTPUT 1 2 3 4 5 6 7 8
1 2 19 12 13 17 7 11

RUN

Pactolus program for the second type arrangement
with time scale of the differential equation

SOLVING EIGEN VALUES CHE490
PACTOLUS DIGITAL ANALOG SIMULATOR PROGRAM

CONFG

BLOCK	CONFIGURATION SPECIFICATION			
	TYPE	INPUT 1	INPUT 2	INPUT 3
1	I	0	21	0
2	I	1	0	0
3	X	76	76	0
4	G	76	0	0
5	G	3	0	0
6	K	0	0	0
7	+	4	5	6
8	G	76	0	0
9	G	3	0	0
10	K	0	0	0
11	+	8	9	10
12	/	7	11	0
13	/	2	11	0
14	G	76	0	0
15	K	0	0	0
16	+	14	15	0
17	/	1	16	0
18	X	12	17	0
19	G	13	0	0
20	G	18	0	0
21	+	19	20	0

END
ICPAR

INITIAL CONDITIONS AND PARAMETERS

BLOCK	IC/PAR1	PAR2	PAR3
2	0.95309	0.0	0.0
1	0.00476	1.00000	0.0
4	-2.00000	0.0	0.0
5	0.18000	0.0	0.0
5	5.00000	0.0	0.0
8	-0.40000	0.0	0.0
9	0.06000	0.0	0.0
10	1.00000	0.0	0.0
14	-0.10000	0.0	0.0
15	1.00000	0.0	0.0
19	-0.00096	0.0	0.0
20	0.10000	0.0	0.0

END
TIMES

INTEGRATION INTERVAL 0.01000000
TOTAL TIME 10.00000000
SAMPLE TIME INCREMENT 0.10000000

END
OUTPT

OUTPUT 1 2 3 4 5 6 7 8
1 2 12 13 21 18 7 11

END
RUN

APPENDIX (7)

- (1) Computer circuit for the trial and error procedure carried out on the conventional analog computer. The numerical settings and the outputs of the components are presented.
- (2) PACTOLUS program with the first type arrangement with or without time scale of the differential equation to check the difference of the results.
- (3) PACTOLUS program with the second type arrangement with or without time scale of the differential equation to assure that both arrangements can be applied on PACTOLUS. Programming on the analog computer; the second arrangement is used for convenient observance of the component-overload, especially as the problem is integrated close to the boundary $y=1.0$.

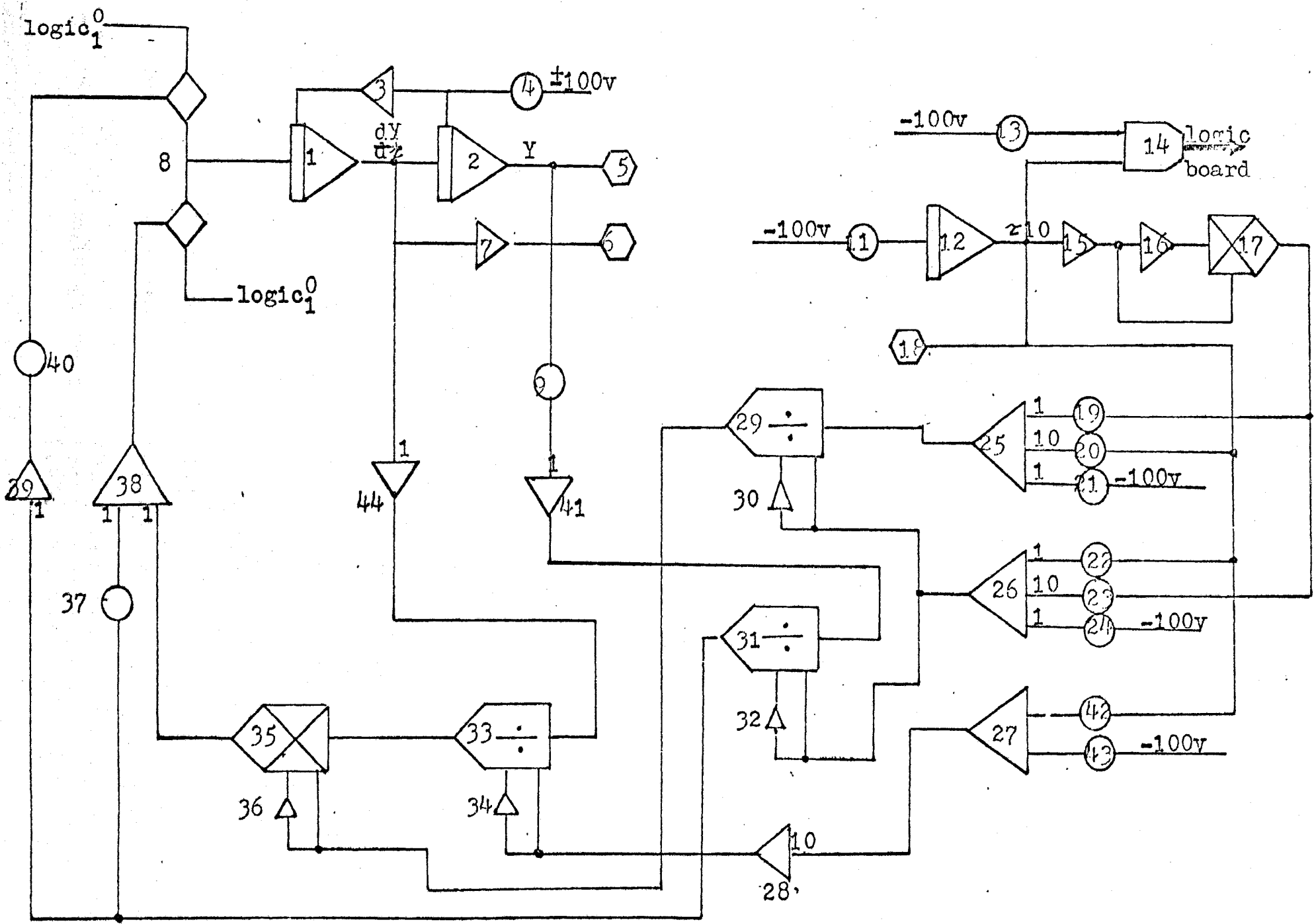


Figure A.1: Conventional analog computer program for Handlos and Baron Model

TABLE A.6: STATIC POT SETTINGS AND AMPLIFIER IDENTIFICATION

(I)			
<u>Amp. No.</u>	<u>Amp. Purpose</u>	<u>Amp. Output</u>	<u>Corresponding Patchboard Element</u>
01	Int.	$-\frac{dY}{d\tau}$	A-2
02	Int.	Y	A-3
03	Inverter or high gain amplifier	Y(0)	C-3
07	Inverter	$\frac{dY}{d\tau}$	2A-9
12	Int.	τ	A-1
15	high gain amplifier	-10τ	B-1
16	inverter	10τ	B-2
17	multiplier (squarer)	τ	A-5
25	+	$(0.18\tau^2 - 2.0\tau + 5)$	B-3
26	+	$10(0.06\tau^2 - 0.4\tau + 1)$	B-4
27	+	$(1 - 0.1\tau)$	D-1
28	High gain amp.	$-10(1 - 0.1\tau)$	C-2
29	divider	$\frac{10(0.18\tau^2 - 2.0\tau + 5)}{(0.06\tau^2 - 0.4\tau + 1)}$	A-6 A-7
30	inverter	$-(0.06\tau^2 - 0.4\tau + 1)$	2B-9
31	divider	$\frac{Y}{(0.06\tau^2 - 0.4\tau + 1)}$	B-5 B-6
32	inverter	$-10(0.06\tau^2 - 0.4\tau + 1)$	2D-9
34	inverter	$10(1 - 0.1\tau)$	2A-10
35	multiplier	$\frac{-0.1(0.18\tau^2 - 2.0\tau + 5)}{(1 - 0.1\tau)(0.06\tau^2 - 0.4\tau + 1)}$	D-4

36	inverter	$\frac{-10(0.18\tau^2 - 2.0\tau + 5)}{(0.06\tau^2 - 0.4\tau + 1)}$	2B-10
38	+	$\frac{d^2 Y}{dz^2}$	D-3
39	inverter	$-\frac{\lambda_n Y}{(0.06\tau^2 - 0.4\tau + 1)}$	2C-9

(II)

<u>Pot No.</u>	<u>Numerical Settings</u>	<u>Corresponding Patchboard Component</u>
04	Y(0) (initial approximation)	BP-2
09	0.1	BP-5
11	0.01	BP-3
13	0.093	BP-10
19	0.18	AP-3
20	0.20	AP-2
21	0.05	AP-4
22	0.40	AP-6
23	0.60	AP-5
24	0.10	AP-7
42	0.10	AP-1
43	0.01	AP-8
37	0.01 λ_n	BP-9
40	0.005 λ_n	BP-8

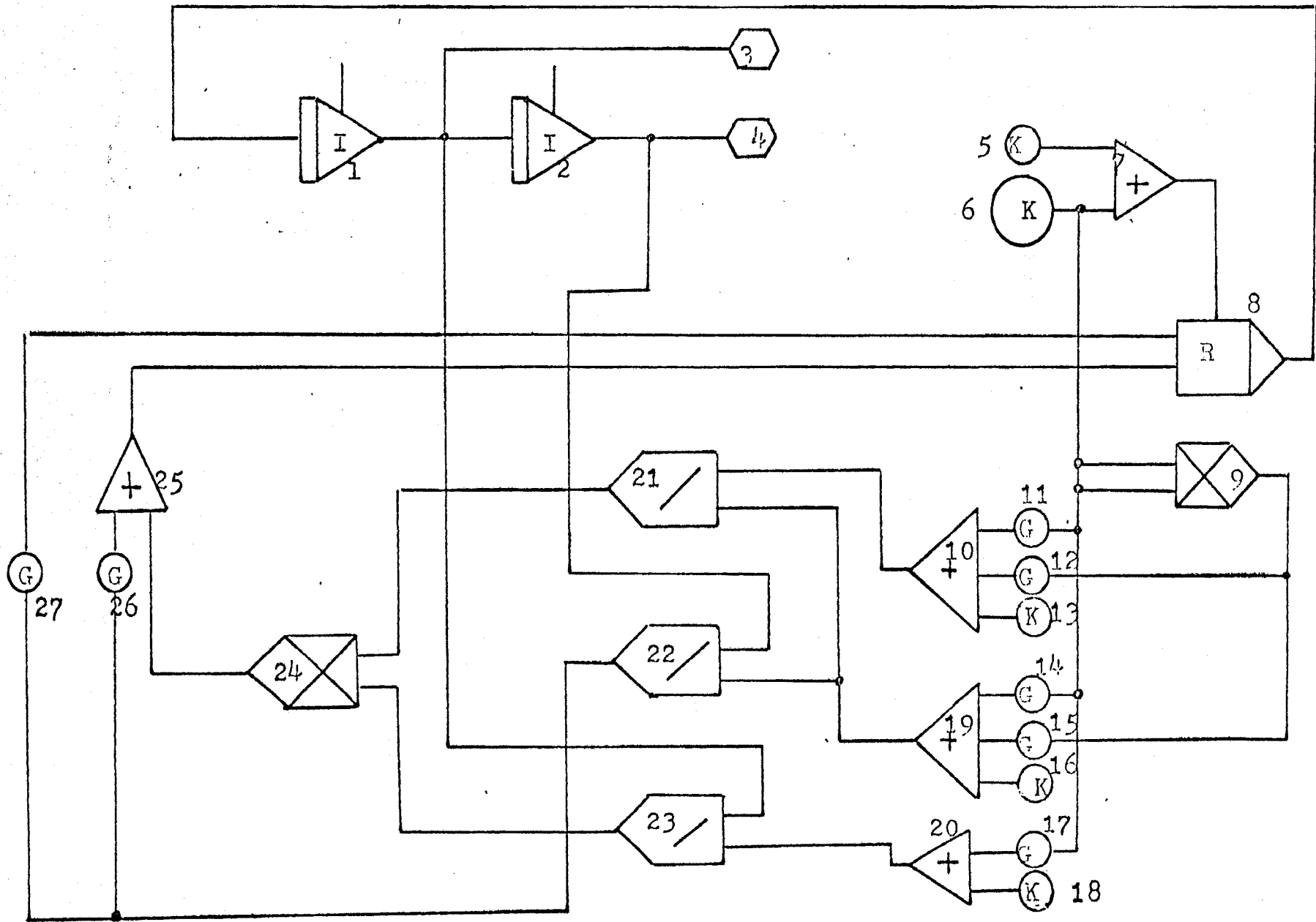


Figure A2: PACTOLUS program with relay switch for $y=1.0$

TABLE A.7: BLOCK REPRESENTATIONS AND NUMERICAL SETTINGS

<u>Block</u>	<u>Type</u>	<u>Output</u>	<u>Numerical Settings</u>
1	I	$\frac{dY}{dy}$	
2	I	Y	
3	output	$\frac{dY}{dy}$	
4	output	Y	
5	K		-0.93 (chosen close to 1.0)
6	K		1.0
7	+		
8	R		
9	x	y^2	
10	+	$(18y^2 - 20y + 5)$	
11	G		-20.0
12	G		18.0
13	K		5.00
14	G		-4.0
15	G		6.00
16	K		1.00
17	G		-1.00
18	K	1.00	
19	+	$(6y^2 - 4.0y + 1)$	
20	+	$(1 - y)$	
21	/	$\frac{(18y^2 - 20y + 5)}{(6y^2 - 4y + 1)}$	

22	/	$\frac{Y}{(6y^2 - 4y + 1)}$
23	/	$\frac{1}{(1-y)} \frac{dY}{dy}$
24	x	$\frac{(18y^2 - 20y + 5)}{(1-y)(6y^2 - 4y + 1)} \frac{dY}{dy}$
25	+	$\frac{d^2Y}{dy^2}$
26	G	$-\lambda_n$
27	G	$-0.5\lambda_n$

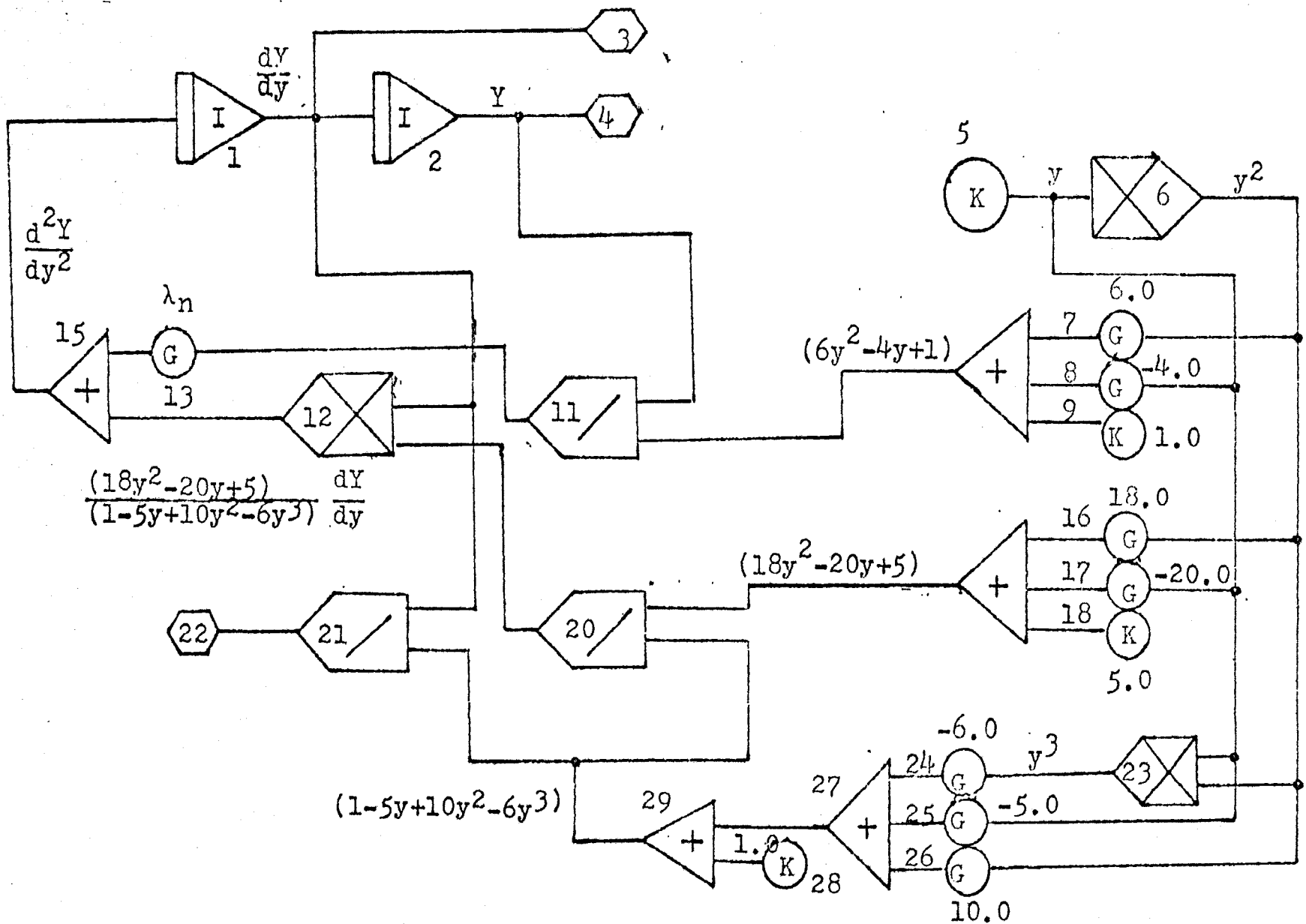


Figure A.3: PACTOLUS program without time scale for the first type circuit arrangement

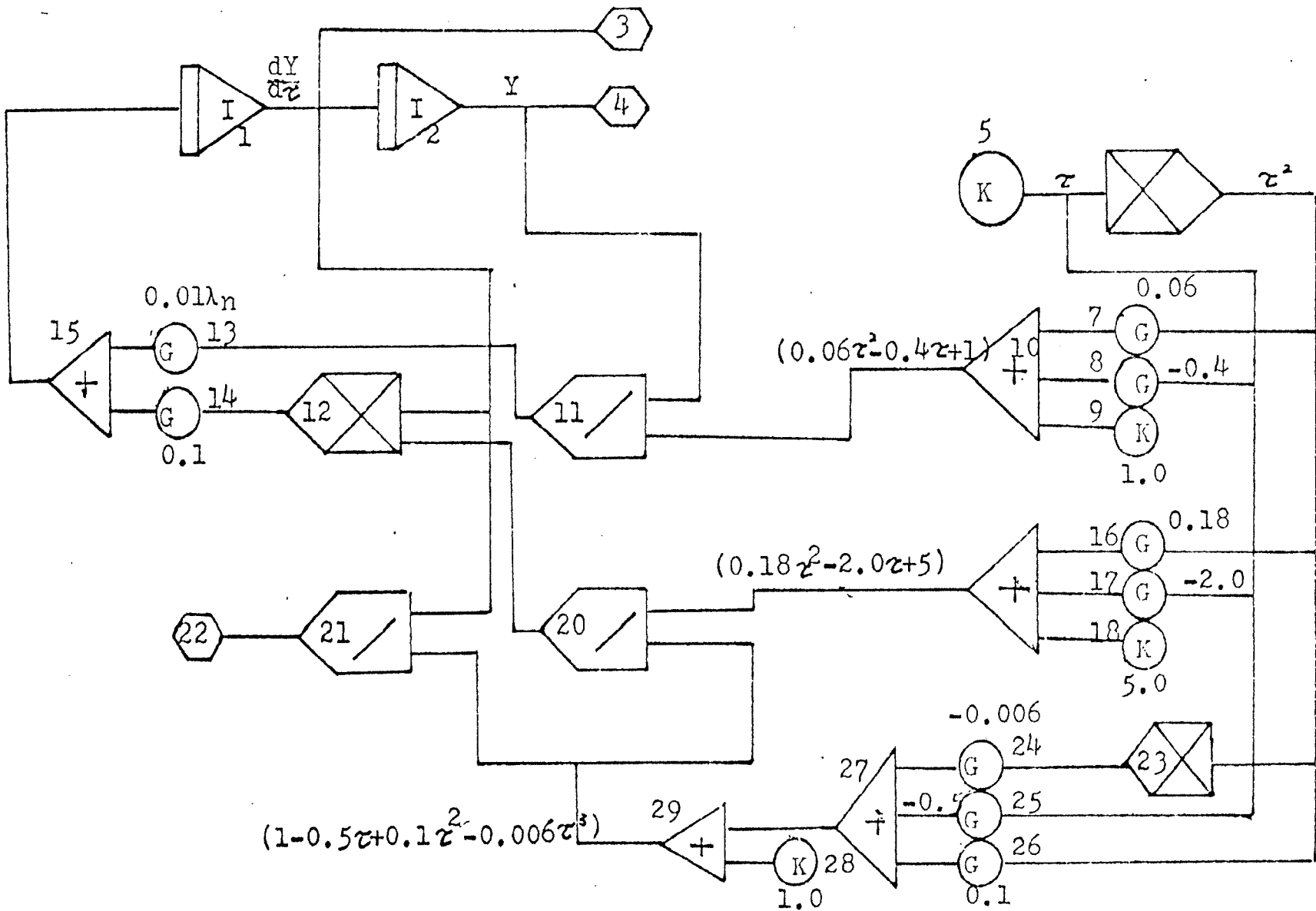


Figure A.4: PACTOLUS program with time scale for the first type circuit arrangement

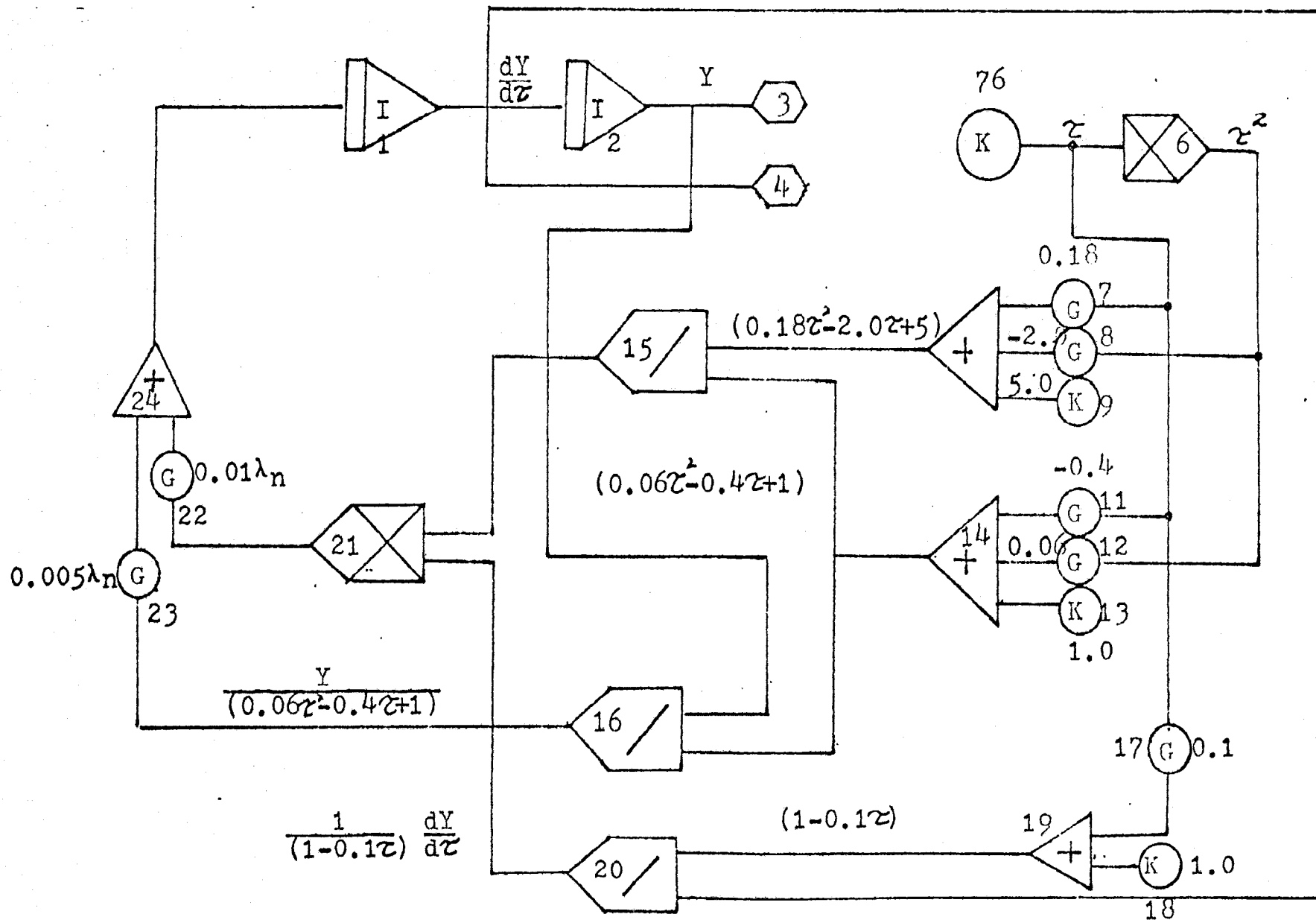


Figure A.5: PACTOLUS program with time scale for the second type circuit arrangement.

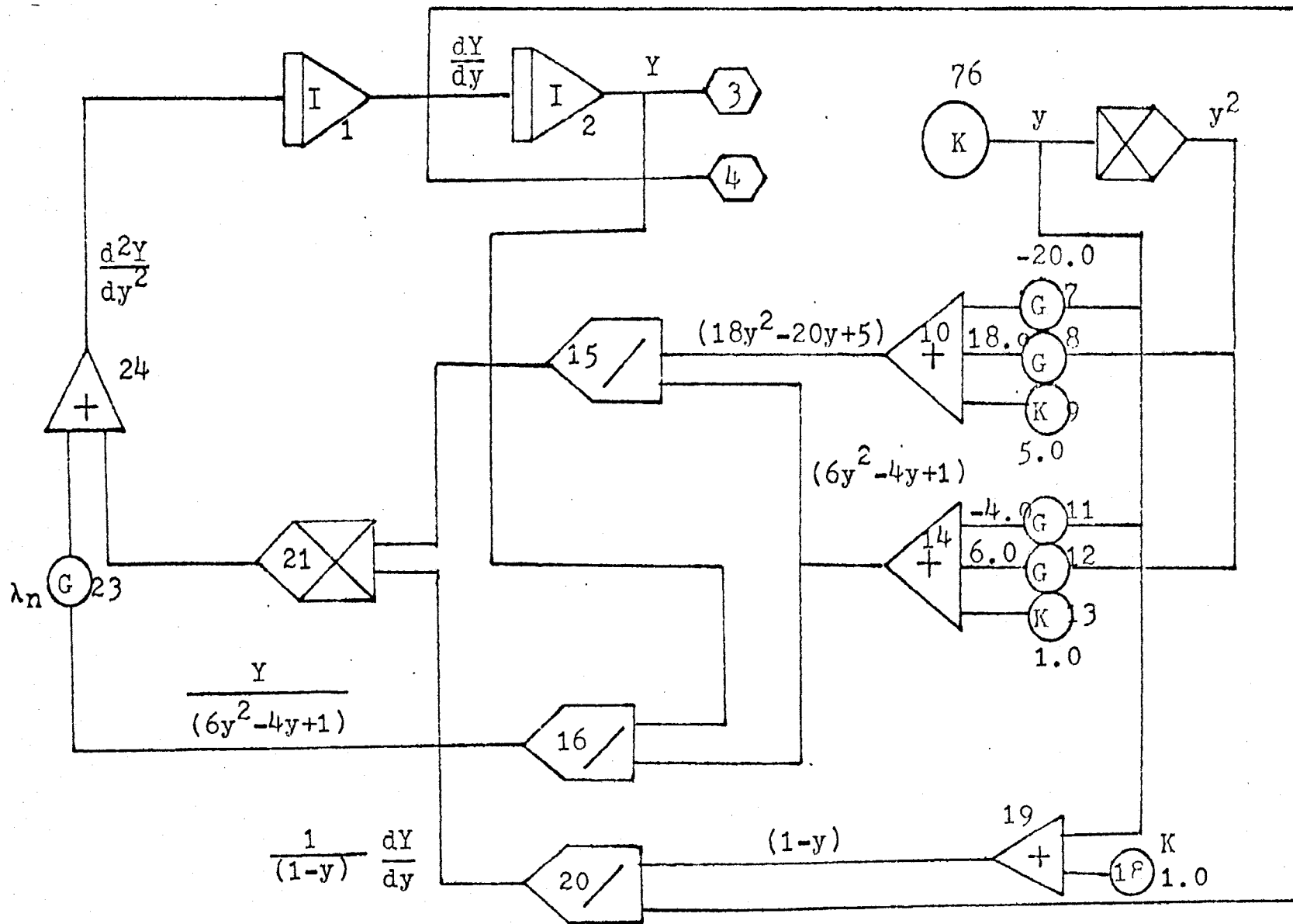


Figure A.6: PACTOLUS program without time scale for the second type of circuit arrangement

APPENDIX 8

- (1) Curves of fraction extracted versus dimensionless time
(Runge-Kutta method by Patel)
- (2) Curve of fraction extracted versus dimensionless time
(Hamming's method by Patel)
- (3) Curve of fraction extracted versus dimensionless time
(Finite-difference method by Patel)

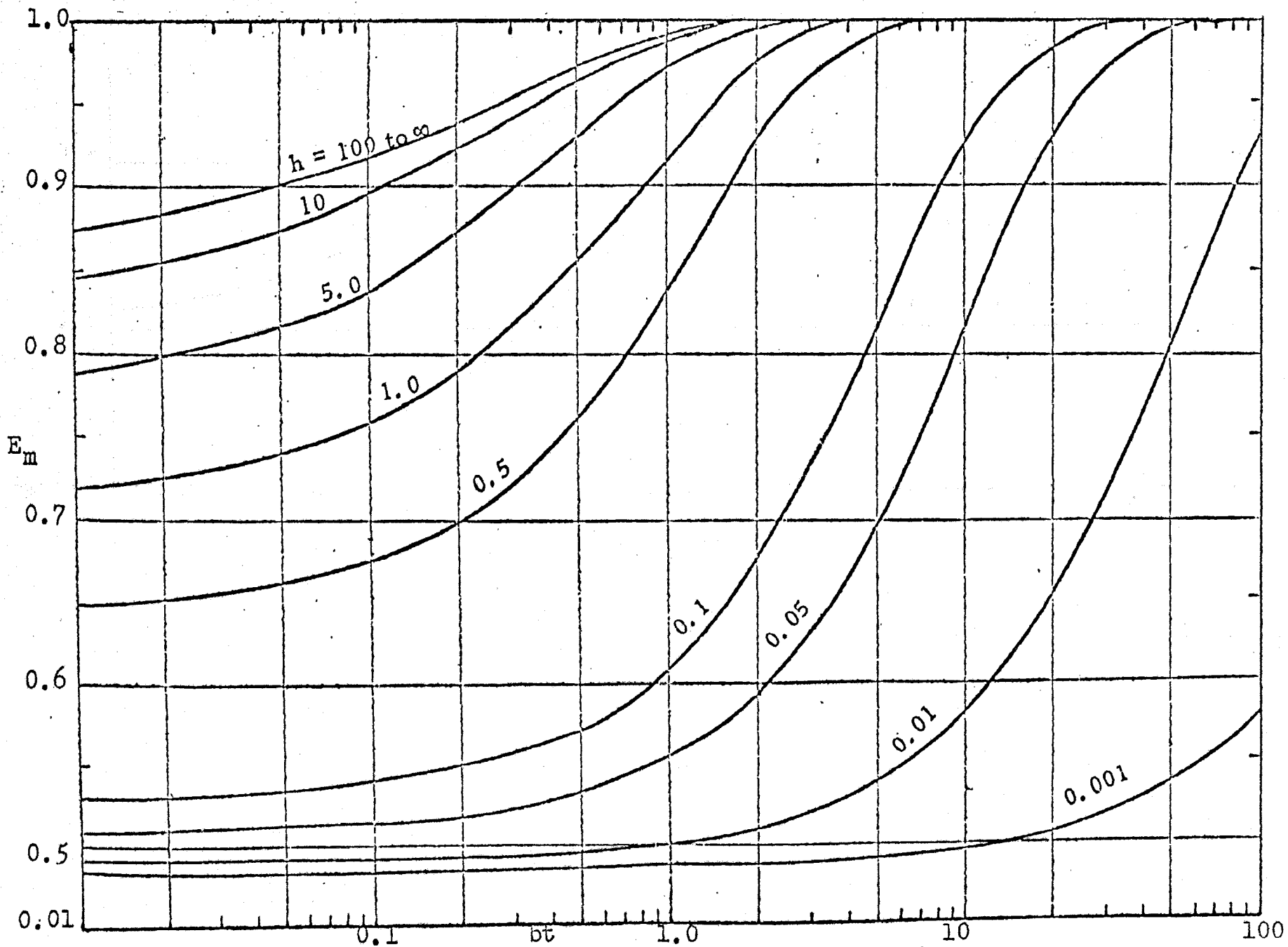


Figure A7: Fraction extracted versus dimensionless time (Runge-Kuta method by Patel)
(28)

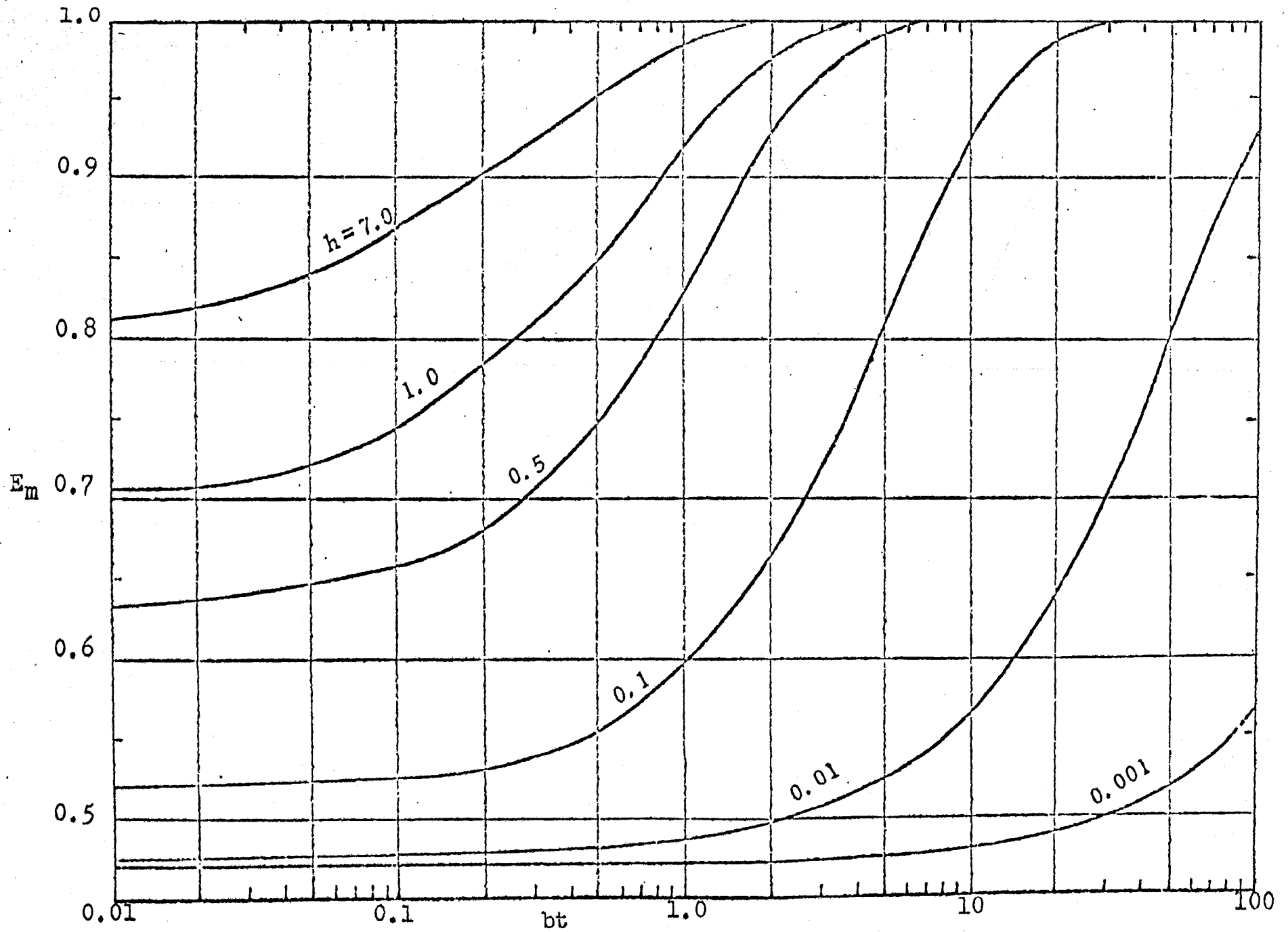


Figure A.8: Fraction extracted versus dimensionless time (Hamming's method by Patel (28)).

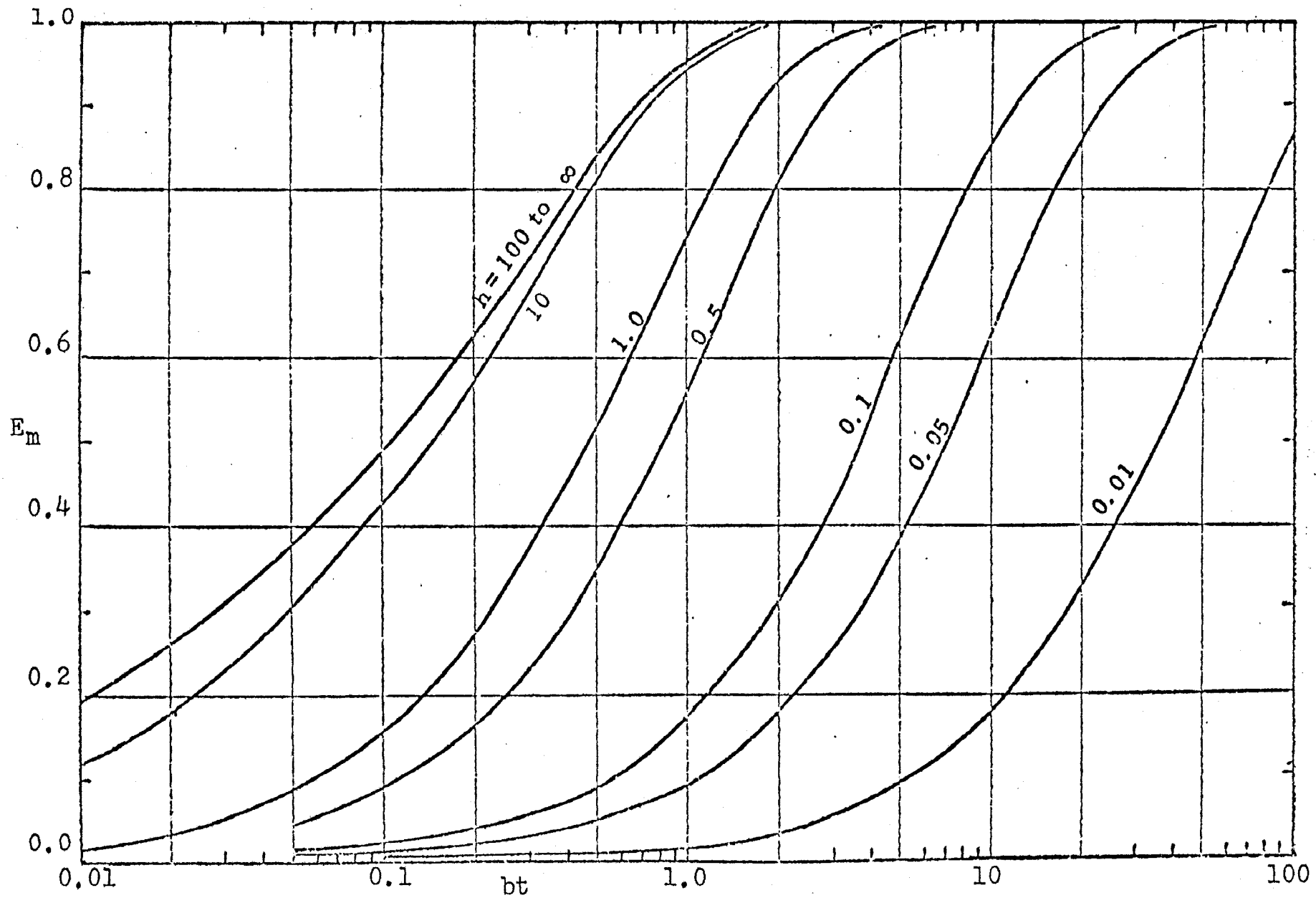


Figure A.9 : Fraction extracted versus dimensionless time(Finite-difference method by Patel (28)).

APPENDIX 9

- (1) Analog computer with its hybrid parts results (when the modified continuous phase resistance $h = 25.0$).
- (2) Analog computer result (when the modified continuous phase resistance $h = 25.0$).

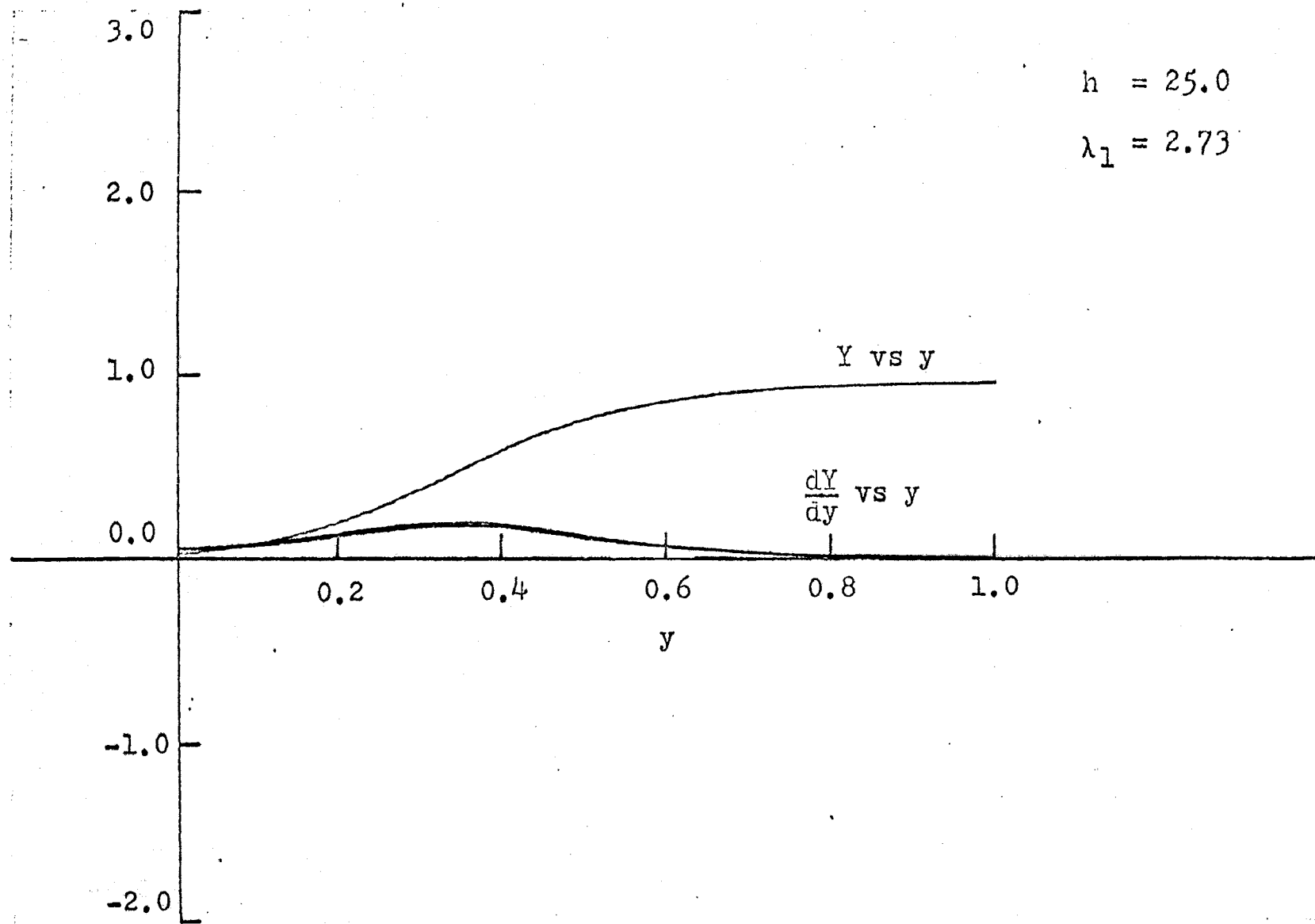


Figure A.10: Solution of Handlos and Baron Model
on an iterative analog computer

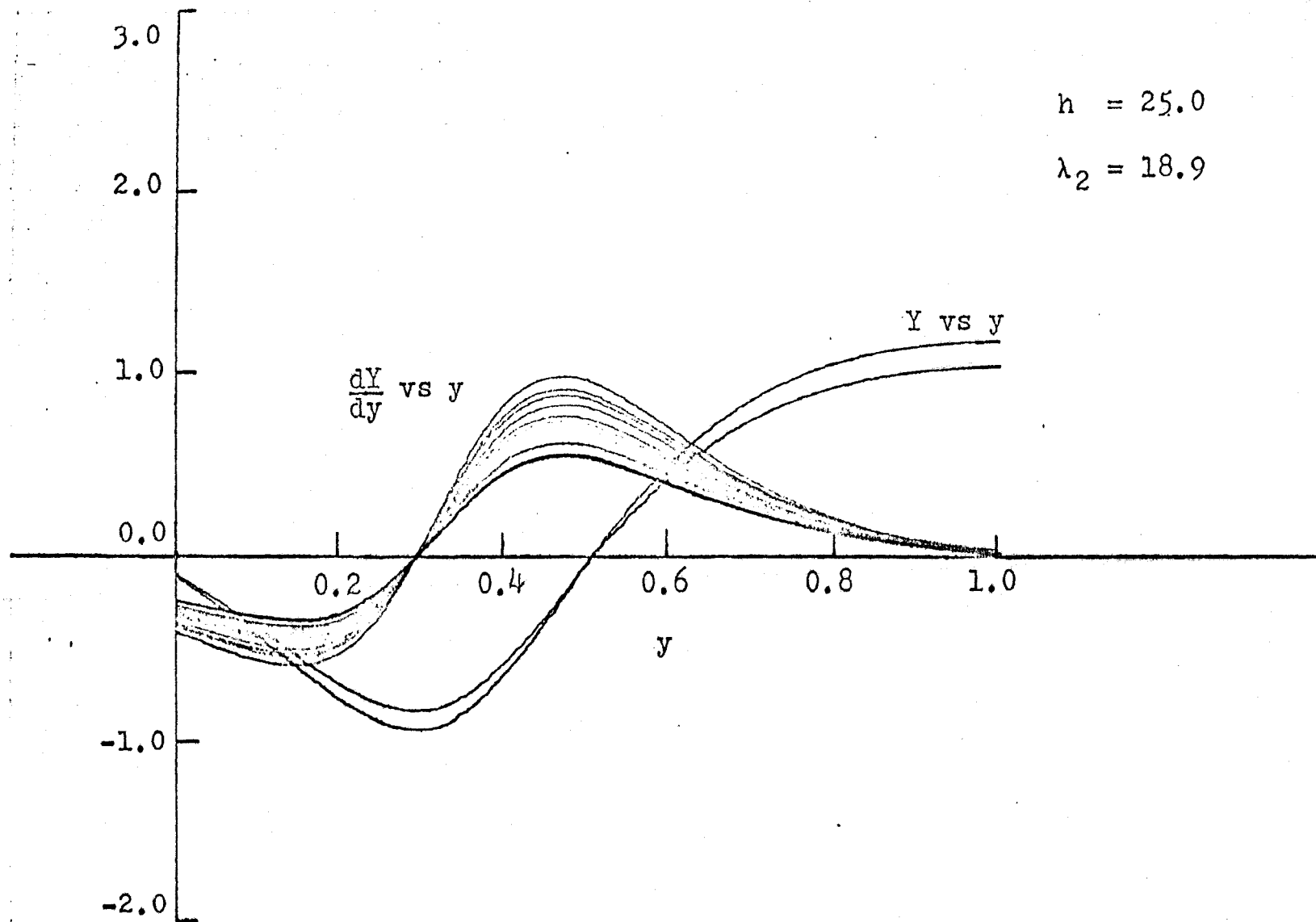


Figure A.11: Solution of Handlos and Baron Model
on an iterative analog computer

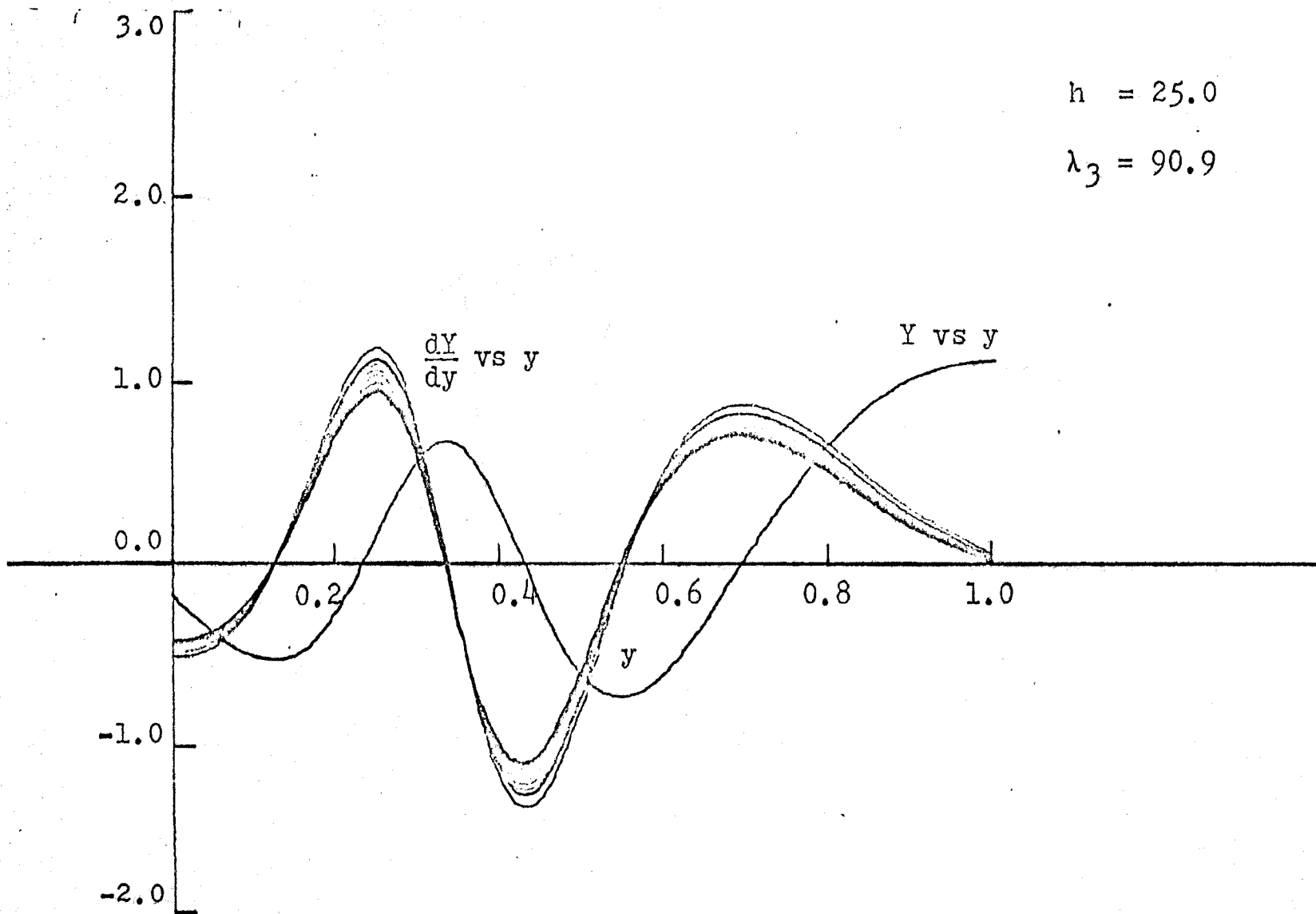


Figure A.12: Solution of Handlos and Baron Model
 on an iterative analog computer

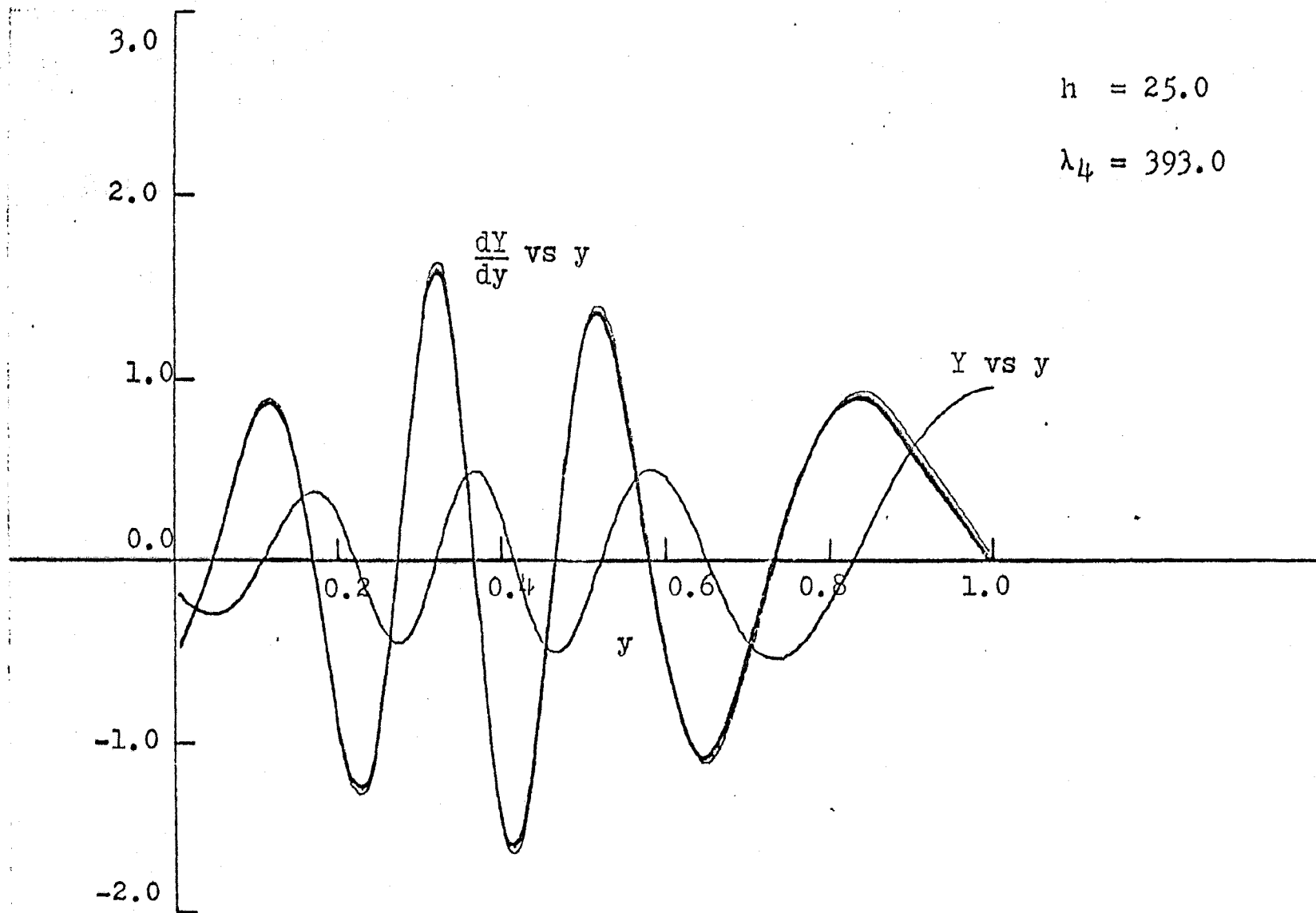


Figure A.13: Solution of Handlos and Baron Model
on an iterative analog computer

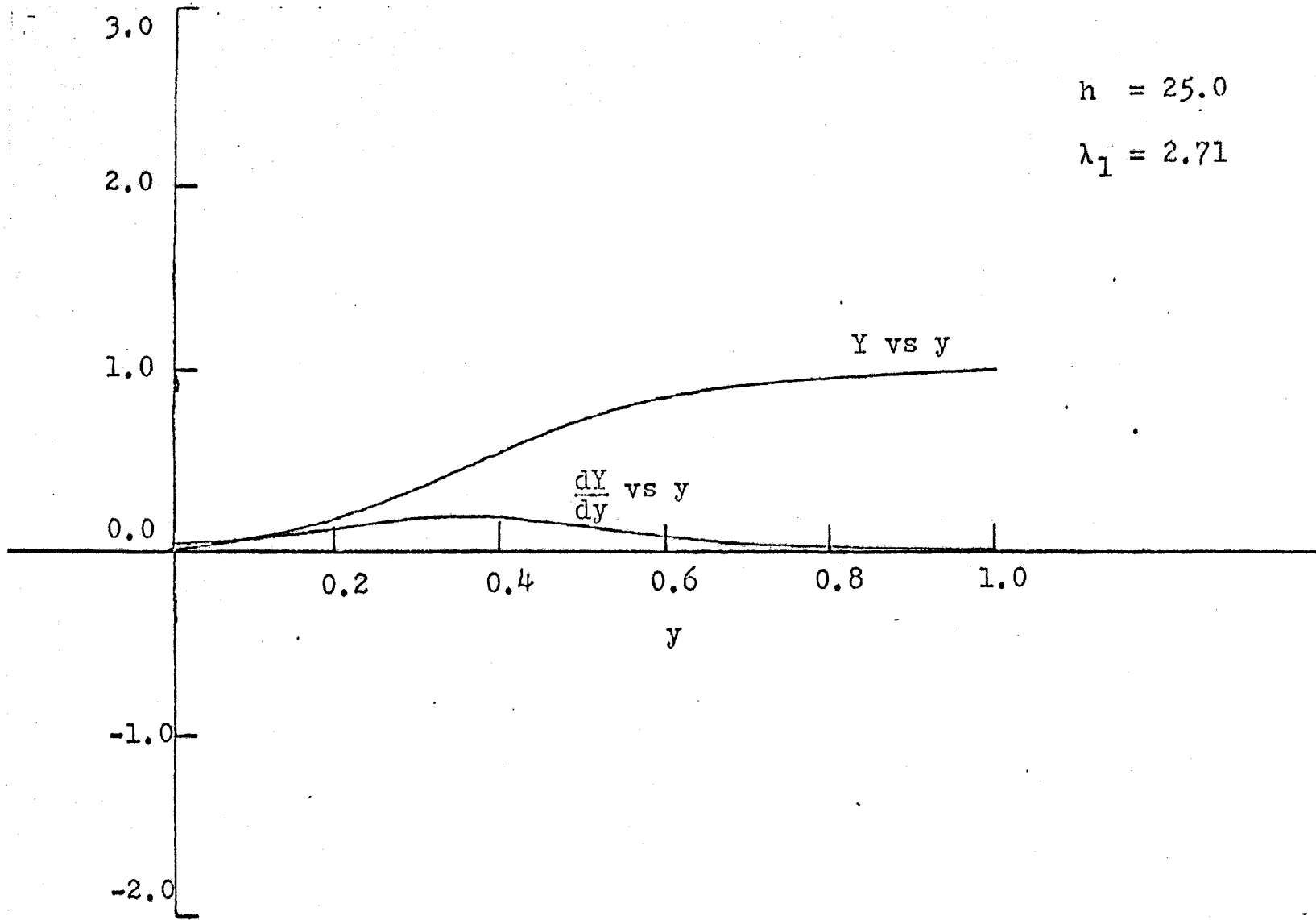


Figure A.14: Solution of Handlos and Baron Model
on a conventional analog computer

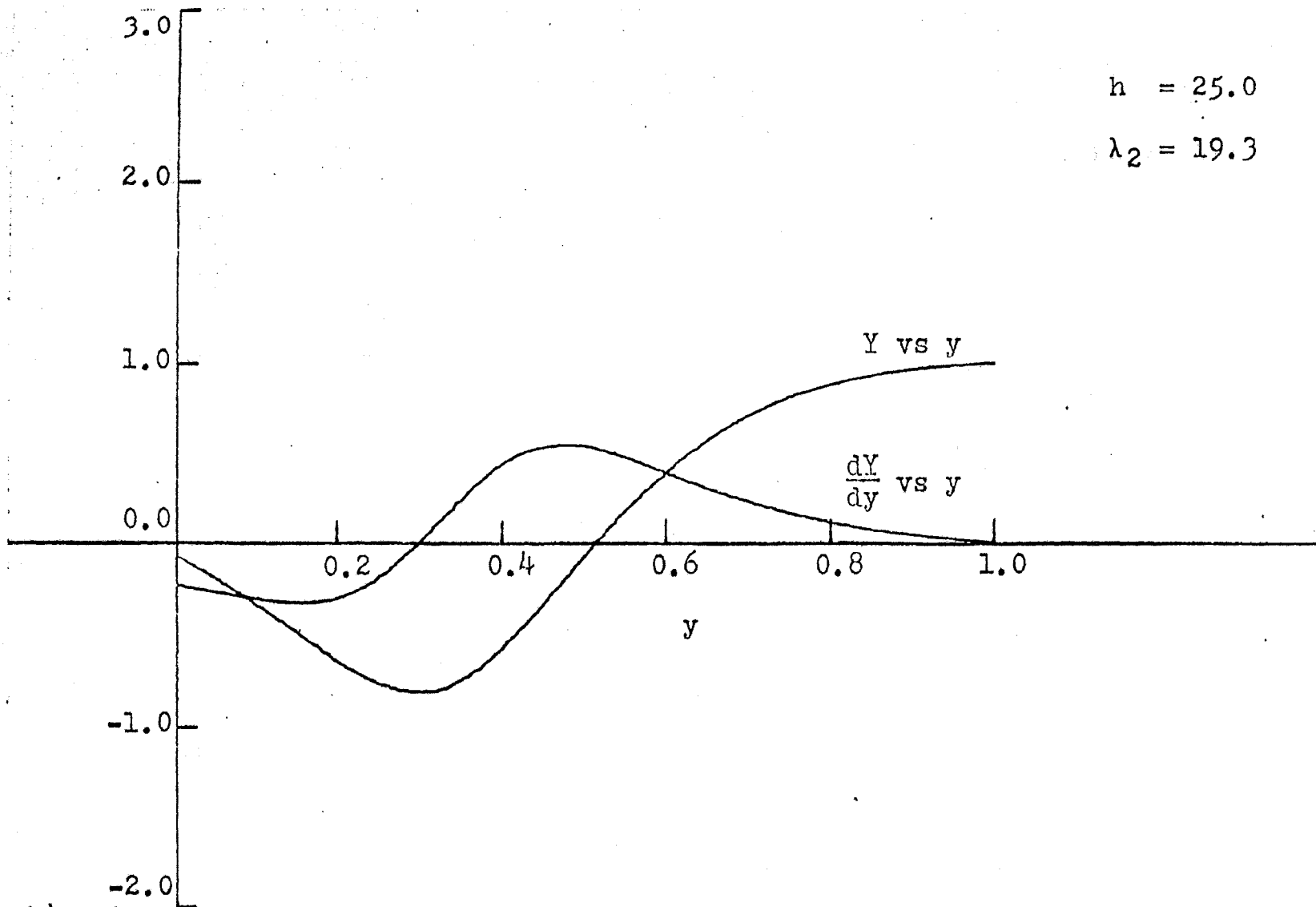


Figure A.15: Solution of Handlos and Baron Model
on a conventional analog computer

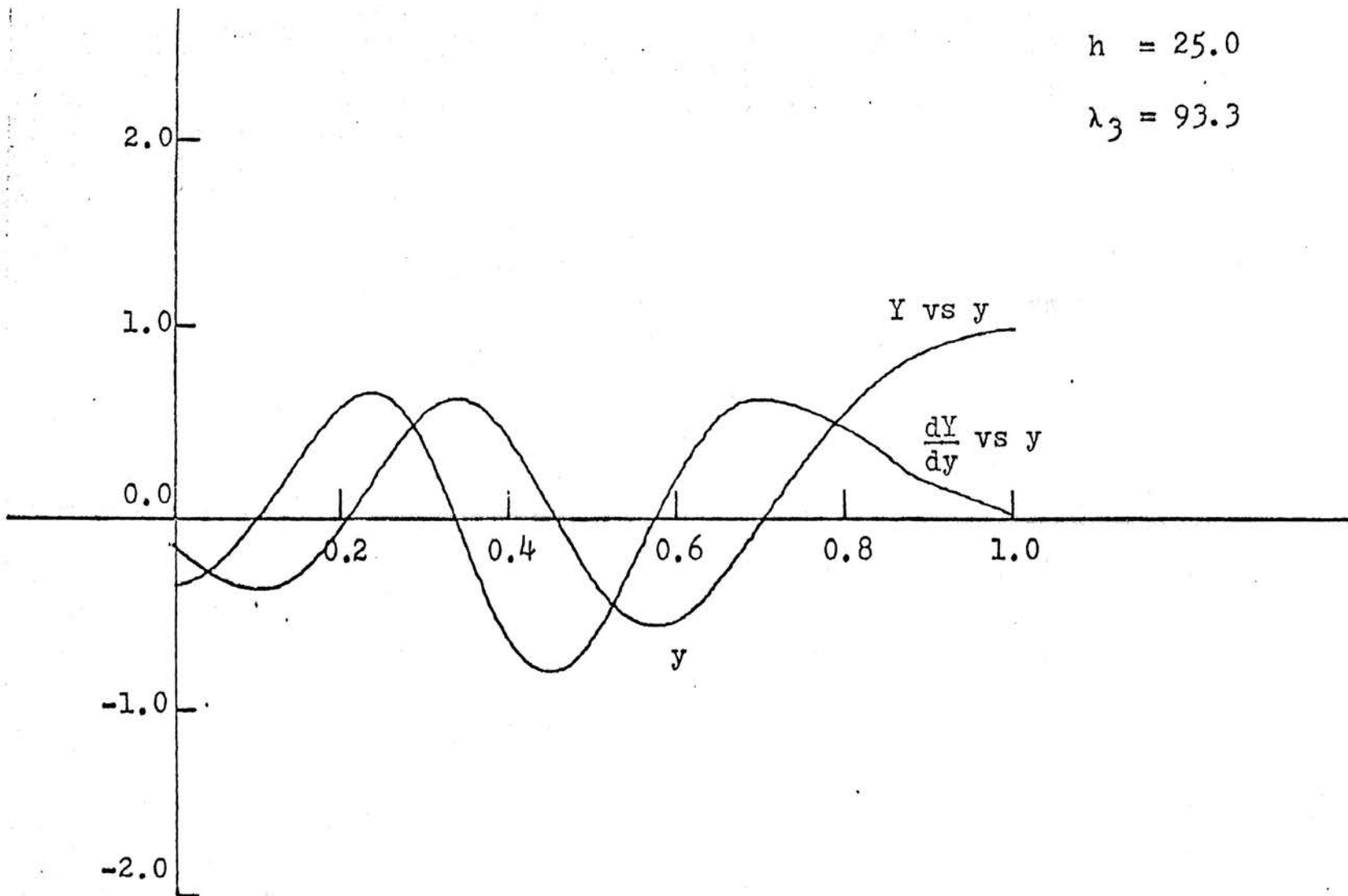


Figure A.16: Solution of Handlos and Baron Model
on a conventional analog computer

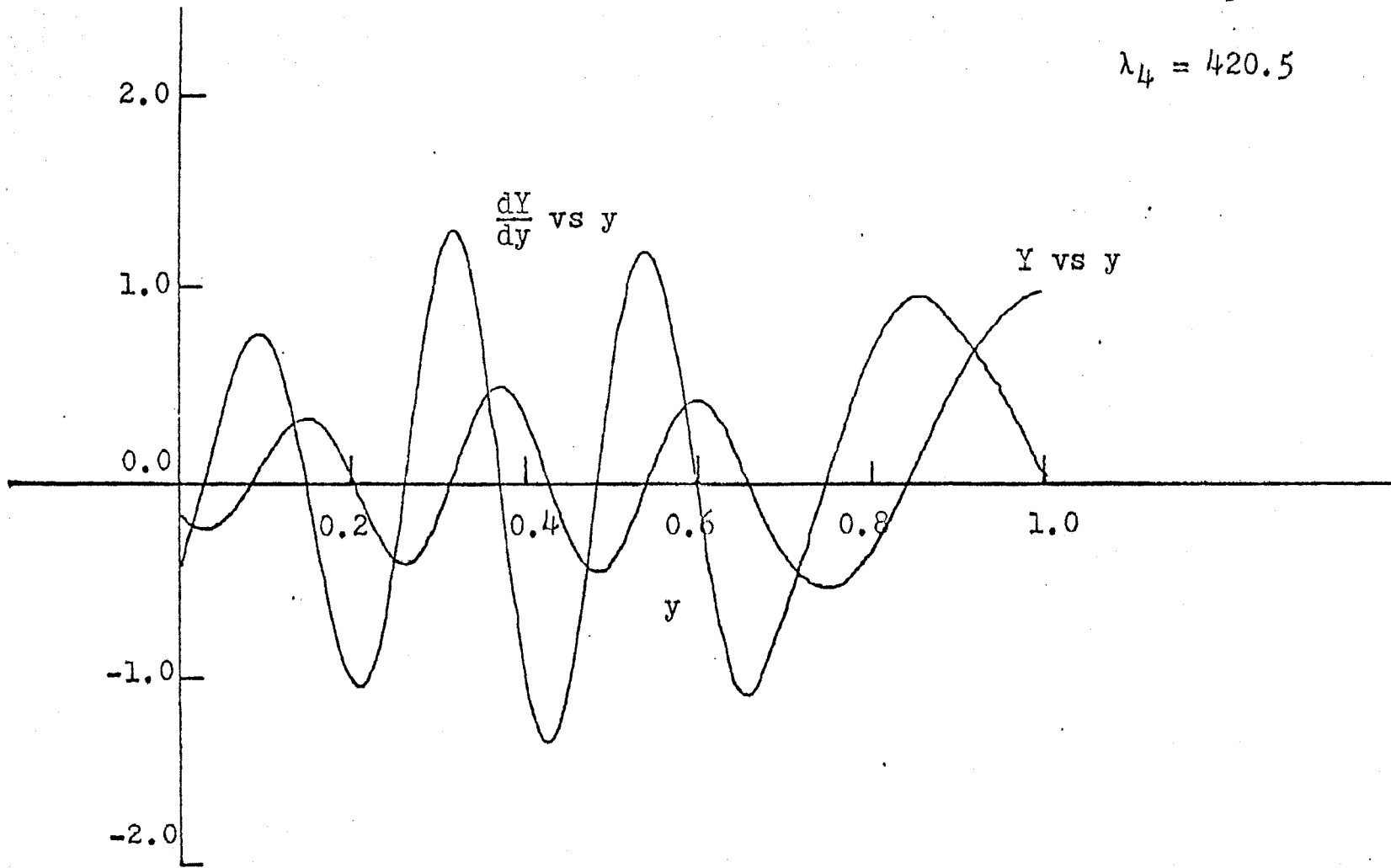


Figure A.17: Solution of Handlos and Baron Model
on a conventional analog computer

APPENDIX 10.1: SCALED EIGENFUNCTIONS GENERATED BY
AN ITERATIVE ANALOG COMPUTER

a	$\frac{dY(0)}{dy} \Big _1$	$\frac{dY(0)}{dy} \Big _2$	$\frac{dY(0)}{dy} \Big _3$	$\frac{dY(0)}{dy} \Big _4$
010	0.000950	-0.000530	0.000482	-0.000270
020	0.002120	-0.001070	0.000782	-0.000570
100	0.008850	-0.005350	0.004560	-0.003000
500	0.046500	-0.028500	0.021700	-0.014750
000	0.087500	-0.061000	0.043700	-0.030000
0000	0.315000	-0.320000	0.230000	-0.160000
0000	0.445000	-0.680000	0.485000	-0.282000
5000	0.558000	-1.430000	1.250000	-0.710000
0000	0.600000	-2.010000	2.040000	-1.390000
0000	0.700000	-2.250000	2.160000	-1.930000
.0000	0.600000	-3.040000	-1.850000	-2.620000
.0000	0.520000	-2.300000	-3.900000	-4.680000
.0000	0.540000	-2.520000	-3.630000	-5.100000
.0000	0.575000	-2.370000	-3.760000	-5.590000
.0000	0.565000	-2.365000	-3.750000	-5.830000
.0000	0.560000	-2.350000	-3.630000	-5.900000
0.00	0.561000	-2.250000	-3.740000	-6.020000
0.00	0.562000	-2.700000	-3.840000	-6.060000
0.00	0.560000	-2.400000	-3.780000	-6.080000
0.00	0.570000	-2.250000	-3.790000	-6.080000
00.0	0.570000	-2.470000	-3.770000	-6.050000
∞	0.570000	-2.200000	-3.800000	-6.070000

APPENDIX 10.2: EIGENFUNCTION OBTAINED FROM A
CONVENTIONAL ANALOG COMPUTER

	$\frac{dY(0)}{dy} \Big _1$	$\frac{dY(0)}{dy} \Big _2$	$\frac{dY(0)}{dy} \Big _3$	$\frac{dY(0)}{dy} \Big _4$
0	0.000955	-0.00055	0.000405	-0.000288
0	0.001910	-0.00110	0.000792	-0.000578
00	0.009450	-0.00553	0.003920	-0.002890
00	0.047500	-0.02960	0.018500	-0.014450
00	0.089000	-0.05790	0.037600	-0.028900
00	0.274000	-0.31000	0.187500	-0.126000
00	0.370000	-0.68000	0.385000	-0.275000
00	0.475000	-1.80000	0.900000	-0.660000
00	0.475000	-2.60000	1.750000	-1.345000
00	0.535000	-2.73000	2.160000	-1.860000
00	0.460000	-3.02000	-2.30000	-2.650000
00	0.500000	-3.05000	-3.33000	-4.130000
00	0.510000	-2.88000	-3.42000	-4.570000
00	0.520000	-2.96000	-3.60000	-4.880000
00	0.525000	-2.90000	-3.60000	-4.850000
00	0.525000	-2.80000	-3.57000	-5.320000
00	0.525000	-2.73000	-3.26000	-5.990000
00	0.530000	-2.77000	-3.32000	-6.290000
00	0.560000	-2.78000	-3.42000	-6.300000
00	0.580000	-2.78000	-3.32000	-6.190000
.0	0.585000	-2.79000	-3.32000	-6.190000
	0.590000	-2.82000	-3.39000	-6.250000

APPENDIX 10.3: SCALED EIGENFUNCTIONS OBTAINEDBY PACTOLUS

h	$\frac{dY(0)}{dy} \Big _1$	$\frac{dY(0)}{dy} \Big _2$	$\frac{dY(0)}{dy} \Big _3$	$\frac{dY(0)}{dy} \Big _4$
.0010	0.00104	-0.00060	0.000480	-0.00030
.0020	0.00203	-0.00122	0.000969	-0.00059
.0100	0.01011	-0.00613	0.004800	-0.00298
.0500	0.47650	-0.03092	0.024000	-0.01490
.1000	0.09135	-0.06255	0.048000	-0.02975
.5000	0.33000	-0.33240	0.243700	-0.14900
.0000	0.47310	-0.68080	0.489500	-0.29800
.5000	0.60200	-1.49300	1.195200	-0.74170
.0000	0.64100	-2.06200	2.055240	-1.46200
.0000	0.64930	-2.20450	2.470000	-2.00180
0.000	0.65460	-2.30470	-1.19140	-2.71200
5.000	0.65970	-2.32800	-3.74090	-4.75200
10.000	0.66000	-2.31330	-3.79600	-5.12200
50.000	0.66110	-2.30370	-3.84580	-5.61660
70.000	0.66120	-2.30460	-3.86370	-5.79500
100.00	0.66123	-2.28140	-3.87520	-5.99100
250.00	0.66150	-2.28144	-3.87520	-5.99170
500.00	0.66170	-2.26770	-3.87760	-5.99170
700.00	0.66166	-2.26990	-3.87200	-5.96400
1000.0	0.66185	-2.27100	-3.87600	-5.96400
∞	0.66176	-2.27430	-3.87700	-5.96500

APPENDIX 11

Digital computer program for evaluating the fraction extracted
 E_m versus dimensionless time bt .

```

/WAT4 CM120210, TIME=1, PAGES=10 D KUD JEFFREY
C CALCULATION OF EXTRACTION  $E_m$  FOR
C SHORT CONTACT TIME AND LONG CONTACT TIME
C LET A REPRESENT EIGEN VALUES
C C REPRESENT THE INITIAL CONDITION OF SLOPE
C H REPRESENT THE CONTINUOUS PHASE RESISTANCE
1 WRITE(3,471)
2 471 FORMAT(//6X, 'H IS THE CONTINUOUS
IPHASE RESISTANCE')
3 WRITE(3,472)
4 472 FORMAT(//6X, 'RESULT OF HANDLOS AND BARON
IMODEL BY TRIAL AND ERROR ON THE
ITERATIVE ANALOG COMPUTER')
5 DO 1 I=1,5
6 READ(1,755)H
7 READ(1,200)BN1,A1
8 READ(1,201)BN2,A2
9 READ(1,202)BN3,A3
10 READ(1,203)BN4,A4
11 755 FORMAT(F10.5)
12 200 FORMAT(2F15.8)
13 201 FORMAT(2F15.8)
14 202 FORMAT(2F15.8)
15 203 FORMAT(2F15.8)
16 WRITE(3,756)H
17 756 FORMAT(//6X, 'H=', F10.5)
18 WRITE(3,700)BN1,BN2,BN3,BN4
19 700 FORMAT(//6X, 'BN1=', F15.4, 3X, 'BN2=', F15.4,
13X, 'BN3=', F15.4, 3X, 'BN4=', F15.4)
20 T=C.C
21 DO 2 J=1,10
22 S=A1*T
23 IF(S.GT. 173)GO TO 401
24 EM=1.-2.*BN1**2/EXP(A1*T)
25 GO TO 31
26 401 EM=1.0
27 31 WRITE(3,102)T,EM
28 102 FORMAT(6X, 'T=', F8.3, 3X, 'EM=', F10.5)
29 2 T=T+C.C1
30 T=C.10
31 DO 3 K=1,10
32 S=A1*T
33 IF(S.GT. 173)GO TO 402
34 EM=1.-2.*BN1**2/EXP(A1*T)
35 GO TO 32
36 402 EM=1.0
37 32 WRITE(3,103)T,EM
38 103 FORMAT(6X, 'T=', F8.3, 3X, 'EM=', F10.5)
39 3 T=T+C.10
40 T=1.C
41 DO 4 L=1,10
42 S=A1*T
43 IF(S.GT. 173)GO TO 403
44 EM=1.-2.*BN1**2/EXP(A1*T)
45 GO TO 33
46 403 EM=1.0
47 33 WRITE(3,104)T,EM

```

```

48      104  FORMAT(6X,'T=',F8.3,3X,'EM=',F10.5)
49      4    T=T+1.0
50      T=10.0
51      DO 5 M=1,10
52      S=A1*T
53      IF(S .GT. 173)GO TO 404
54      EM=1.-2.*BN1**2/EXP(A1*T)
55      GO TO 34
56      404  EM=T.0
57      34  WRITE(3,105)T,EM
58      105  FORMAT(6X,'T=',F8.3,3X,'EM=',F10.5)
59      5    T=T+10.0
60      1    CONTINUE
61      DO 11 I1=1,16
62      READ(1,757)H
63      757  FORMAT(F10.5)
64      READ(1,250)BN1,A1
65      READ(1,251)BN2,A2
66      READ(1,252)BN3,A3
67      READ(1,253)BN4,A4
68      250  FORMAT(2F15.8)
69      251  FORMAT(2F15.8)
70      252  FORMAT(2F15.8)
71      253  FORMAT(2F15.8)
72      WRITE(3,758)H
73      758  FORMAT(//6X,'H=',F10.5)
74      WRITE(3,701)BN1,BN2,BN3,BN4
75      701  FORMAT(//6X,'BN1=',E15.4,3X,'BN2=',E15.4,
13X,'BN3=',E15.4,3X,'BN4=',E15.4)
76      T=0.0
77      DO 12 J1=1,10
78      S1=A4*T
79      IF(S1 .GT. 173)GO TO 71
80      EM4=1.-2.*(BN1**2/EXP(A1*T)+BN2**2/EXP(A2*T)+
1BN3**2/EXP(A3*T)+BN4**2/EXP(A4*T))
81      EM3=1.-2.*(BN1**2/EXP(A1*T)+BN2**2/EXP(A2*T)+
1BN3**2/EXP(A3*T))
82      DEV=(EM4-EM3)/EM4
83      WRITE(3,501)T,EM3,EM4,DEV
84      501  FORMAT(6X,'T=',F8.3,3X,'EM3=',F10.5,3X,'EM4=',
1F10.5,3X,'DEV=',F18.8)
85      GO TO 91
86      71  S11=A1*T
87      IF(S11 .GT. 173)GO TO 81
88      EM=1.-2.*BN1**2/EXP(A1*T)
89      WRITE(3,601)T,EM
90      601  FORMAT(6X,'T=',F8.3,3X,'EM=',F10.5)
91      GO TO 91
92      81  EM=1.0
93      WRITE(3,901)T,EM
94      901  FORMAT(6X,'T=',F8.3,3X,'EM=',F10.5)
95      91  T=T+0.01
96      12  CONTINUE
97      DO 13 K1=1,10
98      S1=A4*T
99      IF(S1 .GT. 150)GO TO 72
100     EM4=1.-2.*(BN1**2/EXP(A1*T)+BN2**2/EXP(A2*T)+

```

```

101      1BN3**2/EXP(A3*T)+BN4**2/EXP(A4*T))
      EM3=1.-2.*(BN1**2/EXP(A1*T)+BN2**2/EXP(A2*T)+
102      1BN3**2/EXP(A3*T))
      DEV=(EM4-EM3)/EM4
103      WRITE(3,502)T,EM3,EM4,DEV
104      502  FORMAT(6X,'T=',F8.3,3X,'EM3=',F10.5,3X,'EM4=',
      1F10.5,3X,'DEV=',E18.8)
      GO TO 92
106      72  S11=A1*T
107      IF(S11.GT.173)GO TO 82
108      EM=1.-2.*BN1**2/EXP(A1*T)
109      WRITE(3,602)T,EM
110      602  FORMAT(6X,'T=',F8.3,3X,'EM=',F10.5)
111      GO TO 92
112      82  EM=1.0
113      WRITE(3,902)T,EM
114      902  FORMAT(6X,'T=',F8.3,3X,'EM=',F10.5)
115      92  T=T+0.1
116      13  CONTINUE
117      DO 14 L1=1,10
118      S1=A4*T
119      IF(S1.GT.150)GO TO 73
120      EM4=1.-2.*(BN1**2/EXP(A1*T)+BN2**2/EXP(A2*T)+
      1BN3**2/EXP(A3*T)+BN4**2/EXP(A4*T))
      EM3=1.-2.*(BN1**2/EXP(A1*T)+BN2**2/EXP(A2*T)+
121      1BN3**2/EXP(A3*T))
      DEV=(EM4-EM3)/EM4
122      WRITE(3,503)T,EM3,EM4,DEV
123      503  FORMAT(6X,'T=',F8.3,3X,'EM3=',F10.5,3X,'EM4=',
      1F10.5,3X,'DEV=',E18.8)
      GO TO 93
126      73  S11=A1*T
127      IF(S11.GT.173)GO TO 83
128      EM=1.-2.*BN1**2/EXP(A1*T)
129      WRITE(3,603)T,EM
130      603  FORMAT(6X,'T=',F8.3,3X,'EM=',F10.5)
131      GO TO 93
132      83  EM=1.0
133      WRITE(3,903)T,EM
134      903  FORMAT(6X,'T=',F8.3,3X,'EM=',F10.5)
135      93  T=T+1.0
136      14  CONTINUE
137      DO 15 M1=1,10
138      S1=A4*T
139      IF(S1.GT.150)GO TO 74
140      EM4=1.-2.*(BN1**2/EXP(A1*T)+BN2**2/EXP(A2*T)+
      1BN3**2/EXP(A3*T)+BN4**2/EXP(A4*T))
      EM3=1.-2.*(BN1**2/EXP(A1*T)+BN2**2/EXP(A2*T)+
141      1BN3**2/EXP(A3*T))
      DEV=(EM4-EM3)/EM4
142      WRITE(3,504)T,EM3,EM4,DEV
143      504  FORMAT(6X,'T=',F8.3,3X,'EM3=',F10.5,3X,'EM4=',
      1F10.5,3X,'DEV=',E18.8)
      GO TO 94
146      74  S11=A1*T
147      IF(S11.GT.173)GO TO 84
148      EM=1.-2.*BN1**2/EXP(A1*T)
149      WRITE(3,604)T,EM
150      604  FORMAT(6X,'T=',F8.3,3X,'EM=',F10.5)
151      GO TO 94
152      84  EM=1.0
153      WRITE(3,904)T,EM
154      904  FORMAT(6X,'T=',F8.3,3X,'EM=',F10.5)
155      94  T=T+10.0
156      15  CONTINUE
157      11  CONTINUE
158      STOP
159      END

```

/DATA

APPENDIX 12: ITERATIVE ANALOG COMPUTER PROGRAM CHECKING

- (1) Static check: Before the computer program is used, all the amplifiers being used have to be checked with the offset while the computer is in VERIFY position. Spot checks on the outputs from the integrators, amplifiers, multipliers, dividers while the computer is in RESET mode are necessary.
- (2) Dynamic check: With the program set up, the computer is allowed to operate for a certain period and is then held at a set of predetermined value of y . The dependent variables can then be compared with those read from the output of the digital-analog simulator.

The indicator on the logic patchboard is used for a double check. It is able to point out clearly the change of the binary logic signal from binary 1 to binary 0 as the independent variable y is approaching unity.

It should be emphasized that the X-Y recorder also has to be calibrated with the computer reference voltage.

APPENDIX (13)

" General information of Model AD-40 iterative analog computer used in this work (3) "

The Applied Dynamics Analog Computer, Model AD-40, is a very precise electronic differential equation analyzer designed to solve linear and non-linear differential equation. This computer is equipped with a patchable control logic system to extend the analog computer's capability for iterative operation requiring logic decisions and sequencing events.

The computing console is shown in Figure, reference (3).. In the standard configuration, this computer contains 40 operational amplifiers, 12 integrator networks, 40 coefficients potentiometers (only 20 pots are available on the computer used in this work), 8 electronic multipliers (including dual squarer, divider), 4 variable diode function generators, 6 comparators, 2 track-hold units, various types of switches, and a complement of parallel programmable logic elements. The analog components are terminated on the removable patchboard on the left, while the logic elements terminate on the patchboard on the right. Hybrid elements, i.e. comparators, track-hold units, logic controlled switches etc. have appropriate termination on both analog and logic patchboard.

The main components contained in the logic patchboard are Logic Gates, Combination Gates/Flip-Flop, Flip-Flops, Registers, Variable Pulsers, Logic Pushbottons, and

indicators. Comparators generate logic signals from analog voltages. Logic components perform logic decisions which produce logic levels for control of problems solutions by either integrator mode control or by logically controlled current switches or function switches.

The capability of patched hybrid and logic components for the control of repetitive or iterative operation expands the solution flexibility of the analog computer.

VITA

The author, Jeffrey Tsai-hwa Kuo, was born on June 23, 1944, in Kwangtung Province, China. He attended Jiann-Kuo Boy's High School in Taiwan, graduating in 1962. After the high school, the author attended National Taiwan University in Taipei, and graduated in the summer, 1966, with a degree of Bachelor of Science in Chemical Engineering. After one year ROTC service in the Chinese Army, he enrolled as a candidate for the Master of Science degree in Chemical Engineering in September, 1967.